STATISTICS OF PHOTON PATHS IN TISSUE DURING DIFFUSE REFLECTANCE SPECTROSCOPY

STATISTICS OF PHOTON PATHS IN TISSUE DURING DIFFUSE REFLECTANCE SPECTROSCOPY

By

ERNEST KWAKU OSEI, B.Sc (Hons).

A Project

Submitted to the School of Graduate Studies

in Partial Fulfilment of the Requirements

for the Degree

Master of Science

(Health and Radiation Physics)

McMaster University

MASTER OF SCIENCE (1991)
(Health and Radiation Physics)

McMASTER UNIVERSITY
Hamilton, Ontario,
Canada.

TITLE: Statistics of Photon Paths in Tissue During Diffuse Reflectance Spectroscopy.

AUTHOR: Ernest Kwaku Osei, B.Sc. (Hons). (University of Science and Technology, Kumasi, Ghana).

SUPERVISOR: Dr. M. S. Patterson

NUMBER OF PAGES: xvi, 116

ABSTRACT

The rapid development of the use of lasers in therapeutic and diagnostic medicine in the past few years has generated interest in measuring the optical properties of tissue. In particular, the development of photodynamic therapy (PDT) has necessitated studies of the optical properties of tissue at wavelengths around 630nm, this being the wavelength at which the photosensitizer commonly used in PDT, namely dihematoporphyrin ether (DHE), is normally activated.

The control of the volume of tissue from which information about the interaction coefficients of the tissue is obtained is an important problem in diffuse reflectance spectroscopy and other applications of light, because it is critical to understanding which tissue volumes are sampled by the injected photons that eventually are re-emitted. This report describes a simple model that predicts the parameters that control the volume of tissue interrogated by photons during reflectance spectroscopy.

In optical fiber based diffuse reflectance spectroscopy, incident radiation is applied at one point on a tissue surface and collected at another point, a radial distance, r, away. Information about the light multiply scattered by the tissue is used to deduce optical scattering and absorption coefficients of the tissue. In this report both steady state and pulse techniques are studied. In the steady state

method, the spatial dependence of the backscattered light is the measured quantity, while the pulse technique uses the temporal broadening of a picosecond (ps) pulse to determine the interaction coefficients.

The relative contribution of a volume element of tissue to the observed signal depends on its location, the measurement geometry and the optical properties of the tissue. Knowledge of this dependence would allow some control of the volume interrogated by reflectance spectroscopy, and would provide insight into the influence of inhomogeneities.

In the work reported here a simple diffusion model of light propagation in tissue based on the Boltzmann radiative transfer equation has been used to derive mathematical expressions for the relative time spent by photons in a given tissue volume element. Using optical interaction coefficients typical of mammalian soft tissues, results are presented for both steady state and pulse irradiation in both semi-infinite and infinite media.

The residency time depth profile calculated by this model for index matched and zero fluence boundary conditions has the same shape as that predicted by Weiss (1989), who used a somewhat different model based on a 3-dimensional random walk theory. These profiles are characterized by a build-up region near the surface and exponential fall far away from the surface in the 'diffusion region'. The influence of the absorption coefficient μ_a and the fiber separation on the residency time as predicted by this model is in good agreement to that predicted

by the random-walk theory (i.e the depth-profile of the residency time tends to sharpen as the absorption coefficient increases. This is attributed to the fact that long trajectories are less likely with large absorption probabilities. As well, the greater the fiber separation, the wider and flatter the depth distribution of the residency time. This is because photons that reach the surface at greater r values have, in general, migrated farther from the immediate vicinity of the source and detector and hence have sampled a larger volume of tissue). All the integrations in this report were performed numerically using the IMSL/LIB on the Microvax computer system in the Hamilton Regional Cancer Center. The adequacy of this numerical integration was tested and was found to be good.

This model therefore suggests that during diffuse reflectance spectroscopy, the volume sampled by re-emitted photons can be controlled by changing parameters such as the fiber separation (in both steady state and time-resolved techniques) and the detection time (in the time-resolved method).

ACKNOWLEDGEMENTS

Writing this project report has been an intensely personal experience which a number of people have been involved directly or indirectly. Since it is impossible to thank all those to whom the author is very much grateful, my gratitude is expressed here to those immediately concerned.

My greatest appreciation and gratitude go to my supervisor **Dr. M. S. Patterson**, without whom this report would not have been in existence. My special thanks again go to him for the patience, tolerance and untiring efforts he exhibited during the course and completion of this project, despite his several commitments.

I equally acknowledge with pleasure the services received from Donna and Ruth, all at the Physics Department, Hamilton Cancer Centre. I am also grateful to all other workers at the Department who gave me insight to the project through informal discussions, especially Swift who allowed me to use her accounts on the Microvax computer system in the Hamilton Regional Cancer Center.

My deep appreciation is extended to my wife, Margaret whose constant advice and encouragement have always sustained me through this project. The encouragements received from my parents, brothers, sisters and friends are also

very much appreciated.

Finally, I cease this opportunity to extend with pleasure my appreciation and thanks to the authorities of McMaster University who gave me the opportunity and financial support to further my education in Canada.

To end, I will express my gratefulness to all those who in diverse ways contributed to make this project a success.

TABLE OF CONTENTS

table of contents (cont.)

table of contents (cont.)

LIST OF FIGURES

CHAPTER ONE

INTRODUCTION.

Among the range of therapeutic procedures used to treat patients with localised malignant tumours, photodynamic therapy (PDT) is a relative newcomer and still an experimental form of treatment. It has been shown (Kessel 1984) to cause significant tumour regression and even cures in early disease. This technique was first performed clinically around 1975 (Dougherty 1975), and involves the destruction of malignant solid tumours by photoactivation of a tumour localizing drug.

In a typical PDT treatment, a photosensitiser, currently dihematoporphyrin ether (DHE) which is a purified form of hematoporphyrin derivative (HPD), is first administered intravenously to the patient. Then after a period of delay of about one to three days to allow accumulation of the drug in the tumour tissue, the volume to be treated is irradiated with visible light, usually at a wavelength of 630nm, this being the longest wavelength at which DHE is normally activated. Upon the absorption of a photon, the photosensitizer, which preferentially accumulates in malignant tissue, is raised to an excited state, which upon non-radiative de-excitation, generates biologically reactive molecular product(s), most likely singlet oxygen ($^1O_2$) which results directly or indirectly in tumour cell death.

The biological response to this new form of cancer treatment primarily depends on several physical factors including the local concentration of the photosensitizing drug in the tumour site, and the amount of activating light reaching the treatment volume (Wilson and Patterson 1986). Much of the on-going research work in PDT has been to develop better understanding of these dependencies. The experimental and theoretical methods used to determine these quantities and other parameters that are of clinical importance such as the tissue optical properties are mostly based on measurements of the light that is diffusely reflected back from the tissue (i.e the reflectance data). For a general review of the physical aspects of PDT and its clinical application the reader is referred to publications by Dougherty (1985) and Wilson and Patterson (1986). The development of this new form of cancer therapy has necessitated studies of the optical properties of tissue at wavelengths around 630nm.

In research work in PDT, and other diagnostic and therapeutic applications of light, the control of the volume of tissue from which information about the interaction coefficients of the tissue is obtained is an important problem, because it is critical to understanding which tissue volume is sampled by the injected photons that eventually are re-emitted from the tissue.

According to Jacques (1989), catheter-based reflectance spectroscopy will measure the optical absorption coefficient of a tissue volume at the catheter tip. Reliable measurements of large volumes are possible in organs (e.g brain, liver,

kidney) and tumours. Measurements of μ_a in smaller tissue volumes would be useful in measuring blood and clots within vessels, the superficial wall of the gastrointestinal and oesophageal tract or the first mm of tissue at a catheter tip which receives strong therapeutic laser irradiation. In these studies, a simple model of light propagation in tissue, based on the diffusion approximation to the radiative transfer equation is developed. This model could predict parameters that control the volume of tissue sampled by the injected photons.

1.1 MODELLING PHOTON PROPAGATION IN TISSUE.

The science of the interaction of light with living systems is usually called photobiology, and 'light' is that part of the electromagnetic spectrum encompassing the ultraviolet, visible and the infra-red regions (Wilson, in press). The propagation of light in biological media is particularly important in many photobiological and photomedical applications, since all photobiological effects results in the first instance, from the absorption of optical energy by tissue components, so that the spatial, and in some cases also the temporal, distribution of light in tissue is a major factor in the final biological result.

Thus the development of accurate and workable theoretical descriptions of light distribution in turbid media can be quite useful. This has created a demand for models that can accurately predict the photon propagation in tissue once the optical properties of the medium are known, or conversely, give the optical properties of the medium when the photon distribution is specified. The most

common approach to developing such appropriate models of light distribution in tissue has been to consider the propagation of light in tissue as the transport of discrete photons, which is described by the Boltzmann radiative transfer equation. Another approach which has been rarely used is to consider it as the propagation of electromagnetic waves (governed by Maxwell's equations) through a dielectric.

In principle, the latter approach, is the most fundamental (Ishimaru 1989) and it is possible to account for the wave-dependent phenomena such as interference, polarization, diffraction, refraction and reflection, and to determine both amplitude and phase dependencies (Wilson 1990). However, its main drawback is the mathematical complexity involved, and as such its usefulness is limited. Fortunately, for most purposes in photobiology, one is primarily interested in the local energy or power (fluence and fluence-rate) within or outside the tissue, rather than in the component amplitudes and phases of the light field (Wilson, in press). For example, in transmission or reflection spectroscopy, the relevant quantity is the fluence or fluence rate of the light which has interacted with, and then propagated out of the tissue.

This allows the light to be described empirically, as equivalent to the propagation of discrete photons whose number density and flow rate define the local fluence rate. Though the photon transport model does not incorporate the wave-dependent effects, it has, nevertheless been successful and useful as a

model to describe the light fluence or fluence rate from and within tissues.

The diffusion theory approximation to the one-speed transport equation, has been used to describe photon propagation in a turbid biological medium. This approach has been suggested by several sources (Wilson in press, Ishimaru 1989, Flock et al 1989, Wilson et al 1989, Profio 1989, Patterson et al 1989 and Reynolds et al 1976). Substantial experimental evidence (Flock et al 1989, Patterson et al 1989 and Wilson et al 1989) indicate that optical propagation in turbid media may be described by a diffusion theory approach. Further substantiation is demonstrated in this report. The diffusion theory applies for optically dense media and only when scattering events are much more probable than absorption events (Duderstadt and Hamilton 1976). This is the case for mammalian tissues in the red and near infra-red regions of the spectrum (Wilson and Patterson 1986, Wilson et al 1988, Flock et al 1987, and Flock 1988), and as a result, the diffusion model has found wide application in tissue optics. But since the model requires diffused light within the tissue, results are not as accurate near boundaries and internal light sources. A formal discussion of the radiative transfer equation and its diffusion approximation is presented in chapters 2 and 3 respectively.

1.2 REFLECTANCE SPECTROSCOPY.

In the form of reflectance spectroscopy used here, collimated light, as for example, a direct beam from a laser, is incident normally on the interface

between a turbid tissue and a transparent medium (usually air) at one point, and the light that is re-emitted at this interface at another point, a radial distance from the point of incidence, into the external transparent medium is measured (Figure 3.5.1). This observed quantity (i.e the reflectance) has been shown by several research groups (Patterson et al 1989, Bonner et al 1981, Weiss et al 1989, Groenhuis et al 1983 and Reynolds et al 1976) to contain informations about parameters of photon interaction within the medium.

In the steady state method, the observable quantities are the number and angular distribution of photons emerging from the surface of the tissue at any point (Patterson et al 1990). The time dependence of these quantities constitute the observable quantities in the time-resolved technique. Since the mean free path of light in tissue is of the order of a few tens of microns (Patterson et al 1990), the photons that escape the tissue usually have been multiply scattered. One goal of tissue optics research has been to deduce the information of interest (e.g absorption and scattering coefficients of the tissue) from the observable parameters. Since there is no straightforward relation between these parameters of interest and the observable quantities, the desired parameters can be obtained by using a physical model of the detection process (Patterson et al 1990).

Some work has already been done in this area by Patterson and co-workers (1989 and 1990), who used the steady state and more recently the time-resolved diffusion approximation of the radiative transfer equation to show that,

the absorption, μ_a, and the transport scattering, $(1-g)\mu_s$, coefficients can be obtained using the spatial or temporal distribution of the diffuse reflectance from a point source. In previous work, Patterson et al (1987) demonstrated that reflectance spectrophotometry is capable of quantifying clinically relevant amounts of hematoporphyrin derivative in realistic phantoms and that DHE can be readily detected in vivo by this technique.

Earlier work in this area was performed by Groenhuis et al (1983) who also used a diffusion model to calculate the number of photons per unit area leaving the surface of a semi-infinite homogeneous medium as a function of the distance from the centre of a normally incident finite collimated beam. Estimation of μ_a and $(1-g)\mu_s$ from measurements of the absolute photon fluence at a number of discrete distances was permitted by the graphical results presented.

In a related study, it has been demonstrated by a somewhat different analysis that surface emission can be used to infer parameters such as the fraction of time that photons re-emitted at the tissue surface have spent at depth z, in the tissue (Weiss et al 1989), the mean path length travelled by the detected photons as a function of the separation between emitting and detecting probes and, the probability of photon absorption as a function of depth (Bonner et al 1987), the root-mean-square (rms) blood cell speed and the number density of blood cells in tissue (Bonner et al 1981).

Feather et al (1981) and Anderson et al (1981) used a reflectance

technique to demonstrate qualitative changes in the amount of pigments such as bilirubin, melanin and haemoglobin in the human skin. The technique has also been used by Reynolds et al (1976) to exploit the different absorption characteristics of haemoglobin and oxyhemoglobin to measure the oxygenation of blood in vivo. Recent work reported by Bacci et al (1986) indicated that measurement of the reflectance spectrum from the skin can be used for the detection of hematoporphyrin in the subcutaneous tissue of mice.

Thus, different information of clinical importance can be inferred by analyzing photons re-emitted from tissue. In this report, therefore, a theoretical model of photon propagation in tissue based on the diffusion approximation to the radiative transfer equation is developed. This study is similar in purpose to that of Weiss et al (1989), who used a rather different approach based on a 3-dimensional random-walk theory. However, by using a somewhat simpler diffusion model, the distributions of the 'residency time' of re-emitted photons are easily determined.

1.3 DIFFUSE REFLECTANCE.

Tissue is a scattering and absorbing medium and, obviously, has a higher refractive index than air. So when a laser beam is incident on a human tissue, at the air-tissue interface, part of the light is reflected back owing to specular reflection. The rest of the light penetrates the tissue where the photons are multiply scattered elastically (i.e scattered without loss of energy) by cytoplasmic

organelles and cell boundaries (Weiss et al 1989). Some photons are absorbed in the tissue and some are reflected back to the surface where they are re-emitted. The absorption and scattering of these photons in the medium are governed by the absorption coefficient, the scattering coefficient μ_s and anisotropy ,g (i.e the average cosine of scatter), respectively. The path length of each photon that successfully escapes the tissue as observable reflectance is not the same. Some photons enter the tissue and are immediately scattered and escape. Other photons wander through the tissue for some time before they migrate to the surface and escape. Therefore the path length, L, is not a single value, but a distribution of path lengths (Delpy et al 1988 and Bonner et al 1987).

In reality the spatial distribution of the light fluence in the irradiated tissue volume depends not only on the absorption and the scattering coefficients of the tissue at any point but also on the heterogeneity of these properties, on the irradiation geometry, on the boundary conditions and on the shape and size of the tissue volume. But for simplicity one usually considers the case of a large volume of optically homogeneous tissue irradiated by a collimated beam incident normally on the tissue surface, (figures 3.4.1.1.1.1 and 3.4.1.1.2.1).

The distribution of diffuse (i.e multiply scattered) reflected light likewise depends critically on the tissue optical properties. As the scattering in tissue increases, the probability of photons being backscattered through the irradiated surface after multiple scattering also increases and it is measured by the diffuse

reflectance (Wilson, in press). In the case of a pure absorbing medium, all the incident photons will be absorbed as expected, so that there will be no reflectance. For a scattering-dominated medium, it has been shown (Patterson et al 1989) from the diffusion theory model of light propagation in tissue that the total diffuse reflectance R_t depends only on the transport albedo (a') of the tissue, $a' = \mu_s'/(\mu_a+\mu_s')$, where $\mu_s' = (1-g)\mu_s$, and in the case of refractive index mismatch at the surface, also on the tissue refractive index.

There are published data on the dependence of the total diffuse reflectance on the transport albedo for various values of the scattering-to-absorption ratios (Wilson 1990). The local diffuse reflectance R(r) is the ratio of the photon flux per unit area on the tissue surface to the incident flux after accounting for the loss due to specular reflection, and the total diffuse reflectance, R_t, is the local diffuse reflectance integrated over the irradiated surface:

$$R_t = \int_0^\infty R(r) 2\pi r dr \qquad 1.1$$

1.4 TIME-RESOLVED REFLECTANCE.

In the previous discussion a steady state condition was assumed as would be obtained for a continuous irradiation or for a pulsed irradiation where the pulse length is large compared to the propagation time of the light in tissue. However, with the introduction of picosecond pulsed laser sources and fast photodetector

systems such as multichannel plate photomultiplier tubes and streak cameras, it has become both feasible and of practical interest in tissue spectroscopy to examine the broadening of the light pulse in tissue (Patterson et al 1989). Light photons take a finite time to propagate in tissue at a speed c′, where c′ = c/n, c is the speed of light in vacuo (expressed in this report as $0.3 mm ps^{-1}$) and n is the refractive index of the medium. Thus the underlying principle of the time-resolved technique is that photons re-emitting a tissue surface are spread in time following an incident short light pulse. This is due to the different path lengths taken in transversing a highly scattering medium such as tissue.

At any particular time, t, following a short incident pulse, for a scattering dominated medium, the total distance, L, (i.e optical path length) travelled by a photon is, L = c′t. For the case of the incident photons that are unscattered, this path length corresponds to the depth below the tissue surface. However, for scattered photons, at time, t, there is a spread (broadening) in the spatial distribution of the photons, and the pattern of photon distribution develops gradually with time. Finally, after the light has become essentially completely diffused, the fluence-time dependence is governed by the absorption. On the tissue surface, the time dependence of the local, R(r,t), and the total, $R_t(t)$, diffuse reflectance also depends initially on the scatter and absorption, but at later times is absorption dominated (Wilson, in press).

Studies of the time course of transmitted light in turbid media have been

performed (Kuga et al 1983). Diagnostic application of time-resolved measurements of reflectance and transmission for spectroscopy (Chance et al 1988 and Delpy et al 1988) and the potential of the time-resolved technique to determine tissue optical properties from R(r,t) (Patterson et al 1989 and Wilson et al 1989) have both been considered.

Ultrashort laser pulses in the femtosecond and picosecond range will therefore probably enjoy increased use in medicine. One application is the disruption of tissue by laser-induced plasma, for example, in ophthalmology, to disrupt the residual lens membrane following ocular lens surgery (Puliafito et al 1983), in urology, to fragment kidney stones (Nishioka et al 1987), and in vascular surgery, to ablate calcified plaque (Prince et al 1987). A second application is ablation of normally non-absorbing tissue by initiating nonlinear absorption with femtosecond pulses (Jacques 1989). A third application is the production of laser induced photochemical reactions, which have been developed principally around the technique of PDT (Gomer 1987).

1.5 TISSUE OPTICAL PROPERTIES.

The interaction of light field with tissue is usually specified by the absorption and the scattering coefficients of the tissue. The angular dependence of the scattering is described by the phase function which is a measure of the relative probability of scattering through a particular angle. In optically turbid tissue (excluding the transparent structure of the eye), the nature of the light field,

i.e the spatial and temporal distribution of light within and from the tissue, depends primarily on the relative contributions of absorption and scattering (Wilson, in press).

The linear (i.e one-photon) absorption and scattering properties of several mammalian tissues have been measured using a variety of in vitro and more recently, in vivo techniques. For example,

1. direct measurement in optically thin tissue samples (Flock et al 1987, Marchesini et al 1989 and Jacques and Prahl 1987),
2. from the diffuse transmittance and reflectance through optically thick samples (Parsa et al 1989, Peters et al and Anderson et al 1981),
3. by 'doping' homogenized tissue with known concentrations of an exogenous absorber (Wilson et al 1986),
4. through 'mapping' of the fluence distributions within intact, bulk tissue (Wilson et al 1985 and Marijnissen et al 1987) and
5. by measuring the spatial and/or temporal distribution of diffusely reflected or transmitted light (Patterson et al 1989, Marijnissen and Star 1984).

Of all these techniques, the last two can be done in vivo. The first technique listed above can yield values of the absorption coefficient, the scattering coefficient, the total attenuation coefficient, μ_t, and the scattering angular distribution or phase function, $S(\theta)$, without the need for any model of light propagation in tissue. The other methods may yield μ_a (the mean free path,

mfp, that a photon travels before absorption occurs is equal to $1/\mu_a$), μ_s (the mean free path between scattering events is equal to $1/\mu_s$) and the scattering anisotropy parameter, g, or some combination of these such as the transport scattering coefficient, μ_s'. However, this requires the application of suitable models of light propagation, such as diffusion theory (Jacques and Prahl 1987, Flock et al 1988) or Monte Carlo simulations (Wilson and Adam 1983, Groenhuis et al 1983 and Flock et al 1988). The experimental and theoretical descriptions of how these parameters are determined and some typical values that have been measured for some soft mammalian tissues can be found elsewhere (Wilson and Patterson 1986 and Wilson 1990).

Around 630nm (Flock et al 1989), the range of interaction coefficients for mammalian soft tissue is $0.01mm^{-1} < \mu_a < 0.5mm^{-1}$, $35mm^{-1} < \mu_s < 70mm^{-1}$ and $0.7 < g < 0.99$. To facilitate the following discussion, the following optical parameters will be assumed as representative values: $\mu_a = 0.01 - 0.2mm^{-1}$ and $\mu_s' = 1.0 - 5.0mm^{-1}$.

1.6 PROJECT PROPOSAL.

The scattering of light by turbid media has been studied extensively in the past (Ishimaru 1978), and its applications include atmospheric optics (Ito 1980 and Weinman and Shipley 1972), optics in the ocean (Jerlov 1976), scattering by stellar and interstellar media (Shihov 1974 and Lee and Jokipii 1975) and optical scattering in biological media (Bonner and Nossal 1981, Patterson et al 1989,

Flock et al 1988 and Wilson et al 1989).

There is therefore a need for better understanding of the migration paths of photons in tissue. The purpose of this project therefore is an attempt to accurately and non-invasively analyze the statistics of photon paths in tissue during both the steady state and time-resolved diffuse reflectance spectroscopy once the bulk scattering and absorption properties of the tissue are specified.

The possible approaches to the solution of this problem include; a Monte Carlo simulation, Random-walk theory and an analytical method (which is based on the diffusion theory). Each of these methods has its own advantages and disadvantages. For example, in the case of Monte Carlo simulation which is performed by tracing individual photon histories, the principal advantage is that complex geometries and inhomogeneities can be modelled in a straightforward manner (Wilson et al 1985). Another advantage is that a variety of physical quantities can be scored during the same run. However, its main drawback is that many photon histories are required to obtain accurate results and this may be expensive in computation time. In some cases, as for example, in the problem being analyzed here, another disadvantage of the Monte Carlo method is that large computer memory will be required. For computational efficiency, which is important, especially in routine clinical use of light, fast, though approximate analytical approach may be used. This is the method that would be used in this report.

1.7 SIGNIFICANCE OF RESULTS.

The main results of this report will be mathematical expressions for the average residency time in an elemental tissue volume of a photon that is injected into a tissue and subsequently is re-emitted through a small area dA, on the tissue surface, a radial distance, r, from the point of injection. From these expressions one can deduce some characteristics of the migration paths of those photons that contribute to diffuse surface reflectance measurements at any point, once the bulk optical properties of the tissue are specified.

The relative contribution of an elemental volume of tissue to the observed signal depends on the residency time of those photons in that volume element. This quantity in turn depends on the location of the volume element, the measurement geometry and the optical properties of the tissue. Knowledge of this dependence would allow some control of the volume interrogated by reflectance spectroscopy, and would provide insight into the influence of inhomogeneities. Though the objective in this report is not to deduce the optical properties of tissue, the model could certainly be used to determine μ_a and $(1-g)\mu_s$ (Patterson et al 1990).

The results should also pertain to other variety of bio-medically important measurements, particularly when the receiving and transmitting fibers of the probes are far apart from each other. For example, in Doppler laser techniques (Weiss et al 1989), it frequently is important to determine the depth of penetration

of injected photons, both for those absorbed within the tissue and those re-emitted from the irradiated surface. The distribution of the absorption depths is critical in evaluating therapeutic procedures such as laser ablation and photo-chemical therapy (Dougherty et al 1978 and Dorion et al 1983). Unfortunately, the model used here is restricted to those photons that eventually are re-emitted on the tissue surface, however, it is worth mentioning that this analysis can certainly be used to determine absorption depths.

The model could be used to determined the distribution of depths sampled by the diffusely reflected photons since it corresponds to the average residency time at a given depth, z (Bonner et al 1987). Such distribution is important for interpreting remote-sensing measurements such as laser Doppler evaluation of microcirculatory blood flow (Tahmoush et al 1983), spectroscopic sensing of tissue oxygenation (Reynolds et al 1976 and Johnson 1970) and fluorescence (Dougherty et al 1978 and Doiron et al 1983).

1.8 SCOPE OF WORK.

In the work reported here, a simple diffusion model of light propagation in tissue has been used to investigate the statistics of photon paths in tissue during both the steady state and time-resolved diffuse reflectance spectroscopy. Two irradiation geometries are considered: an infinite medium with an isotropic point source of photons (figure 3.4.1.2.1) and a semi-infinite medium (the probability that a photon reaches a tissue boundary other than the illuminated surface before

being absorbed or re-emitted is negligibly small) with a collimated beam of photons (figure 3.4.1.1.1.1 and 3.4.1.1.2.1).

In chapter 2, the fundamental parameters of the propagation medium are defined and the radiative transfer equation is derived. Since the solution of this equation is very difficult to obtain, the diffusion approximations are introduced subject to some boundary conditions. One of the two boundary conditions incorporates index mismatch. The solutions of the diffusion equation for both irradiation geometries are presented in chapter 3. Using these solutions, approximate analytical expressions for the relative time spent by re-emitted photons in an infinitesimal volume element dV at r' in a semi-infinite medium are obtained. A similar expression for photons emitted from a point source and observed in a point detector in an infinite medium is also derived. The residency time at depth z, obtained by Weiss et al (1989) for a semi-infinite medium, is also introduced.

In chapter 4, the results and a discussion on the computational methods used are presented. The results obtained in the semi-infinite medium with a zero boundary condition in the steady state method are compared to that of Weiss et al (1989).

The significance of an inhomogeneous medium and slab geometry on the photon residency time distribution in tissue are considered to be outside the scope of this report.

The geometrical presentation of the model to be analyzed is illustrated in figures 3.4.1.1.1.1, 3.4.1.1.2.1 and 3.4.1.2.1. In figures 3.4.1.1.1.1 and 3.4.1.1.2.1, a narrow collimated infinitesimally short pulsed light beam is incident normally on the surface of a semi-infinite homogeneous medium at a point O(0,0,0) at time t = 0. Photons enter the medium and are scattered by scattering sites. Some are absorbed in the medium and some are reflected back to the surface where they are re-emitted. A detector is positioned on the surface at a point D(r,0,0), a radial distance, r, from the point of incidence. Two techniques are considered: The steady state technique and the time-resolved method. In the steady state method, experimental data consist of measurements of the reflected intensity on the tissue surface, taken as a function of the distance, r, from the point of incidence of photons. In the time-resolved technique, the measured quantity is the reflected intensity, taken as a function of both r and time t. The coordinate system measures penetration of the medium in terms of the coordinate, z, which is positive in the downward direction (into the medium), and the coordinates x,and y, measured perpendicular to the z-axis.

In figure 3.4.1.2.1, a point source of photons is placed in an infinite medium at S(0,0) and a point detector is positioned at a point D(r,0), a distance r, from the source, and measures the spatial dependence of the multiply scattered light or the temporal broadening of a picosecond pulse.

CHAPTER TWO

THEORY I

2.1 ASSUMPTIONS OF THE RADIATIVE TRANSFER THEORY.

In order to determine the distribution of photons in a random medium such as tissue, one must investigate the process of photon transport, that is, the motion of the photons as they stream about in the tissue, frequently being scattered by scattering sites and eventually either being absorbed in or escaping from the medium. Such investigation requires accounting for both the photon motion and the photon interactions in the tissue. As discussed under section 1.1, the transport model (which assume that light photons propagating through tissue can be treated as neutral particles and that wave phenomena can be ignored) is a feasible approach to the problem of photon transport in tissue.

The variables which characterize the state of an individual photon include; its position, $\underline{r}$, the direction of motion, $\underline{\Omega}$, and the time, t, at which the photon is observed. It will be assumed that the photons are mononergetic and that scattering is elastic (i.e there is no photon energy loss in the process). Further more, fluorescence of the medium will be ignored. Thus, all photons within the medium will have the same wavelength or energy. It is important to make mention here that both inelastic scatter and fluorescence can be included

(Moulton 1990) but will require a more complicated model.

2.2 DEFINITIONS OF THE FUNDAMENTAL PARAMETERS OF THE PROPAGATION MEDIUM.

The fundamental quantity of interest is the photon angular density $n(\underline{r},\underline{\Omega},t)$, (units: $m^{-3}Sr^{-1}$), defined such that

$$n(\underline{r},\underline{\Omega},t)d^3rd\underline{\Omega}$$

is the expected number of photons in d^3r about $\underline{r}$ moving in solid angle $d\underline{\Omega}$ about the direction $\underline{\Omega}$ at time t. The photon density (i.e the number of photons per unit volume at a position $\underline{r}$ at time t, units: m^{-3}), is therefore defined as the angle integral of the photon angular density, i.e

$$N(\underline{r},t) = \int_{4\pi} n(\underline{r},\underline{\Omega},t)d\underline{\Omega} \qquad 2.1$$

Other quantities of interest are the radiance, energy fluence rate and photon angular flux, defined as follows; The radiance, $L(\underline{r},\underline{\Omega},t)$,(units: $Wm^{-2}Sr^{-1}$), is related to the photon angular density by the equation

$$L(\underline{r},\underline{\Omega},t) = h\upsilon c' n(\underline{r},\underline{\Omega},t) \qquad 2.2$$

where $h\upsilon$ is the energy of an individual photon and c' is the speed of light in the medium.

Similarly the energy fluence rate, $F(\underline{r},t)$, (units: Wm^{-2}) is defined as

$$F(\underline{r},t) = h\nu c' N(\underline{r},t) \qquad 2.3$$

It is also common to define the photon angular flux, (units: $m^{-2}s^{-1}Sr^{-1}$), as;

$$\varphi(\underline{r},\Omega,t) = c' n(\underline{r},\Omega,t) \qquad 2.4$$

and the photon fluence rate, (units: $m^{-2}s^{-1}$), as the angle integral of the photon angular flux, i.e

$$\phi(\underline{r},t) = \int_{4\pi} \varphi(\underline{r},\Omega,t)\, d\Omega = c' N(\underline{r},t) \qquad 2.5$$

A related concept is the photon angular current density (units: $s^{-1}Sr^{-1}$), defined as

$$J(\underline{r},\Omega,t) = c'\Omega n(\underline{r},\Omega,t) = \Omega\varphi(\underline{r},\Omega,t) \qquad 2.6$$

and the photon current density, (units: s^{-1}), is

$$J(\underline{r},t) = c' \int_{4\pi} \Omega n(\underline{r},\Omega,t)\, d\Omega = \int_{4\pi} \Omega\varphi(\underline{r},\Omega,t)\, d\Omega \qquad 2.7$$

Finally, it is necessary to define the various interaction coefficients before an exact equation describing photon transport in a turbid biological medium can be developed. The attenuation of visible light in tissue can be considered as due essentially to absorption and elastic scattering. The absorption coefficient, $\mu_a(\underline{r},t)$, is the probability that a photon will be absorbed per unit infinitesimal path length at a position $\underline{r}$ in the medium at time t, and is related to the rate

$$\mu_a(\underline{r},t)\varphi(\underline{r},\underline{\Omega},t)d^3rd\underline{\Omega}$$

at which photons in $d^3rd\underline{\Omega}$ at $(\underline{r},\underline{\Omega},t)$ are absorbed. Similarly the differential scattering coefficient $\mu_s(\underline{r},\underline{\Omega}'\rightarrow\underline{\Omega},t)$, which is the probability per unit infinitesimal path length per unit solid angle of photon scatter from an initial direction $\underline{\Omega}'$ to a final direction $\underline{\Omega}$ is such that

$$\mu_s(\underline{r},\underline{\Omega}'\rightarrow\underline{\Omega},t)\varphi(\underline{r},\underline{\Omega}',t)d^3rd\underline{\Omega}$$

represents the rate at which photons moving in the direction $\underline{\Omega}'$ are scattered to the new direction $\underline{\Omega}$. The total scattering coefficient, $\mu_s(\underline{r},t)$, i.e the probability that a photon will be scattered per unit infinitesimal path length at a position $\underline{r}$ in the medium at time t, is given by the integral of the differential scattering coefficient over all final directions, i.e

$$\mu_s(\underline{r},t) = \int_{4\pi} \mu_s(\underline{r},\underline{\Omega}'\rightarrow\underline{\Omega},t)d\underline{\Omega} \qquad 2.8$$

Note, it has been assumed, as is generally the case, that, the scattering and absorption coefficients are independent of the original direction of the photon. An assumption that is reasonable for a random medium, such as tissue (Wilson et al 1985). The total attenuation coefficient, $\mu_t(\underline{r},t)$, sometimes referred to as the extinction coefficient, is the sum of the absorption and scattering coefficients,

$$\mu_t(\underline{r},t) = \mu_a(\underline{r},t) + \mu_s(\underline{r},t) \qquad 2.9$$

and its inverse, $[\mu_t(r,t)]^{-1}$, is the mean free path between photon interactions. The

scattering phase function, S(θ), describes the angular dependence of the scattering, where θ is the angle between the incident beam and the scattered photon in the scattering plane. S(θ) is given by

$$S(\theta) = \left(\frac{2\pi}{\mu_s}\right)\frac{d\mu_s(\Omega \rightarrow \Omega')}{d\Omega'} \qquad 2.10$$

where the integral of S(θ) over 4π Sr is unity. In most models of light propagation, a useful simplifying parameter often used is the average cosine of scatter, denoted by g, (Duderstadt and Hamilton 1976),

$$g = \int_{-1}^{1} S(\theta)\cos\theta\, d(\cos\theta) \qquad 2.11$$

Thus, g = 0 represents isotropic scattering, while 0 < g ≤ 1 represents forward scattering.

2.3 THE TRANSPORT EQUATION.

Now, consider an arbitrary volume, V, of surface area, S, located anywhere within the tissue. The objective is to examine this 'control' volume carefully to determine how the photon population within it changes. It is evident that the total number of photons in V at a time, t, travelling in a direction, $\underline{\Omega}$, in $d\underline{\Omega}$ can be obtained by integrating the photon angular density over the entire volume, i.e

$$\left[\int_V n(r,\underline{\Omega},t)\, d^3r\right] d\underline{\Omega}$$

Hence the time rate of change of the number of photons in V must be given by

a balance relation such that

$$\frac{\partial}{\partial t}\left[\int_V n(\underline{r},\underline{\Omega},t)\,d^3r\right]d\underline{\Omega} = \begin{matrix}\textit{Gain of photons}\\ \textit{in V}\end{matrix} - \begin{matrix}\textit{Loss of photons}\\ \textit{in V}\end{matrix} \qquad 2.12$$

If it is assumed that, the arbitrary volume V is chosen not to be time dependent, then,

$$\frac{\partial}{\partial t}\left[\int_V n(\underline{r},\underline{\Omega},t)\,d^3r\right]d\underline{\Omega} = \left[\int_V \frac{\partial}{\partial t} n(\underline{r},\underline{\Omega},t)\,d^3r\right]d\underline{\Omega} \qquad 2.13$$

The various ways by which photons can appear (i.e the gain mechanisms) or disappear (i.e the loss mechanisms) in the volume will now be considered and they shall be represented by mathematical expressions.

2.3.1 GAIN MECHANISMS.

There are two main gain mechanisms that contribute to the population of photons in the chosen volume, V. First of all, there is the gain due to photon sources in the volume. If the source density $S(\underline{r},\underline{\Omega},t)$ is specified so that

$$S(\underline{r},\underline{\Omega},t)\,d^3r\,d\underline{\Omega}$$

is the rate at which photons are produced in d^3r at $\underline{r}$ moving in $d\underline{\Omega}$ about $\underline{\Omega}$, then, the production of photons in V is

$$\left[\int_V S(\underline{r},\underline{\Omega},t)\,d^3r\right]d\underline{\Omega}$$

The second gain term in the volume is that due to those photons which initially were in a different direction $\underline{\Omega}'$, and then suffering a scattering collision in V

which changes their initial direction into the direction of interest $\underline{\Omega}$. If the probability of scattering from $\underline{\Omega}'$ to $\underline{\Omega}$ is given in terms of the differential scattering coefficient, $\mu_s(\underline{r},\underline{\Omega}'\rightarrow\underline{\Omega},t)$, then the rate at which those photons moving in the direction $\underline{\Omega}'$ are scattered to the direction of interest $\underline{\Omega}$ is

$$[\int_V c'\mu_s(\underline{r},\underline{\Omega}'\rightarrow\underline{\Omega},t)n(\underline{r},\underline{\Omega}',t)d^3r]d\underline{\Omega}$$

However, contributions from any initial direction, $\underline{\Omega}'$, must be considered, hence the total rate becomes,

$$[\int_V d^3r\int_{4\pi} d\underline{\Omega}'c'\mu_s(\underline{r},\underline{\Omega}'\rightarrow\underline{\Omega},t)n(\underline{r},\underline{\Omega}',t)]d\underline{\Omega}$$

2.3.2 LOSS MECHANISMS.

Conversely, there are some loss mechanisms that occur in the volume which results in loss of photons. The two most significant loss mechanisms are the loss due to the net leakage of photons from the volume V, and the loss due to those photons in V suffering a collision. If $j(\underline{r},\underline{\Omega},t)$ is the photon angular current density, then the net rate at which photons in the direction $\underline{\Omega}$ pass out through a small surface element $d\underline{S}$ is

$$\int_S j(\underline{r},\underline{\Omega},t)dS$$

and utilising the relation in equation 2.6, the expression above can be rewritten

in terms of the photon angular density as

$$c' \int_S \underline{\Omega} n(\underline{r},\underline{\Omega},t) dS$$

But it would be more convenient to convert the surface integral above to a volume integral, similar to the other terms. The common way to convert such surface integral to volume integral is to use Gauss's theorem:

$$\int_S dS \cdot A(\underline{r}) = \int_V d^3r \nabla \cdot A(\underline{r}) \qquad 2.14$$

to write

$$[c' \int_S \underline{\Omega} n(\underline{r},\underline{\Omega},t) dS] d\underline{\Omega} = [c' \int_V \nabla \cdot \underline{\Omega} n(\underline{r},\underline{\Omega},t) d^3r] d\underline{\Omega} \qquad 2.15$$

It is obvious that an absorption interaction removes a photon from V. By definition a scattering collision changes a photon direction, but since one is only keeping track of photons in V with this specific direction $\underline{\Omega}$, a scattering collision can also be considered to amount to loss of photons. The rate at which photons suffer collisions at a point $\underline{r}$ at time t is

$$c' \mu_t(\underline{r},t) n(\underline{r},\underline{\Omega},t)$$

Hence integrating this collision rate over the entire volume V, gives the total loss due to collision in the volume as

$$[c'\int_V \mu_t(r,t)n(r,\Omega,t)d^3r]d\Omega$$

If all these terms are now combined such that

$$\textit{The time rate of change of photons in V} = \textit{Gain terms in V} - \textit{Loss terms in V} \qquad 2.16$$

Then,

$$[\int_V \frac{\partial}{\partial t}n(r,\Omega,t)d^3r]d\Omega = [\int_V S(r,\Omega,t)d^3r]d\Omega - [c'\int_V \nabla\Omega n(r,\Omega,t)d^3r]d\Omega + [c'\int_V d^3r\int_{4\pi} d\Omega(\Omega'\rightarrow\Omega)n(r,\Omega',t) - [c'\int_V \mu_t(r,t)n(r,\Omega,t)d^3r]d\Omega \qquad 2.17$$

or

$$\int_V d^3r[\frac{\partial}{\partial t}n(r,\Omega,t) + c'\Omega\nabla n(r,\Omega,t) + c'\mu_t(r,t)n(r,\Omega,t) - \int_{4\pi} d\Omega' c'\mu_s(r,\Omega'\rightarrow\Omega,t)n(r,\Omega,t) - S(r,\Omega,t)]d\Omega = 0 \qquad 2.18$$

Notice that, it has rightly been written,

$$c'\nabla\Omega = c'\Omega\nabla \qquad 2.19$$

since $\underline{\Omega}$ does not depend on $\underline{r}$.

Recall that the volume V being examined was chosen to be arbitrary, that is to say, equation 2.18 must hold for any volume V in the medium. However, the only way this can occur is if the integrand itself were to vanish (Duderstadt and Hamilton 1976). Hence,

$$S(r,\Omega,t) = \frac{\partial}{\partial t}n(r,\hat{\Omega},t) + c'\hat{\Omega}\nabla n(r,\hat{\Omega},t) + c'\mu_t(r,t)n(r,\hat{\Omega},t) - \int_{4\pi} d\hat{\Omega}' c'\mu_s(\hat{\Omega}'\rightarrow\hat{\Omega})n(r,\hat{\Omega}t) \qquad 2.20$$

Using equation 2.4, equation 2.20 can be rewritten in terms of the photon angular flux density, i.e

$$S(r,\Omega,t) = \frac{1}{c'}\frac{\partial}{\partial t}\varphi(r,\Omega,t) + \Omega\nabla\varphi(r,\Omega,t) + \mu_t(r,t)\varphi(r,\Omega,t) - \int_{4\pi} d\Omega'\mu_s(\Omega\rightarrow\Omega)\varphi(r,\Omega',t) \qquad 2.21$$

Equation 2.21 is the classical Boltzman transport equation. It is a far more fundamental and exact description of the photon population in a medium, and the fundamental cornerstone on which almost all of the various approximate methods used in photon transport are based. Its major drawback, however, is that, despite all the assumptions that were made to derive it, it is usually very difficult to solve for any but the simplest modelled problems. Applications to practical situations generally requires further, even more restrictive approximations (Moulton 1990).

2.4 SOLUTION OF THE TRANSPORT EQUATION.

An analytical solution of the transport equation is possible, but only under a few conditions (Wilson and Patterson 1988). Thus the Boltzmann transport equation is usually solved numerically on a computer. Chandrasekhar (1950), has solved the transport equation for a homogeneous, semi-infinite, isotropically

scattering medium irradiated with a collimated beam of infinite extend. And a similar solution has been presented by Rybick (1971) for a similar medium irradiated with a narrow collimated beam. There are a number of numerical techniques which have evolved to handle more general conditions such as anisotropic scattering and slab geometries (Wilson and Patterson 1985). The most direct method is that of discrete ordinates described by Duderstadt and Hamilton (1976), which amounts to a numerical solution of a discrete version of the transport equation. The solution for the general case of finite beam and a 3-dimensional geometry containing inhomogeneities still represents a formidable computing task (Wilson and Patterson 1986).

CHAPTER THREE

THEORY II

3.1 THE PHOTON DIFFUSION EQUATION.

Another way of solving the transport equation is to simplify it from an **integro-differential** (i.e containing both derivatives in space and time as well as integral over angle) equation to a partial differential equation which can then be solved by standard techniques.The transport equation can be rewritten in terms of the angle-integrated flux, $\phi(\underline{r},t)$, i.e

$$\phi(\underline{r},t) = \int_{4\pi} \varphi(\underline{r},\underline{\Omega},t)\, d\underline{\Omega} \qquad 3.1$$

Integrating the Boltzmann transport equation 2.21 over all directions, $\underline{\Omega}$, i.e

$$\int_{4\pi} d\underline{\Omega}\, S(\underline{r},\underline{\Omega},t) = \frac{1}{c'}\int_{4\pi} d\underline{\Omega}\frac{\partial}{\partial t}\varphi(\underline{r},\underline{\Omega},t) + \int_{4\pi} d\underline{\Omega}\,\underline{\Omega}\nabla\varphi(\underline{r},\underline{\Omega},t) + \int_{4\pi} d\underline{\Omega}\,\mu_t(\underline{r},t)\varphi(\underline{r},\underline{\Omega},t) - \int_{4\pi}\int_{4\pi} d\underline{\Omega}\,\mu_s(\underline{\Omega}'\rightarrow\underline{\Omega})\varphi(\underline{r},\underline{\Omega}',t) \qquad 3.2$$

or rearranging the terms gives

$$\int_{4\pi} d\Omega S(r,\Omega,t) = \frac{1}{c'}\frac{\partial}{\partial t}\int_{4\pi} d\Omega\varphi(r,\Omega,t) + \nabla\int_{4\pi} d\Omega\Omega\varphi(r,\Omega,t) + \mu_a(r,t)\int_{4\pi} d\Omega\varphi(r,\Omega,t) - \int_{4\pi} d\Omega'\int_{4\pi} d\Omega\mu_s(\Omega'\rightarrow\Omega)\varphi(r,\Omega',t) \quad 3.3$$

Using the relations summarized in table 3.1.1 and equation 2.9, the transport equation simplifies to

$$S(r,t) = \frac{1}{c'}\frac{\partial}{\partial t}\phi(r,t) + \nabla\cdot J(r,t) + \mu_a(r,t)\phi(r,t) \quad 3.4$$

Now, according to Fick's law which is also occasionally referred to as the diffusion approximation,

$$J(r,t) = -D(r,t)\nabla\phi(r,t) \quad 3.5$$

where D(r,t) is know as the diffusion coefficient defined as,

$$D(r,t) = [3\mu_{tr}(r,t)]^{-1} \quad 3.6$$

μ_{tr} is the transport cross section, defined such that,

$$\mu_{tr}(r,t) = \mu_t(r,t) - g\mu_s(r,t) \quad 3.7$$

where g is the average cosine of the scattering angle in a photon scattering collision. Using equations 3.7, and 2.9, equation 3.6 can be rewritten as,

$$D(r,t) = [3\{\mu_a(r,t) + (1-g)\mu_s(r,t)\}]^{-1} \quad 3.8$$

It is assumed here that the differential scattering coefficient depends only on the

cosine of the angle between $\underline{\Omega}$ and $\underline{\Omega}'$. It should be noted that equation 3.5 is valid, if it is used to describe the photon flux far away from boundaries or isolated sources as it is assumed here. It is further assumed that the propagation medium is only weakly absorbing, and the photon current is changing slowly on a time scale comparable to the mean time between collisions (Duderstadt and Hamilton 1976).

Substituting equation 3.5 into equation 3.4, the time dependent photon diffusion equation is derived as

$$S(r,t) = \frac{1}{c'}\frac{\partial}{\partial t}\phi(r,t) - D(r,t)\nabla^2\phi(r,t) + \mu_a(r,t)\phi(r,t) \qquad 3.9$$

So far, the description of the interaction parameters of the propagation medium has been generalized. This is necessary in some cases. For example, the determination of the spatial dependence of the absorption and scattering coefficients may be the goal of an imaging problem, while the time dependence of these parameters may indicate metabolic response to some external stimulus (Moulton 1990). However, for simplicity in this report, it will be assumed that the medium in which the photons are propagating is uniform or homogeneous such that the diffusion and the absorption coefficients do not depend on position. Furthermore the properties of the medium are assumed to be constant in time. Then the diffusion equation simplifies to,

$$S(r,t) = \frac{1}{c'}\frac{\partial}{\partial t}\phi(r,t) - D\nabla^2\phi(r,t) + \mu_a\phi(r,t) \qquad 3.10$$

The diffusion theory is attractive because of its simplicity and because the differential equation obtained above can be solved even for complex geometries using numerical techniques. When solving this equation, it must be remembered that only photons which have been scattered at least once in the medium may satisfy the equation (Duderstadt and Hamilton 1976).

TABLE 3.1.1 For isotropic photon sources and scattering (Duderstadt and Hamilton 1976)

$$4\pi = \int_{4\pi} d\underline{\Omega}$$

$$\phi(\underline{r},t) = \int_{4\pi} \varphi(\underline{r},\underline{\Omega},t)d\underline{\Omega}$$

$$S(\underline{r},t) = \int_{4\pi} S(\underline{r},\underline{\Omega},t)d\underline{\Omega}$$

$$\mathbf{J}(\underline{r},t) = \int_{4\pi} \underline{\Omega}\varphi(\underline{r},\underline{\Omega},t)d\underline{\Omega}$$

$$\mu_s(\underline{r},t) = \int_{4\pi} \mu_s(\underline{r},\underline{\Omega}'\rightarrow\Omega,t)d\Omega$$

3.2 INITIAL AND BOUNDARY CONDITIONS.

Since the photon diffusion equation has derivatives in both space and time, one must assign suitable boundary and initial conditions to complete the specification of any problem. Since the diffusion equation itself is only an approxi-

mation to the more exact transport equation, one can use the transport theory boundary condition as a guide in the development of appropriate diffusion boundary conditions (Duderstadt and Hamilton 1976). The appropriate initial condition involves specifying the photon flux, $\phi(\underline{r},t)$, for all positions $\underline{r}$ at the initial time, t = 0. And since only a single time derivative appears in the equation, the initial condition can be chosen to be the specification of the initial value of the photon flux for all positions, i.e

$$\textit{Initial condition}: \quad \phi(\underline{r},0) = \phi_o(\underline{r}) \tag{3.11}$$

Generally, there are no photons within the volume of interest prior to irradiation. As a result the initial distribution of photons is assumed to be identically zero everywhere in the volume.

$$\phi(\underline{r},t) = 0 \qquad t < 0 \tag{3.12}$$

The presence of photon sources within the volume, V, depends on the irradiation geometry. The illumination of the surface with a temporally narrow pulse of mono-directional light may be expressed mathematically by defining $S(\underline{r},\underline{\Omega},t) = 0$ in V and incorporating the incident beam into the initial and boundary conditions so that the photon flux at ∂V is $\phi(r_{\partial V},\underline{\Omega},t)$ for all $\underline{\Omega}\cdot\underline{n} < 0$, where $\underline{n}$ is the outward normal to ∂V (Moulton 1990).

Alternatively, the initial scattering events could be written as an internal

source function,

$$S(\underline{r},\underline{\Omega},t) = f(\underline{\Omega}\cdot\underline{\Omega}_o)\delta(\underline{\Omega}_o c't+\underline{r}_o-r)\exp(-\mu_t c't) \qquad 3.13$$

where $\underline{r}_o$ is the initial position. The presence of the phase function describes the angular distribution of first scatters while the δ-function defines the temporarily narrow, mono-directional nature of the incident beam. The attenuation of the beam through scatter and absorption is described by the exponential decay (Moulton 1990).

The boundary conditions depend on the particular physical problem of interest (Duderstadt and Hamilton 1976). It has been demonstrated that a useful approach is to set the diffuse fluence rate to zero at an extrapolated boundary some distance beyond the actual surface, i.e

$$\phi(r_{\partial V}+\underline{n}r_e,t) = 0 \qquad 3.14$$

The application of this boundary condition forces the fluence rate to zero outside the volume of interest on the surface described by $(\underline{r}_{\partial V}+\underline{n}r_e)$. According to Hamilton and Duderstadt (1976), if the interface is between tissue and a non-scattering medium with the same refractive index, this extrapolated boundary is located at

$$z_e = 0.7104\lambda_{tr} = (0.7104)3D \qquad 3.15$$

where λ_{tr} is the transport mean free path. Hemenger (1977), has demonstrated that a mismatch in the index of refraction at the surface of the medium , for example, an air-tissue interface, can be accounted for by changing the position of this extrapolated boundary.

The development of such expressions for the position of the extrapolated boundary in terms of the optical properties of the medium has been pursued by many other authors (Moulton 1990). For the purposes of this report only two of the most commonly used expressions for the position of the extrapolated boundaries and the zero boundary condition will be used. Specifically, the influence of the Milne, and the Marshak extrapolated boundary conditions and the zero boundary condition developed by Patterson et al (1989), on the average residency time at a depth z of re-emitted photons will be considered. The Marshak extrapolated boundary condition incorporates an index-mismatch at the boundary, while the Milne extrapolated boundary and the zero boundary conditions are generally considered for an index-matched boundary.

Moulton (1990), has presented a detailed discussion on the exact as well as approximate boundary conditions often used in photon transport. The results, even for the relatively simple approximate boundary conditions are still complex and require further simplifications. It was demonstrated that the expression for the position of the extrapolated boundary which results from the solution of the Milne problem can be obtained when $(1-a')<<1$ as,

$$z_{e,Milne} \approx \frac{1}{\mu_s'} 0.710446[1-0.0199(1-a')^2+...] \qquad 3.16$$

where the dimensionless parameter $a' = \mu_s'/\mu_{tr}$ and is referred to as the transport albedo. The corresponding expression obtained from the Marshak problem for an index-mismatched boundary condition was shown to be,

$$z_{e,Marshak} \approx \frac{2D}{\kappa}\{1+\frac{4}{3}\frac{(D\mu_a)}{\kappa^2}+\frac{16}{5}\frac{(D\mu_a)^2}{\kappa^4}+...\} \qquad 3.17$$

where

$$\kappa = \frac{(1-R_o)(1-\mu_c^2)}{(1+R_o)+(1-R_o)\mu_c^3}, \quad R_o = (\frac{n_m-n_V}{n_m+n_V})^2, \quad \theta_c = \sin^{-1}(\frac{n_v}{n_m}) \qquad 3.18$$

and

$$\mu_c = \cos(\theta_c)$$

n_V and n_m are the refractive indices of a non-scattering medium (taken here to be equivalent to that of air, i.e, 1.0) and the medium of interest (taken here to be tissue i.e 1.4) respectively.

Patterson et al have demonstrated that, for such applications where the probe fibers are wide apart compared to the extrapolation length, the pulse shape is insensitive to the exact location of the extrapolated boundary, hence for simplicity one could ignore the extrapolation length and assume that the fluence rate vanishes on the true (physical) boundary,

$$\phi(r_{\partial V},t) = 0 \qquad 3.19$$

Application of this boundary condition forces the fluence rate to zero on the physical boundary of the volume at all times, though the true fluence rate is non-zero on this boundary (Duderstadt and Hamilton 1976).

3.3 SOLUTION OF THE DIFFUSION EQUATION.

3.3.1 THE FUNDAMENTAL SOLUTION.

Moulton (1990), has recently determined the solution of the diffusion equation in various geometries and for different boundary conditions. This was accomplished through the development of the appropriate Green's function. Using the properties of the fundamental solution, $E(\underline{r}_n,t)$, of the n-dimensional diffusion equation

$$\delta(t)\delta(\underline{r}_n) = \frac{1}{c'}\frac{\partial}{\partial t}E(\underline{r}_n,t) - D\nabla_n^2 E(\underline{r}_n,t) + \mu_a E(\underline{r}_n,t) \qquad 3.20$$

in an infinite medium such that the initial and boundary conditions are

$$E(\underline{r}_n,0) = 0$$
$$\lim_{|\underline{r}_n|\to\infty} E(\underline{r}_n,t) = 0 \qquad 3.21$$

it was demonstrated that,

$$E(\underline{r}_n,t) = 1_+(t)c'(4\pi Dc')^{-\frac{n}{2}}t^{-\frac{n}{2}}\exp(-\frac{|\underline{r}_n|^2}{4Dc't}-\mu_a c't) \qquad 3.22$$

where $1_+(t)$ is the Heaviside step function

$$1_+(t) = \begin{cases} 1 & t\geq 0 \\ 0 & t<0 \end{cases} \qquad 3.23$$

Considering only the positive times, the fundamental solution in n-dimensional spherical coordinates for an infinite medium is

$$E(\underline{r}_n,t) = c'(4\pi Dc')^{-\frac{n}{2}}t^{-\frac{n}{2}}\exp(-\frac{|\underline{r}_n|^2}{4Dc't}-\mu_a c't) \qquad 3.24$$

3.3.2 INFINITE MEDIUM.

It will be assumed that the diffuse photon fluence rate, $\phi(\underline{r},t)$, satisfies the diffusion equation given by equation 3.10. Then utilizing the fundamental solution above, the fluence rate per incident photon at $\underline{r}$ in 3-dimensional spherical coordinates for an infinite medium can be obtained as

$$\phi(\underline{r},t) = c'(4\pi Dc')^{-\frac{3}{2}}t^{-\frac{3}{2}}\exp(-\frac{|\underline{r}|^2}{4Dc't}-\mu_a c't) \qquad 3.25$$

3.3.3 SEMI-INFINITE MEDIUM.

3.3.3.1 ZERO BOUNDARY CONDITION.

The problem posed in figure 3.3.3.1.1 can be solved by using equation 3.25

and making two assumptions. The first assumption is that all the incident photons are initially isotropically scattered at a depth z_o, directly below the source fiber on the tissue surface, where z_o is actually the mean distance between scattering events and is defined as

$$z_o = [(1-g)\mu_s]^{-1} \qquad 3.26$$

so that the actual source term can be represented by the simple delta function described below.

$$S(r,t) = \delta(z-z_o)\delta(t) \qquad 3.27$$

According to Patterson et al (1989), this localization of the first interactions will not produce inaccuracies for measurements of the fluence rate made far from the source or for detection times which are long after pulse incidence. The second assumption which has already been discussed under section 3.2, is that the fluence rate should be set to zero on the physical boundary, (z = 0). As demonstrated by Patterson et al (1989), this boundary condition can be met by adding a negative or image source of photons to the infinite medium problem as shown in figure 3.3.3.1.1

The fluence rate per incident photon (units: $mm^{-2}s^{-1}$) at any point in the medium can then be written in cylindrical coordinates as the sum of contributions

Semi–Infinite Homogeneous Medium
Irradiated with a Pencil Beam.
Boundary Condition: $\varphi(r,0,t) = 0$
or $\varphi(r,0) = 0$

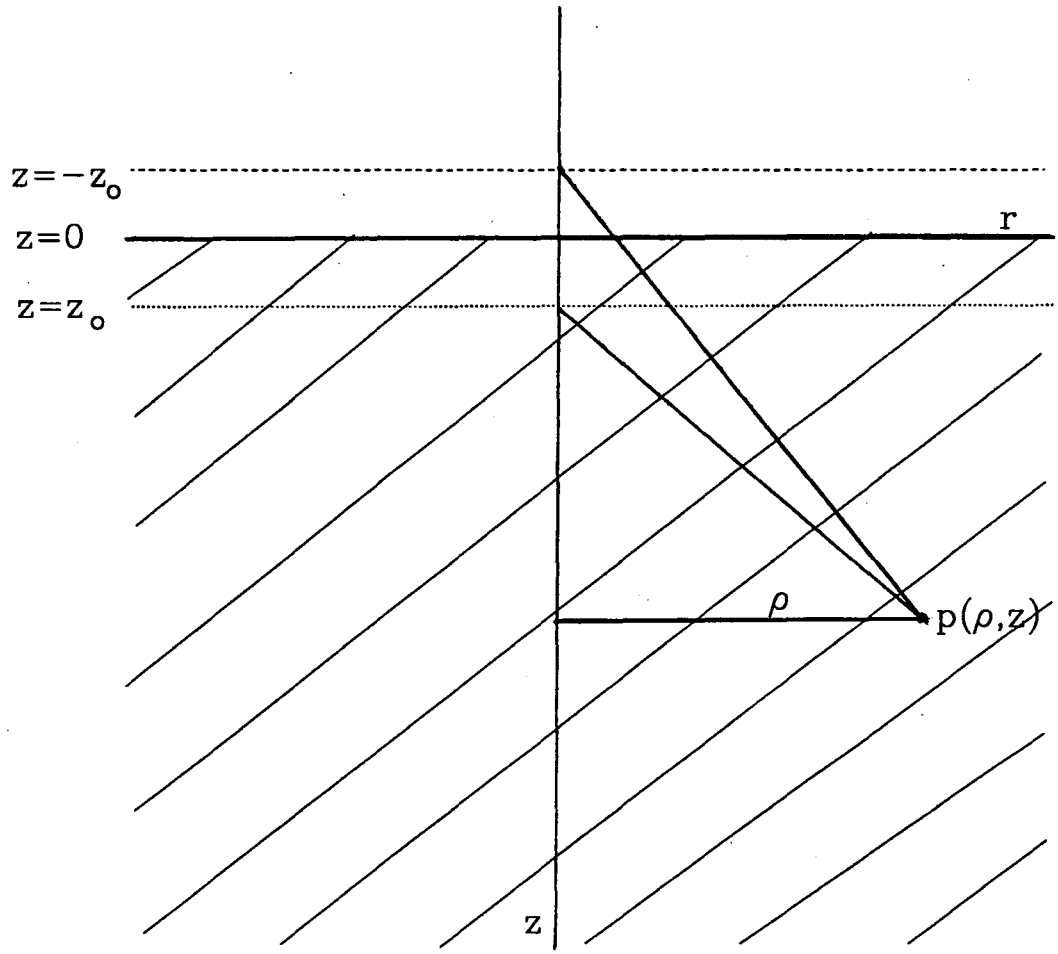

Figure 3.3.3.1.1

A collimated pencil beam normally incident upon the surface of a semi–infinite homogeneous medium. The beam is assumed to create an isotropic photon source at a depth z_o. The boundary condition is met by assuming an image source at $z = -z_o$.

from the two sources, i.e

$$\phi(\rho,z,t) = c'(4\pi Dc')^{-\frac{3}{2}} t^{-\frac{3}{2}} \exp(-\mu_a c' t)\{e^{-\frac{(z-z_o)^2+\rho^2}{4Dc't}} - e^{-\frac{(z+z_o)^2+\rho^2}{4Dc't}}\} \qquad 3.28$$

Hence the photon density per incident photon, N(ρ,z,t), (units: mm^{-3}) is easily obtained from equation 3.28 by just dropping the factor c', (see equation 2.5). i.e

$$N(\rho,z,t) = (4\pi Dc')^{-\frac{3}{2}} t^{-\frac{3}{2}} \exp(-\mu_a c' t)\{e^{-\frac{(z-z_o)^2+\rho^2}{4Dc't}} - e^{-\frac{(z+z_o)^2+\rho^2}{4Dc't}}\} \qquad 3.29$$

The number of photons reaching the surface per unit area per unit time per incident photon can be calculated from Fick's law

$$J(r,t) = -D\nabla\phi(\rho,z,t)_{|z=0} \qquad 3.30$$

which leads to the final expression for the diffuse reflectance, R(r,t) (units: $m^{-2}s^{-1}$), determined by Patterson et al (1989) for a 3-dimensional radially symmetric problem as,

$$\begin{aligned} R(r,t) &= |J(r,t)| \\ &= z_o(4\pi Dc')^{-\frac{3}{2}} t^{-\frac{5}{2}} \exp(-\mu_a c' t) e^{-\frac{r^2+z_o^2}{4Dc't}} \end{aligned} \qquad 3.31$$

3.3.3.2 EXTRAPOLATED BOUNDARY CONDITION.

The extrapolated boundary condition described by equation 3.14 for a 3-

dimensional semi-infinite geometry is

$$\phi(r,-z_e,t) = 0 \qquad 3.32$$

and the source function is as given by equation 3.27. The solution of this problem is obtained by placing an image source of photons at $z = -z_p$ where $z_p = z_o+2z_e$ as shown in figure 3.3.3.2.1. Utilizing the solution for the infinite medium problem, the assumption that the fluence rate vanishes on the surface $z = -z_e$, and that all the incident photons are initially isotropically scattered at z_o, the fluence rate per incident photon at any point in the medium can be written in cylindrical coordinates as,

$$\phi(\rho,z,t) = c'(4\pi Dc')^{-\frac{3}{2}} t^{-\frac{3}{2}} \exp(-\mu_a c' t)\{e^{-\frac{(z-z_o)^2+\rho^2}{4Dc't}} - e^{-\frac{(z+z_p)^2+\rho^2}{4Dc't}}\} \qquad 3.33$$

hence the photon density per incident photon becomes,

$$N(\rho,z,t) = (4\pi Dc')^{-\frac{3}{2}} t^{-\frac{3}{2}} \exp(-\mu_a c' t)\{e^{-\frac{(z-z_o)^2+\rho^2}{4Dc't}} - e^{-\frac{(z+z_p)^2+\rho^2}{4Dc't}}\} \qquad 3.34$$

The diffuse reflectance per unit area per unit time per incident photon is determined from Fick's law by Moulton (1990) for a radially symmetric 3-dimensional geometry as,

Semi–Infinite Homogeneous Medium Irradiated with a Pencil Beam.
Boundary Condition: $\varphi(r,-z_e,t) = 0$
or $\varphi(r,-z_e) = 0$

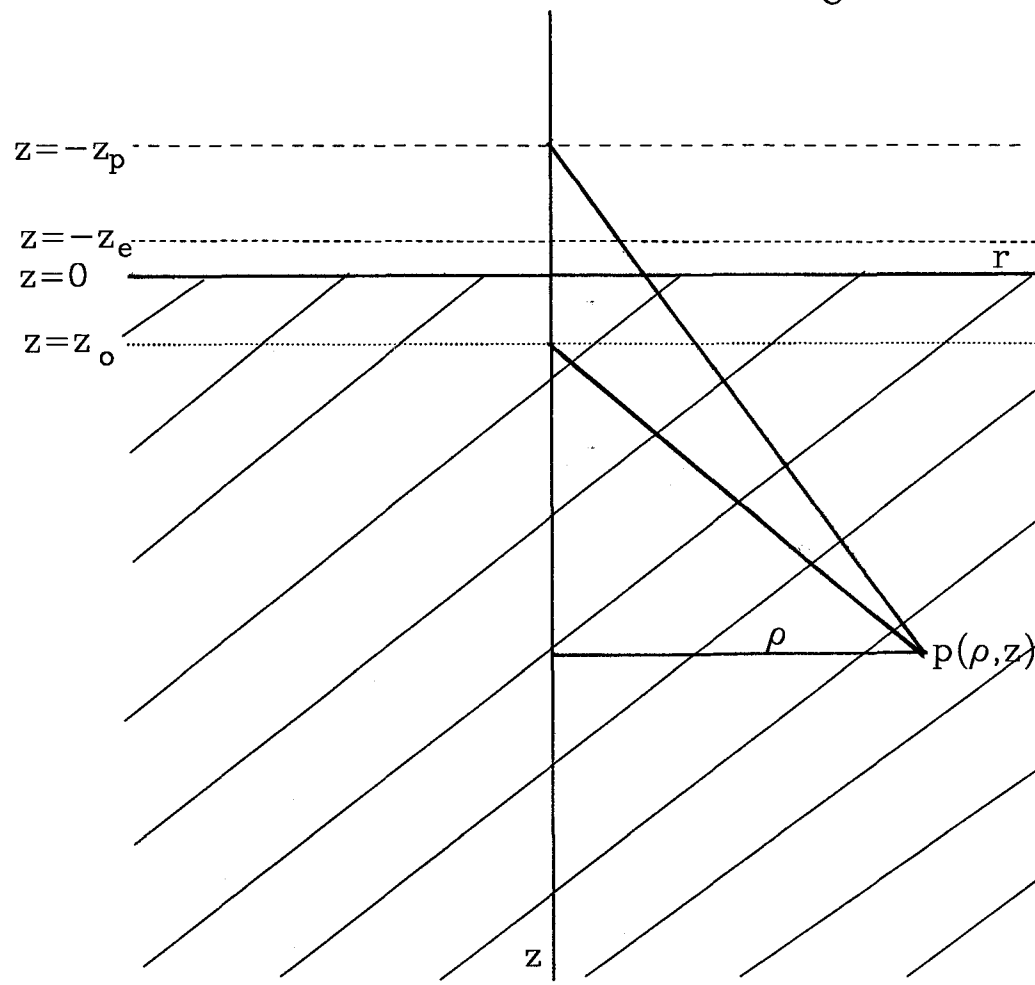

Figure 3.3.3.2.1

A collimated pencil beam normally incident upon the surface of a semi–infinite homogeneous medium. The beam is assumed to create an isotropic photon source at a depth z_o. The boundary condition is met by assuming an image source at $z = -z_p$, $(z_p = z_o + 2z_e)$.

$$R(r,t) = \frac{1}{2}(4\pi Dc')^{-\frac{3}{2}} t^{-\frac{5}{2}} \exp(-\mu_a c' t)\{z_o e^{-\frac{r^2+z_o^2}{4Dc't}} + z_p e^{-\frac{r^2+z_p^2}{4Dc't}}\} \qquad 3.35$$

3.4 STATISTICS OF THE RESIDENCY TIME OF RE-EMITTED PHOTONS.

3.4.1 PULSE STATE.

3.4.1.1 SEMI-INFINITE MEDIUM.

3.4.1.1.1 ZERO BOUNDARY CONDITION.

Assume N_p photons enter the tissue (see figure 3.4.1.1.1.1) at time t = 0 ps. The number of photons that will leave the tissue surface through dA about $\underline{r}$ in a time interval dt at time t is

$$N_p R(r,t)\,dA\,dt$$

where R(r,t) is the photon diffuse reflectance given by equation 3.31. The total time (pico-seconds, ps) spent by these photons in the tissue before they exit through dA at ($\underline{r}$,t) is

$$tN_p R(r,t)\,dA\,dt$$

To determine what fraction of this total time is spent in an elemental volume dV about some arbitrary location $\underline{r}'$ in the medium, consider a time interval dt' at time t' during the propagation of the photons in the tissue. Then the number

of photons in dV during this time interval is

$$N_p N(\rho,z,t')dV$$

where N(ρ,z,t') is the probability of finding a photon in the vicinity of $\underline{r}'$ at time t' after entry into the tissue (i.e the photon density per incident photon). And it is obtained from equation 3.29 as

$$N(\rho,z,t') = (4\pi Dc')^{-\frac{3}{2}} t'^{-\frac{3}{2}} \exp(-\mu_a c' t') \{ e^{-\frac{(z-z_o)^2+\rho^2}{4Dc't'}} - e^{-\frac{(z+z_o)^2+\rho^2}{4Dc't'}} \} \quad 3.36$$

The probability that a photon which is in dV in the tissue at ($\underline{r}'$,t') will escape through dA on the tissue surface at ($\underline{r}$-$\underline{r}'$,t-t') thereafter, is the so called escape function (units: $mm^{-2}ps^{-1}$), which from equation 3.31 and the geometry of the problem in figure 3.4.1.1.1.1 is obtained as,

$$E(r,z,t,\rho,\theta,t') = z_o(4\pi Dc')^{-\frac{3}{2}} (t-t')^{-\frac{5}{2}} e^{-\mu_a c'(t-t')} e^{-\frac{r^2+z^2+\rho^2-2r\rho\cos(\theta)}{4Dc'(t-t')}} \quad 3.37$$

Thus, the joint probability of a photon escaping from the tissue in the vicinity of $\underline{r}$ after a time t through dA on the tissue surface having been in dV in the tissue in the vicinity of $\underline{r}'$ at time t' after entry into the tissue will be

$$N_p N(\rho,z,t')dVE(r,z,t,\rho,\theta,t')dAdt$$

Photons that reach dV in the vicinity of $\underline{r}'$ at time t' will have different paths in the tissue because some photons enter the medium and are immediately

Semi-Infinite Homogeneous Medium
Irradiated with a Pencil Beam.
Boundary Condition: $\varphi(r,0,t) = 0$
or $\varphi(r,0) = 0$

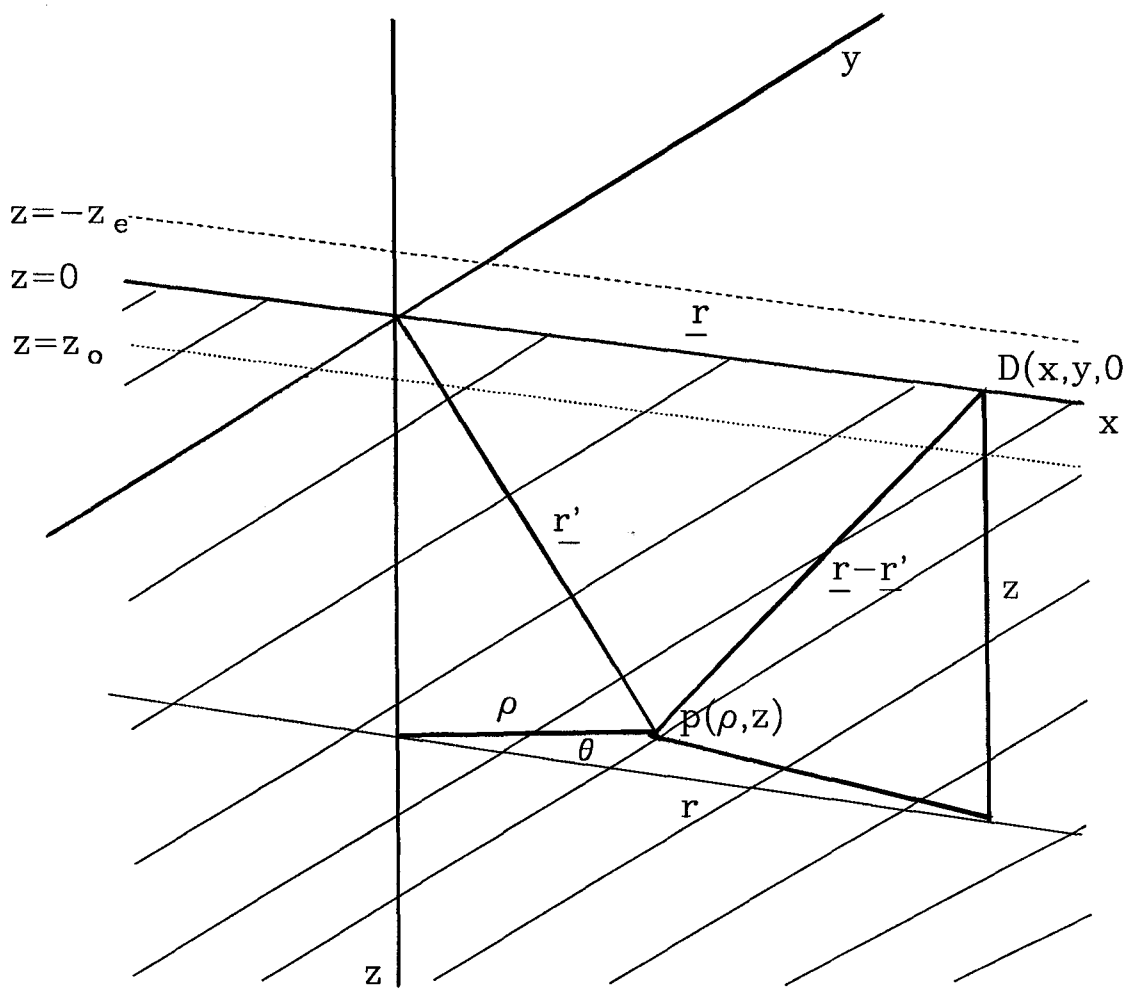

Figure 3.4.1.1.1

A geometrical presentation of the model being analyzed. Photons enter the medium at 0(0,0,0) at t=0. A detector positioned at D(x,y,0) measures the reflectance as a function of r (steady state) or r and t (pulse state). The boundary condition is $\varphi(r,0,t)=0$ or $\varphi(r,0)=0$.

scattered into dV while others wander through the tissue for some time before they reach dV. We must consider all possible times t', that contribute to the time the photons spend in dV in the tissue at ($\underline{r}'$,t') and still escape at ($\underline{r}$,t) through dA on the irradiated surface. This can easily be calculated by taking the time integral of the expression above, i.e,

$$dT(r,z,t,\rho,\theta) = N_p dV dA dt \int_{\frac{|\underline{r}'|}{c'}}^{t-\frac{|\underline{r}-\underline{r}'|}{c'}} N(\rho,z,t')E(r,z,t,\rho,\theta,t')dt' \qquad 3.38$$

The lower limit of the integration is the time for a direct flight of a photon from the point of incidence to dV (i.e the shortest time a photon will take to reach dV), and the upper limit is the maximum time taken by an incident photon to eventually reach dV after wandering through the tissue and still escape at $\underline{r}$. Substituting for N(ρ,z,t') and E(r,z,t,ρ,θ,t'), the residency time dT(r,z,t,ρ,θ) (in picoseconds) of re-emitted photons at (z,ρ) and source-detector distance r is obtained as

$$dT(r,z,t,\rho,\theta) = N_p dV dA dt \int_{LL}^{UL} K_1 t'^{-\frac{3}{2}}(t-t')^{-\frac{5}{2}} e^{-\frac{r^2+z^2+\rho^2-2r\rho\cos(\theta)}{4Dc'(t-t')}} \times \exp(-\mu_a c' t')\left(e^{-\frac{(z-z_0)^2+\rho^2}{4Dc't'}} - e^{-\frac{(z+z_0)^2+\rho^2}{4Dc't'}}\right)dt' \qquad 3.39$$

where

$$LL = \frac{(z^2+\rho^2)^{\frac{1}{2}}}{c'}, \qquad UL = t-\frac{[r^2+z^2+\rho^2-2r\rho\cos(\theta)]^{\frac{1}{2}}}{c'} \qquad 3.40$$

and

$$K_1 = z_o(4\pi Dc')^{-3}$$

which can be evaluated numerically. The residency time at depth z is critical to interpreting data in a situation in which the measured property (e.g micro-circulatory blood flow) is not uniform with depth in the tissue (Weiss et al 1989). It should be noted that the entire expression has units of time, as it should, since it represents the total time spent by N_p photons in an elemental volume dV in the medium before re-emitting at the tissue surface. The integrand itself has units of mm^{-5} and will be represented by $L(r,z,t,\rho,\theta)$, i.e

$$L(r,z,t,\rho,\theta) = \int_{LL}^{UL} K_1 t'^{-\frac{3}{2}}(t-t')^{-\frac{5}{2}} e^{-\mu_a c' t} e^{-\frac{r^2+z^2+\rho^2-2r\rho\cos(\theta)}{4Dc'(t-t')}} \{e^{-\frac{(z-z_o)^2+\rho^2}{4Dc't'}} - e^{-\frac{(z+z_o)^2+\rho^2}{4Dc't'}}\}dt' \qquad 3.41$$

Notice that the volume integral of $dT(r,z,t,\rho,\theta)$ should just be equal to the total time spent by the photons in the medium before they exit, i.e,

$$N_p dAdt\int_V L(r,z,t,\rho,\theta)d^3r' = tN_p R(r,t)dAdt \qquad 3.42$$

or

$$\int_V L(r,z,t,\rho,\theta)d^3r' = tR(r,t) \qquad 3.43$$

Suppose, instead of calculating the absolute amount of time photons spent in dV one is interested in calculating the relative amount of time spent by these photons in the volume element. This would just be the normalised form of the residency time in the volume element, $dT_n(r,z,t,\rho,\theta)$. From equations 3.39, and the expression for the total time photons spent in the medium it can easily be shown to be,

$$dT_n(r,z,t,\rho,\theta) = \frac{N_p dV dA dt \int_{LL}^{UL} K_1 t'^{-\frac{3}{2}}(t-t')^{-\frac{5}{2}} e^{-\mu_a c' t} e^{-\frac{r^2+z^2+\rho^2-2r\rho\cos(\theta)}{4Dc'(t-t')}} \times \{e^{-\frac{(z-z_o)^2+\rho^2}{4Dc't'}} - e^{-\frac{(z+z_o)^2+\rho^2}{4Dc't'}}\}dt'}{tN_p dA dt(4\pi Dc')^{-\frac{3}{2}} t^{-\frac{5}{2}} z_o \exp(-\mu_a c' t) e^{-\frac{r^2+z^2}{4Dc't}}} \qquad 3.44$$

or

$$dT_n(r,z,t,\rho,\theta) = \frac{dV \int_{LL}^{UL} K_1 t'^{-\frac{3}{2}}(t-t')^{-\frac{5}{2}} e^{-\mu_a c' t} e^{-\frac{r^2+z^2+\rho^2-2r\rho\cos(\theta)}{4Dc'(t-t')}} \times \{e^{-\frac{(z-z_o)^2+\rho^2}{4Dc't'}} - e^{-\frac{(z+z_o)^2+\rho^2}{4Dc't'}}\}dt'}{t(4\pi Dc')^{-\frac{3}{2}} t^{-\frac{5}{2}} z_o \exp(-\mu_a c' t) e^{-\frac{r^2+z_o^2}{4Dc't}}} \qquad 3.45$$

$dT_n(r,z,t,\rho,\theta)$ is unitless as it should, since it represents the relative amount of

time a photon spent in dV before escaping at the surface. Notice that the normalization was to the total time photons spent in the medium before they escape at ($\underline{r}$,t).

3.4.1.1.2 EXTRAPOLATED BOUNDARY.

The escape function is obtained from equation 3.35 and the geometry of figure 3.4.1.1.2.1 as

$$E(r,z,t,\rho,\theta,t') = \frac{1}{2}(4\pi Dc')^{-\frac{3}{2}}(t-t')^{-\frac{5}{2}}e^{-\mu_a c'(t-t')}\{z_o e^{-\frac{r^2+z^2+\rho^2-2r\rho\cos(\theta)}{4Dc'(t-t')}} + z_p e^{-\frac{r^2+z^2+\rho^2-2r\rho\cos(\theta)}{4Dc'(t-t')}}\} \quad 3.46$$

and the probability of finding a photon in dV in the vicinity of $\underline{r}'$ at time t' after entry into the tissue (i.e the photon density per incident photon) is obtained from equation 3.34 by substituting t by t'. i.e

$$N(\rho,z,t') = (4\pi Dc')^{-\frac{3}{2}}t'^{-\frac{3}{2}}\exp(-\mu_a c't')\{e^{-\frac{(z-z_o)^2+\rho^2}{4Dc't'}} - e^{-\frac{(z+z_p)^2+\rho^2}{4Dc't'}}\} \quad 3.47$$

Utilizing the same discussion under section 3.4.1.1.1, for the zero boundary condition, the total time dT(r,z,t,ρ,θ), spent by N_p photons in an elemental volume dV in the tissue, assuming the fluence rate is set to zero on the extrapolated boundary z = $-z_e$, becomes

Semi–Infinite Homogeneous Medium
Irradiated with a Pencil Beam.
Boundary Condition: $\varphi(r,-z_e,t) = 0$
or $\varphi(r,-z_e) = 0$

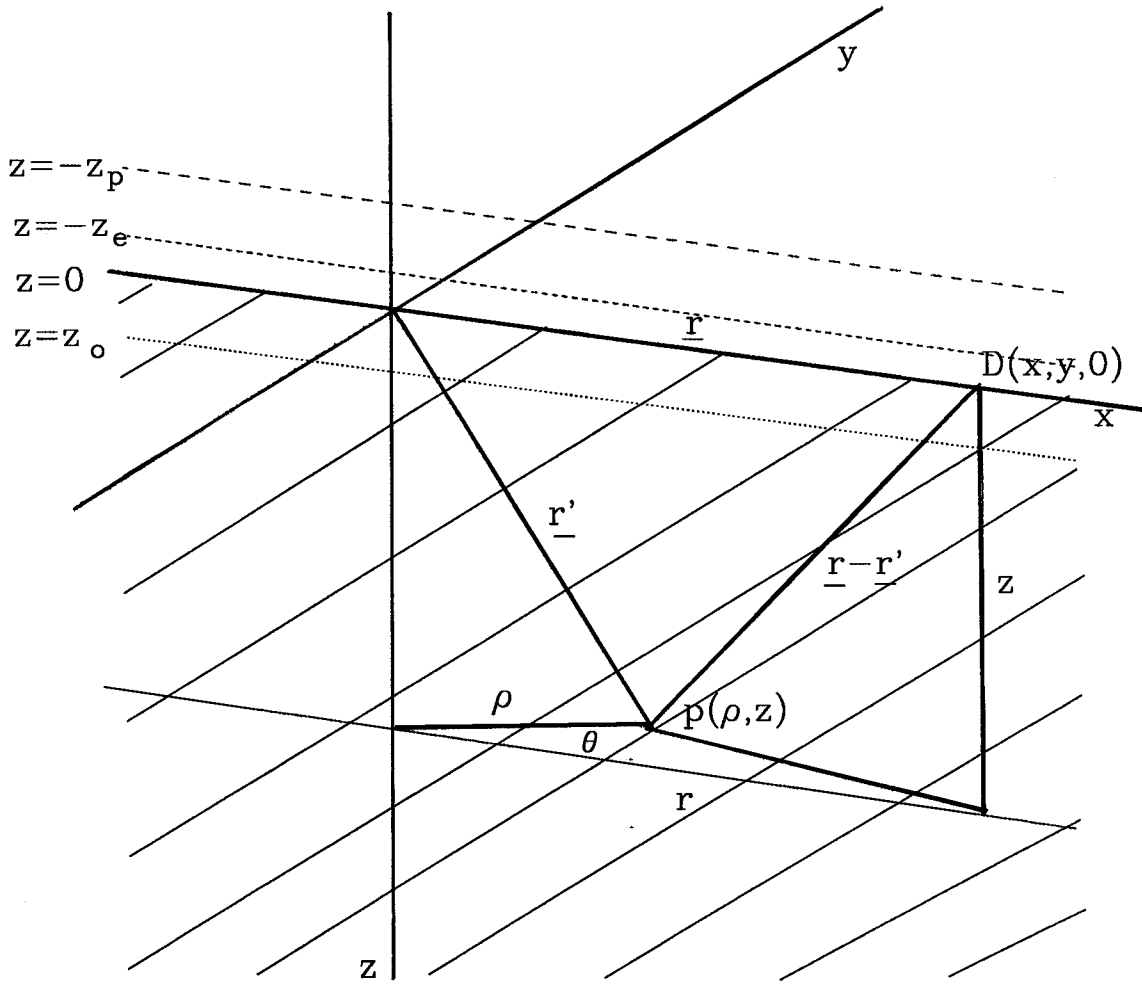

Figure 3.4.1.1.2.1

A geometrical presentation of the model being analyzed. Photons enter the medium at O(0,0,0) at t=0. A detector positioned at D(x,y,0) measures the reflectance as a function of r (steady state) or r and t (pulse state). The boundary condition is $\varphi(r,-z_e,t)=0$ or $\varphi(r,-z_e)=0$.

$$dT(r,z,t,\rho,\theta) = \frac{1}{2}N_p dV dA dt \int_{LL}^{UL} K_2 t'^{-\frac{3}{2}}(t-t')^{-\frac{5}{2}}\{z_o e^{-\frac{r^2+z^2+\rho^2-2r\rho\cos(\theta)}{4Dc'(t-t')}} + z_p e^{-\frac{r^2+z^2+\rho^2-2r\rho\cos(\theta)}{4Dc'(t-t')}}\}\{e^{-\frac{(z-z_o)^2+\rho^2}{4Dc't'}} - e^{-\frac{(z+z_p)^2+\rho^2}{4Dc't'}}\}e^{-\mu_a c' t} dt' \quad 3.48$$

where

$$K_2 = (4\pi Dc')^{-3}$$

and L(r,z,t,ρ,θ) is therefore given as

$$L(r,z,t,\rho,\theta) = \frac{1}{2}\int_{LL}^{UL} K_2 t'^{-\frac{3}{2}}(t-t')^{-\frac{5}{2}} e^{-\mu_a c' t}\{z_o e^{-\frac{r^2+z^2+\rho^2-2r\rho\cos(\theta)}{4Dc'(t-t')}} + z_p e^{-\frac{r^2+z^2+\rho^2-2r\rho\cos(\theta)}{4Dc'(t-t')}}\}\{e^{-\frac{(z-z_o)^2+\rho^2}{4Dc't'}} - e^{-\frac{(z+z_p)^2+\rho^2}{4Dc't'}}\}dt' \quad 3.49$$

The normalized (to the total time spent by photons in the medium) version of equation 3.48 is

$$dT_n(r,z,t,\rho,\theta) = \frac{dV\int_{LL}^{UL} K_2 t'^{-\frac{3}{2}}(t-t')^{-\frac{5}{2}} e^{-\mu_a c' t}\{z_o e^{-\frac{r^2+z^2+\rho^2-2r\rho\cos(\theta)}{4Dc'(t-t')}} + z_p e^{-\frac{r^2+z^2+\rho^2-2r\rho\cos(\theta)}{4Dc'(t-t')}}\}\{e^{-\frac{(z-z_o)^2+\rho^2}{4Dc't'}} - e^{-\frac{(z+z_p)^2+\rho^2}{4Dc't'}}\}dt'}{t(4\pi Dc')^{-\frac{3}{2}} t^{-\frac{5}{2}} \exp(-\mu_a c' t)\{z_o e^{-\frac{r^2+z_o^2}{4Dc't}} + z_p e^{-\frac{r^2+z_p^2}{4Dc't}}\}} \quad 3.50$$

3.4.1.2 INFINITE MEDIUM.

The problem analyzed in this report can also be solved for a point source and a point detector situated in an infinite medium.

Similar to the reflectance problem for a semi-infinite medium already discussed, assume N_p photons are emitted from a point source situated in an infinite medium at S(0,0) at time t = 0 ps, (figure 3.4.1.2.1). The photon density in dV at $\underline{r}$ at any time t thereafter can easily be determined. Given that a photon is in dV at $\underline{r}$ at time t, to determine how much time it has spent in dV′ about some arbitrary location $\underline{r}_1$ in the medium, consider a time interval dt′ at time t′ after being emitted from the source in the medium. Then the number of photons in dV′ at $\underline{r}_1$ during this time interval is

$$N_p N(x,y,t')dV'$$

where N(x,y,t′) is obtained from equation 3.25 as

$$N(x,y,t') = (4\pi Dc')^{-\frac{3}{2}} t'^{-\frac{3}{2}} \exp(-\mu_a c' t') e^{-\frac{x^2+y^2}{4Dc't'}} \qquad 3.51$$

The probability that a photon which is in dV′ at ($\underline{r}_1$,t′) will be in dV at ($\underline{r}_2$,t-t′) thereafter is just

$$N(r-x,y,t-t')dV$$

where

$$N(r-x,y,t-t') = (4\pi Dc')^{-\frac{3}{2}} (t-t')^{-\frac{3}{2}} e^{-\mu_a c'(t-t')} e^{-\frac{(r-x)^2+y^2}{4Dc'(t-t')}} \qquad 3.52$$

Therefore, the combined probability of detecting a photon in dV at ($\underline{r}$,t) having

Infinite Homogeneous Medium with a Point Source and Point Detector.

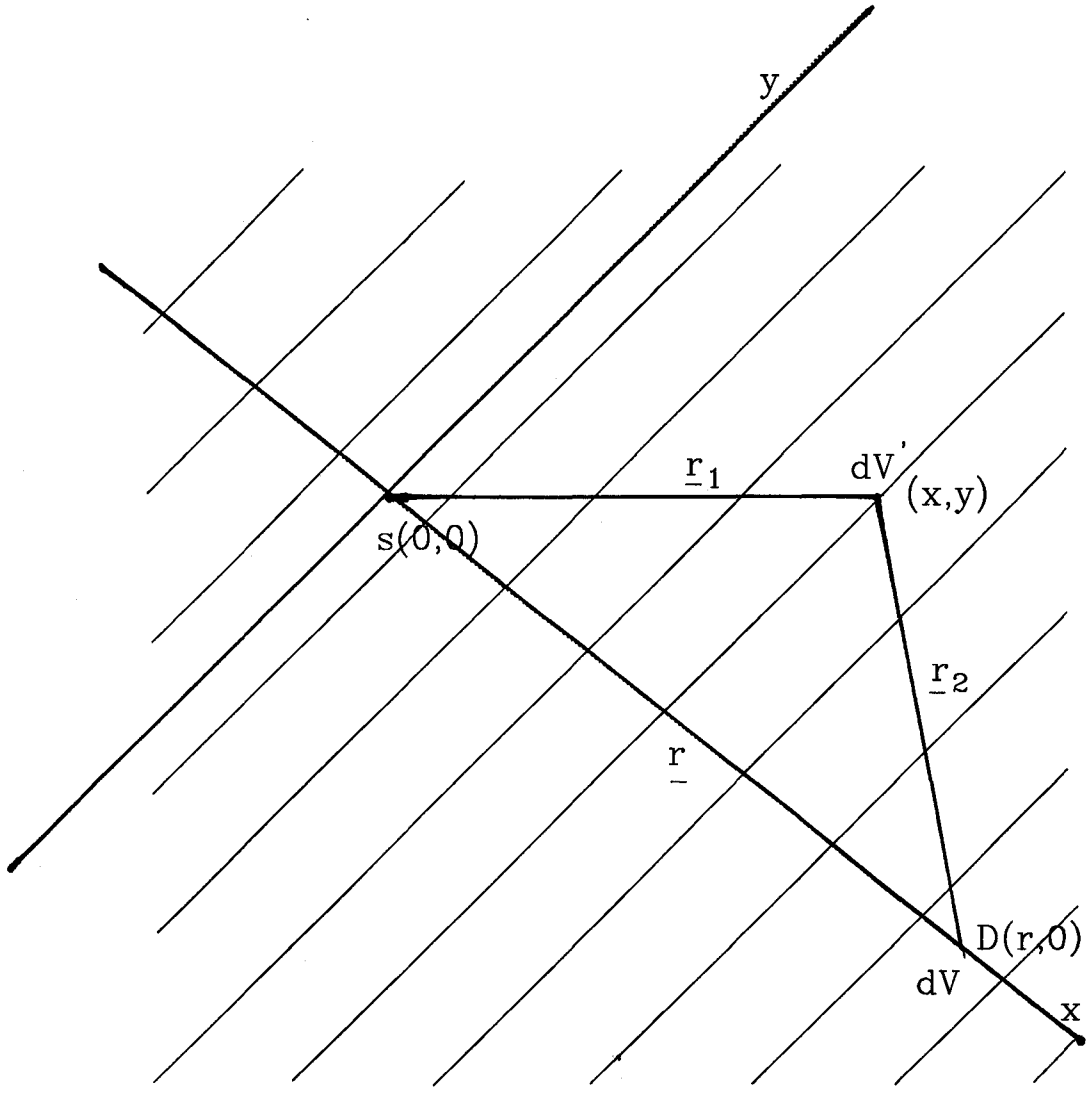

Figure 3.4.1.2.1

An isotropic point source of photons is positioned in an infinite homogeneous medium at s(0,0). A point detector situated at D(r,0) measures the number of photons reaching dV as a function of r (steady state) or r and t (pulse state). Calculated values are symmetrical about the line y = 0.

been in dV′ at ($\underline{r}_1$,t′) after emission from the source is

$$N_p N(x,y,t')dV'dt'N(r-x,y,t-t')dV$$

Considering all possible times t′ that contribute to this time function, the residency time dT(r,x,y) of a photon in dV′ at ($\underline{r}$,t′) that was detected in dV at ($\underline{r}$,t) is

$$dT(r,x,y,t) = N_p dV'dV \int_{\frac{|r_1|}{c'}}^{t-\frac{|r_2|}{c'}} N(x,y,t')N(r-x,y,t-t',)dt' \qquad 3.53$$

substituting for N(x,y,t′) and N(r-x,y,t-t′), the residency time in dV′ of a photon detected in dV becomes

$$dT(r,x,y,t) = N_p dV'dV \int_{\frac{|r_1|}{c'}}^{t-\frac{|r_2|}{c'}} K_2 t'^{-\frac{3}{2}}(t-t')^{-\frac{3}{2}} e^{-\mu_a c't} e^{-\frac{x^2+y^2}{4Dc't'}} e^{-\frac{(r-x)^2+y^2}{4Dc'(t-t')}} dt' \qquad 3.54$$

where

$$K_2 = (4\pi Dc')^{-3}, \quad |\underline{r}_1| = (x^2+y^2)^{\frac{1}{2}} \quad \textit{and} \quad |\underline{r}_2| = [(r-x)^2+y^2]^{\frac{1}{2}}$$

As expected once again, the entire expression has units of time. And as usual we will represent the integrand by L(r,x,y,t), i.e

$$L(r,x,y,t') = \int_{\frac{(x^2+y^2)^{\frac{1}{2}}}{c'}}^{t-\frac{[(r-x)^2+y^2]^{\frac{1}{2}}}{c'}} K_2 t'^{-\frac{3}{2}}(t-t')^{-\frac{3}{2}} e^{-\mu_a c' t} e^{-\frac{x^2+y^2}{4Dc't'}} e^{-\frac{(r-x)^2+y^2}{4Dc'(t-t')}} dt' \qquad 3.55$$

3.4.2 STEADY STATE.

The discussion so far has been concerned with the relation between time-resolved reflectance to the photon residency time distribution in tissue. One can easily proceed to the solution of the steady state problem. Two methods are proposed: The first method is simply the time integral of the time-resolved problem. The second method is based on the diffusion approximation to the steady state radiative transfer equation. The first method is expensive in computation time. On the other hand, the second method gave relatively quick results, and hence was used to determine most of the results in the steady state method.

3.4.2.1 PHOTON RESIDENCY TIME FROM THE TIME INTEGRAL OF THE TIME-RESOLVED PROBLEM.

3.4.2.1.1 SEMI-INFINITE MEDIUM.

3.4.2.1.1.1 ZERO BOUNDARY CONDITION.

The total number of photons that exit at r through dA (figure 3.4.1.1.1.1) in the steady state, i.e assuming a continuous irradiation of photons on the tissue

surface is

$$N_p dA \int_0^\infty R(r,t)\,dt$$

where R(r,t) is given by equation 3.31. The total time spent by the photons in the medium before they exit through dA at $\underline{r}$ is

$$N_p dA \int_0^\infty tR(r,t)\,dt$$

The total amount of this time spent in dV in the vicinity of $\underline{r}'$ in the tissue, $dT(r,z,\rho,\theta)$, is just

$$dT(r,z,\rho,\theta) = \int_0^\infty dT(r,z,t,\rho,\theta)\,dt = N_p dV dA \int_0^\infty L(r,z,t,\rho,\theta)\,dt \qquad 3.56$$

If equation 3.56 is normalized to the total time spent by the photons in the medium before they exit through dA about $\underline{r}$ on the tissue surface, one would obtain the normalized form of the residency time, $dT_n(r,z,\rho,\theta)$, in the steady state as

$$dT_n(r,z,\rho,\theta) = \frac{N_p dV dA \int_0^\infty L(r,z,t,\rho,\theta)\,dt}{N_p dA \int_0^\infty tR(r,t)\,dt} \qquad 3.57$$

or

$$dT_n(r,z,\rho,\theta) = \frac{dV\int_0^{\infty} L(r,z,t,\rho,\theta)dt}{\int_0^{\infty} tR(r,t)dt} \qquad 3.58$$

$L(r,z,t,\rho,\theta)$ is given by equation 3.41. Substituting for $L(r,z,t,\rho,\theta)$ and $R(r,t)$ equation 3.58 becomes

$$dT_n(r,z,\rho,\theta) = \frac{dV\int_0^{\infty}[\int_{LL}^{UL} K_1 t'^{-\frac{3}{2}}(t-t')^{-\frac{5}{2}} e^{-\mu_a c' t} e^{-\frac{r^2+z^2+\rho^2-2r\rho\cos(\theta)}{4Dc'(t-t')}} \times \{e^{-\frac{(z-z_o)^2+\rho^2}{4Dc't'}} - e^{-\frac{(z+z_o)^2+\rho^2}{4D't'}}\}dt']dt}{\int_0^{\infty} t(4\pi Dc')^{-\frac{3}{2}} t^{-\frac{5}{2}} z_o \exp(-\mu_a c' t) e^{-\frac{r^2+z_o^2}{4Dc't}} dt} \qquad 3.59$$

Equation 5.59 above is just the time integral of the time-resolved problem, i.e the time integral of equation 3.45.

3.4.2.1.1.2 EXTRAPOLATED BOUNDARY CONDITION.

The influence of extrapolated boundary conditions on the residency time in the steady state technique can be determined. Substituting for $L(r,z,t,\rho,\theta)$ using equation 3.49 and $R(r,t)$ from equation 3.35 in equation 3.58, the residency time incorporating extrapolated boundary conditions is obtained as

$$dT_n(r,z,\rho,\theta)=\frac{dV\int_0^{\infty}[\int_{LL}^{UL} K_2 t'^{-\frac{3}{2}}(t-t')^{-\frac{5}{2}} e^{-\mu_a c' t}\{z_o e^{-\frac{r^2+z^2+\rho^2-2r\rho\cos(\theta)}{4Dc'(t-t')}} + z_p e^{-\frac{r^2+z^2+\rho^2-2r\rho\cos(\theta)}{4Dc'(t-t')}}\}\{e^{-\frac{(z-z_o)^2+\rho^2}{4Dc't'}} - e^{-\frac{(z+z_p)^2+\rho^2}{4Dc't'}}\}dt']dt}{\int_0^{\infty} t(4\pi Dc')^{-\frac{3}{2}} t^{-\frac{5}{2}} \exp(-\mu_a c' t)\{z_o e^{-\frac{r^2+z_o^2}{4Dc't}} + z_p e^{-\frac{r^2+z_p^2}{4Dc't}}\}dt} \quad 3.60$$

The equation above is the time integral of equation 3.50.

3.4.2.1.2 INFINITE MEDIUM.

In a similar way the total amount of time spent in dV′ in the steady state, dT(r,x,y), about some arbitrary location $\underline{r}_1$ in an infinite medium (figure 3.4.1.2.1) before being detected in an elemental volume dV at $\underline{r}_2$ thereafter in the medium is

$$dT(r,x,y) = \int_0^{\infty} dT(r,x,y,t)dt = N_p dV' dV \int_0^{\infty} L(r,x,y,t)dt \quad 3.61$$

where L(r,x,y,t) is given by equation 3.55. Substituting for L(r,x,y,t), dT(r,x,y) becomes

$$dT(r,x,y)=N_p dV dV' \int_0^{\infty}[\int_{\frac{|r_1|}{c'}}^{t-\frac{|r_2|}{c'}} K_2 t'^{-\frac{3}{2}}(t-t')^{-\frac{3}{2}} e^{-\mu_a c' t} e^{-\frac{x^2+y^2}{4Dc't'}} e^{-\frac{(r-x)^2+y^2}{4Dc'(t-t')}} dt']dt$$

Equation 3.62 above is the time integral of equation 3.54. And the integrand is

represented by L(r,x,y)

$$L(r,x,y) = \int_0^{\infty}\left[\int_{\frac{|r_1|}{c'}}^{t-\frac{|r_2|}{c'}} K_2 t'^{-\frac{3}{2}}(t-t')^{-\frac{3}{2}}\exp(-\mu_a c' t')\,\theta^{-\frac{x^2+y^2}{4Dc't'}}\,\theta^{-\frac{(r-x)^2+y^2}{4Dc'(t-t')}}dt'\right]dt \quad 3.63$$

3.4.2.2 PHOTON RESIDENCY TIME FROM THE STEADY STATE TRANSFER EQUATION.

During the derivation of the time dependent diffusion equation (equation 3.10), the energy dependence of the transport equation was eliminated, the medium was assumed to be homogeneous, properties of the medium were assumed to be constant in time and scattering was assumed isotropic in the interest of simplifying the model. Attention can now be turned to the remaining time and spatial variables. Let the time variable be completely eliminated by considering only steady state transport problems. Then equation 3.10 simplifies to

$$-D\nabla^2\phi(\underline{r}) + \mu_a\phi(\underline{r}) = S(\underline{r}) \quad 3.64$$

This is the diffusion approximation to the steady state radiative transfer equation for a homogeneous medium (Duderstadt and Hamilton 1976). The solution of this differential equation for $S(\underline{r}) = \delta(\underline{r})$, for the photon fluence far enough from the source is (Patterson et al 1989)

$$\phi(r) = \frac{e^{-\mu_{eff} r}}{4\pi D r} \qquad 3.65$$

where

$$\mu_{eff} = \{3\mu_a[\mu_a + (1-g)\mu_s]\}^{\frac{1}{2}} \qquad 3.66$$

is the effective attenuation coefficient (units: mm^{-1}).

For the case of point source in a semi-infinite medium, the fluence (units: mm^{-2}) per incident photon (see figure 3.4.1.1.1.1) about $\underline{r}'$ in the tissue for a zero boundary condition is therefore written as the sum of the contributions from the two sources:

$$\phi(z,\rho) = \frac{1}{4\pi D}\left[\frac{\exp\{-\mu_{eff}[(z-z_o)^2+\rho^2]^{\frac{1}{2}}\}}{[(z-z_o)^2+\rho^2]^{\frac{1}{2}}} - \frac{\exp\{-\mu_{eff}[(z+z_o)^2+\rho^2]^{\frac{1}{2}}\}}{[(z+z_o)^2+\rho^2]^{\frac{1}{2}}}\right] \qquad 3.67$$

The reflectance (units: mm^{-2}) at a distance, r, from the point of incidence has been shown by Patterson et al (1989) to be

$$R(r) = |-D\nabla\phi(r,z,\rho)|_{z=0} = \frac{z_o}{2\pi}\frac{\exp[-\mu_{eff}(r^2+z_o^2)^{\frac{1}{2}}]}{r^2+z_o^2}\left[\mu_{eff} + \frac{1}{(r^2+z_o^2)^{\frac{1}{2}}}\right] \qquad 3.68$$

The photon escape function (units: mm^{-2}) is easily derived from equation 3.68 and the geometry of figure 3.4.1.1.1.1 as

$$E(r,z,\rho,\theta) = \frac{z_o}{2\pi}\frac{\exp[-\mu_{eff}|\underline{r}-\underline{r}'|]}{|\underline{r}-\underline{r}'|^2}[\mu_{eff}+\frac{1}{|\underline{r}-\underline{r}'|}] \qquad 3.69$$

where

$$|\underline{r}-\underline{r}'| = \{r^2+z^2+\rho^2-2r\rho\cos(\theta)\}^{\frac{1}{2}}$$

The adequacy of the integrations which were performed numerically by the computer can now be tested by comparing the results of the residency time obtained from the time integral of the time-resolved problem to that obtained from the diffusion approximation to the steady state radiative transfer equation.

It has been shown from the time integral of the time-resolved problem that, the total time spent by N_p photons in an elemental tissue volume dV in the vicinity of $\underline{r}'$ in the steady state is

$$N_p dV dA \int_0^\infty L(r,z,t,\rho,\theta)dt$$

where $L(r,z,t,\rho,\theta)$ is given by equation 3.41 or 3.49. If an absorber of volume dV and extra absorption $\Delta\mu_a$ is assumed to be located at $\underline{r}'$ in the tissue, then the number of photons that will escape the tissue at $\underline{r}$ through dA will be reduced by

$$N_p dV dA \Delta\mu_a c' \int_0^\infty L(r,z,t,\rho,\theta)dt$$

Using the diffusion approximation to the steady state radiative transfer equation

approach, it can be shown that, the absorber will reduce the signal leaving the tissue at $\underline{r}$ by

$$N_p dV \Delta \mu_a \phi(z,\rho) E(r,z,\rho,\theta) dA$$

Comparing the two expressions above we should have

$$N_p dV dA \Delta \mu_a c' \int_0^\infty L(r,z,t,\rho,\theta) dt = N_p dV \Delta \mu_a \phi(z,\rho) E(r,z,\rho,\theta) dA \qquad 3.70$$

or

$$\int_0^\infty L(r,z,t,\rho,\theta) dt = \frac{1}{c'} \phi(z,\rho) E(r,z,\rho,\theta) \qquad 3.71$$

which affirms the fact that the time integral of the time-resolved problem for the solution of the steady state problem is in fact proportional to the product of the photon fluence and the escape function obtained directly from the diffusion approximation to the steady state radiative transfer equation. So that instead of using the time consuming expression on the L.H.S of equation 3.71, one could use the expression on the R.H.S which gives relatively quick results. A graphical presentation of this comparison is presented in figure 4.2.2.5 for typical values

of the optical parameters.

Therefore the residency time of re-emitted photons in a volume element dV at $\underline{r}'$ in the tissue before escaping through dA at $\underline{r}$ on the tissue surface, for zero boundary condition is derived as

$$dT(r,z,\rho,\theta) = K_3\left[\frac{\exp\{-\mu_{eff}[(z-z_o)^2+\rho^2]^{\frac{1}{2}}\}}{[(z-z_o)^2+\rho^2]^{\frac{1}{2}}} - \frac{\exp\{-\mu_{eff}[(z+z_o)^2+\rho^2]^{\frac{1}{2}}\}}{[(z+z_o)^2+\rho^2]^{\frac{1}{2}}}\right] x\frac{\exp\{-\mu_{eff}|\underline{r}-\underline{r}'|\}}{|\underline{r}-\underline{r}'|^2}\left[\mu_{eff}+\frac{1}{|\underline{r}-\underline{r}'|}\right] \quad 3.72$$

where

$$K_3 = \frac{z_o}{8\pi^2 Dc'}$$

If this expression is normalized to the total number of photons leaving the medium in the vicinity of $\underline{r}$ per unit area, R(r), then equation 3.72 becomes

$$dT_n(r,z,\rho,\theta) = K_3\left(\frac{\exp\{-\mu_{eff}[(z-z_o)^2+\rho^2]^{\frac{1}{2}}\}}{[(z-z_o)^2+\rho^2]^{\frac{1}{2}}} - \frac{\exp\{-\mu_{eff}[(z+z_o)^2+\rho^2]^{\frac{1}{2}}\}}{[(z+z_o)^2+\rho^2]^{\frac{1}{2}}}\right) x\left(\frac{\exp[-\mu_{eff}|\underline{r}-\underline{r}'|]}{|\underline{r}-\underline{r}'|^2}\left[\mu_{eff}+\frac{1}{|\underline{r}-\underline{r}'|}\right]\right)\left(\frac{z_o}{2\pi}\frac{\exp[-\mu_{eff}(r^2+z_o^2)^{\frac{1}{2}}]}{r^2+z_o^2}\right)^{-1} x\left(\mu_{eff}+\frac{1}{(r^2+z_o^2)^{\frac{1}{2}}}\right)^{-1} \quad 3.73$$

The corresponding expression that incorporates extrapolated boundary conditions can also be shown to be

$$dT_n(r,z,\rho,,\theta) = K_4\left(\frac{\exp\{-\mu_{eff}[(z-z_o)^2+\rho^2]^{\frac{1}{2}}\}}{[(z-z_o)^2+\rho^2]^{\frac{1}{2}}} - \frac{\exp\{-\mu_{eff}[(z+z_p)^2+\rho^2]^{\frac{1}{2}}\}}{[(z+z_p)^2+\rho^2]^{\frac{1}{2}}}\right)$$
$$x\left(z_o\frac{\exp[-\mu_{eff}|r-r'|]}{|r-r'|^2}[\mu_{eff}+\frac{1}{|r-r'|}]+z_p\frac{\exp[-\mu_{eff}|r-r'|]}{|r-r'|^2}[\mu_{eff}+\frac{1}{|r-r'|}]\right)$$
$$x\left(z_o\frac{\exp\{-\mu_{eff}(r^2+z_o^2)^{\frac{1}{2}}\}}{r^2+z_o^2}[\mu_{eff}+\frac{1}{(r^2+z_o^2)^{\frac{1}{2}}}]+z_p\frac{\exp\{-\mu_{eff}(r^2+z_p^2)^{\frac{1}{2}}\}}{r^2+z_p^2}x[\mu_{eff}+\frac{1}{(r^2+z_p^2)^{\frac{1}{2}}}]\right)^{-1} \quad 3.74$$

where

$$K_4 = \frac{1}{8\pi^2 Dc'} \quad 3.75$$

The mean penetration depth of an incident photon can now be determine from this model and compared with results from the 3-dimensional random walk theory model. The average penetration depth of a photon that eventually escapes at the tissue surface at a distance r from the point of incidence can be determine by integrating equation 3.72 over all ρ and θ and normalized to its volume integral, i.e

$$dT_n(r,z) = \frac{\int_0^{2\pi}\int_0^{\infty} dT(r,z,\rho,\theta)\rho\, d\rho\, d\theta}{\int_0^{2\pi}\int_0^{\infty}\int_0^{\infty} dT(r,z,\rho,\theta)\rho\, d\rho\, dz\, d\theta} \qquad 3.76$$

where dT(r,z,ρ,θ) is given by equation 3.72. This final expression is similar to equation 3.77 obtained by Weiss et al (1989) and based on a 3-dimensional random walk theory.

3.5 PHOTON RESIDENCY TIME FROM RANDOM WALK THEORY.

Weiss et al (1989) have analyzed the scattering process of photons in tissue in terms of a random walk on a simple cubic lattice. The following assumptions were made in the analysis:

1. The tissue is of semi-infinite extent,
2. Scattering of the photons is isotropic,
3. Beer's law applies to photon absorption in the tissue,
4. The surface, z = 0, consist of absorbing sites, so that any photon reaching the surface will be trapped there and will contribute to the reflected intensity, and
5. Properties of the tissue are taken to be isotropic.

The model for his analysis is shown schematically in figure 3.5.1. A laser beam impinges on a human tissue and is scattered by scattering sites. Some photons are absorbed in the tissue and some are reflected back to the surface where they are re-emitted. For the purpose of comparison, only one result of

Semi–Infinite Homogeneous Medium Irradiated with a Pencil Beam. Boundary Condition: $\varphi(r,0) = 0$

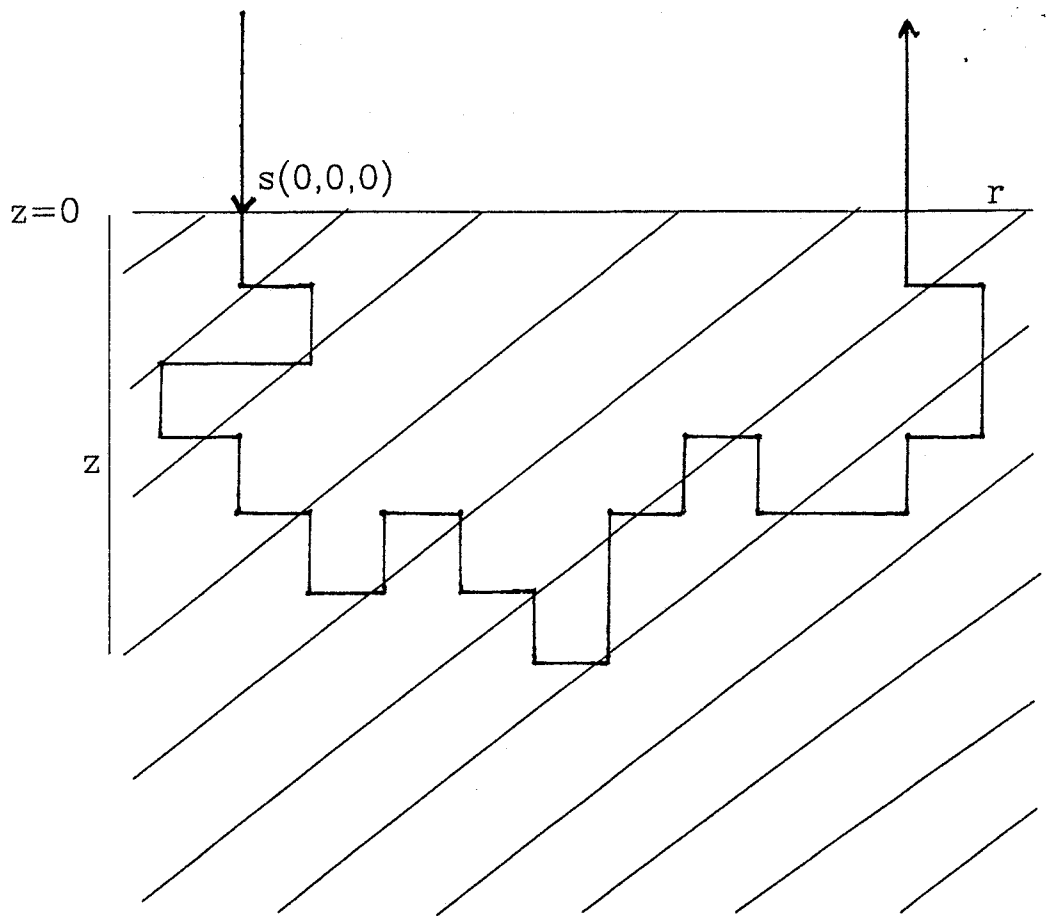

Figure 3.5.1

A collimated pencil beam normally incident upon the surface of a semi–infinite homogeneous medium. The path represents a cartoon of a typical path travelled by a photon inserted into the medium at s(0,0,0) and exiting at a point on the surface at a radial distance r from the point of entry. (Weiss et al 1989).

interest will be stated, but for a detailed description of the analysis, the reader is referred to Weiss et al (1989). The end result of the calculation, which is the normalized form of the fraction of time that photons re-emitted at a distance, r, from the initial injection point have spent at depth, z, is

$$p(r,z) = \frac{4r(6\mu)^{\frac{1}{2}}z}{r^2+4z^2}\{1+\frac{1}{[6\mu(r^2+4z^2)]^{\frac{1}{2}}}\}\exp\{r(6\mu)^{\frac{1}{2}}-[6\mu(r^2+4z^2)]^{\frac{1}{2}}\} \quad 3.77$$

A plot of p(r,z) as a function of z is shown in figure 4.2.2.5 for typical values of μ, where $\mu = \mu_a L$, ($L = 1/\mu_s'$).

CHAPTER FOUR

RESULTS AND DISCUSSION

4.1 INTRODUCTION.

The purpose of this report has been to develop a model that relates the fundamental optical properties of tissue, (i.e μ_a and μ_s'), the radial distance along the tissue surface between the point of incidence and the point of re-emission and detection of photons, to the time that photons have spent in an elemental volume dV in the tissue. In addition to these relations which were developed for both the steady state and the time-resolved methods, the influence of delaying the detection time (in the pulse state technique) on the residency time was also of interest.

These residency times can be indirectly measured experimentally in phantoms, as is currently being done by research groups at the Hamilton Regional Cancer Centre, but, so far, no work has been done in living tissues. Knowledge of the residency time would allow some insight into the depth distribution of injected photons that are eventually re-emitted. In this respect, once the characteristic scattering and absorption parameters for a given homogeneous tissue are specified, for the wavelength to be used in diagnosis or therapy, other relevant information can be obtained according to the model. For

instance, one could infer the volume sampled by the re-emitted photons.

4.2 RESULTS.

4.2.1 TIME-RESOLVED TECHNIQUE.

A model has been developed, which can be used to determine non invasively the residency time of diffusely re-emitted photons in an elemental tissue volume. The development of the time-resolved and spatial distribution of the residency time of the re-emitted photons has been possible by the use of the diffusion approximation to the time dependent and the time independent radiative transfer equation respectively.

The solution of the Boltzmann transport equation for the fluence rate per incident photon at a point $\underline{r}$ in 3-dimensional cylindrical coordinates in an infinite homogeneous medium was first developed. This was used to solve the problem posed in figure 3.4.1.1.1.1 for a semi-infinite homogeneous medium. The fluence rate per incident photon at ($\underline{r}$,t) inside the medium was mathematically derived (equation 3.28) and hence the reflectance (i.e the number of photons leaving the tissue surface) per unit area per unit time per incident photon at a radial distance r, from the point of incidence was obtained. The latter equation (i.e equation 3.31), as it has already been discussed, has been used extensively by a number of authors (Patterson et al 1989 and Chance et al 1989) to pursue the determination of the optical properties of tissue directly from the temporal dependence of the diffuse reflectance.

The influence of extrapolated boundary conditions on the fluence rate and hence on the reflectance which are mathematically shown in equations 3.33 and 3.35 respectively have been studied extensively by Moulton (1990). These equations (3.28, 3.31, 3.33 and 3.35) have been the cornerstone of the analysis in this report.

The calculations of the integrals have been done numerically using the IMSL/LIB on the Microvax computer system in the Hamilton Regional Cancer Centre. The results of these calculations for typical values of the optical properties of soft tissue are presented in this chapter. The results presented have been in most cases for a mismatched refractive index at the tissue surface, as for example, between a transparent medium (e.g air) and a turbid biological tissue. This is usually the case in practical applications, where photons are incident on the interface between air and living tissue. The index of refraction of the transparent medium from which photons are being incident is considered here to be equivalent to that of air, having a value of 1.0 and that of the medium through which the photons propagate is taken to be that of soft tissue with a value of 1.4.

Figures 4.2.1.1, 4.2.1.2, 4.2.1.3, 4.2.1.4, 4.2.1.5, 4.2.1.6 and 4.2.1.7 show the normalized (to the total time photons spent in tissue before escaping at the surface) version of the residency time in an elemental volume as a function of depth in tissue for pulse irradiation. These residency time depth distributions were

made along a line midway between the source and detection fibers. The curves have been calculated using equation 3.50, and except for figures 4.2.1.2, 4.2.1.4 and 4.2.1.6 which were calculated for 'late times', the detection time, t, has been taken at the time, t_{max}, at which the maximum number of re-emitted photons are detected on the tissue surface (i.e $R_{max}(r,t_{max})$). The Marshak approximation (equation 3.17) was used to calculate the position of the extrapolated boundary. The terms 'early time' used in this report refers to t_{max} and 'late time' means delaying the detection time of the re-emitted photons. Here, the late time values have been taken as the time at which the number of re-emitted photons on the tissue surface has fallen to $(1/10)^{th}$ of its maximum value. The time at which the peak occurs in the reflectance-time spectrum for a zero boundary condition can easily be obtained from the relation

$$\frac{d}{dt}\log_e[R(r,t)] = -\frac{5}{2t} - \mu_a c' + \frac{r}{4Dc't} = 0 \qquad 4.1$$

It has been demonstrated by Wilson et al (1989) that

$$t_{max} = \frac{1}{2c'}\left\{\left[\left(\frac{5}{2\mu_a}\right)^2 + \frac{3\mu_s'}{\mu_a}(r^2+z_o^2)\right]^{\frac{1}{2}} - \frac{5}{2\mu_a}\right\} \qquad 4.2$$

The corresponding result incorporating an extrapolated boundary condition which has been used in most cases here is not straightforward. The values of t_{max} for the extrapolated boundary condition used in this report has therefore been

obtained, using equation 3.35, by numerically calculating R(r,t) for various values of t, fiber separation r, and typical values of μ_a, μ_s' and noting the time (t_{max}) of maximum reflectance ($R_{max}(r,t_{max})$). The corresponding late time value is then determined by noting the time at which R(r,t) has fallen to $(1/10)^{th}$ $R_{max}(r,t_{max})$.

The influence of the various fundamental optical parameters μ_a and μ_s' on the depth distribution of the residency time for early detection times are demonstrated in figures 4.2.1.3 and 4.2.1.5 respectively. Figures 4.2.1.4 and 4.2.1.6 show the same residency time depth distribution as in figures 4.2.1.3 and 4.2.1.5 but for late detection times. The fiber separation is r = 30mm, and the μ_a and μ_s' values are typical of soft mammalian tissue. It is interesting to note that the depth distribution tends to sharpen as the absorption coefficient increases, and this is readily understood, because long trajectories are less likely with large absorption probabilities. In some of the results a scattering to absorption ratio of 5:1 has been used which may be too small but it should be mentioned here that, generally good results could be obtained in the diffusion theory if the scattering to absorption ratio is about 10:1. Figures 4.2.1.1 and 4.2.1.2 show the normalized form of the residency time as a function of depth for various values of the fiber separation. The main difference between these two plots is that, the former has been determined for early detection times and the latter for late times. The most significant implication is that, the greater the fiber separation the wider and flatter the depth distribution. The effect of delaying the detection time of the emergent

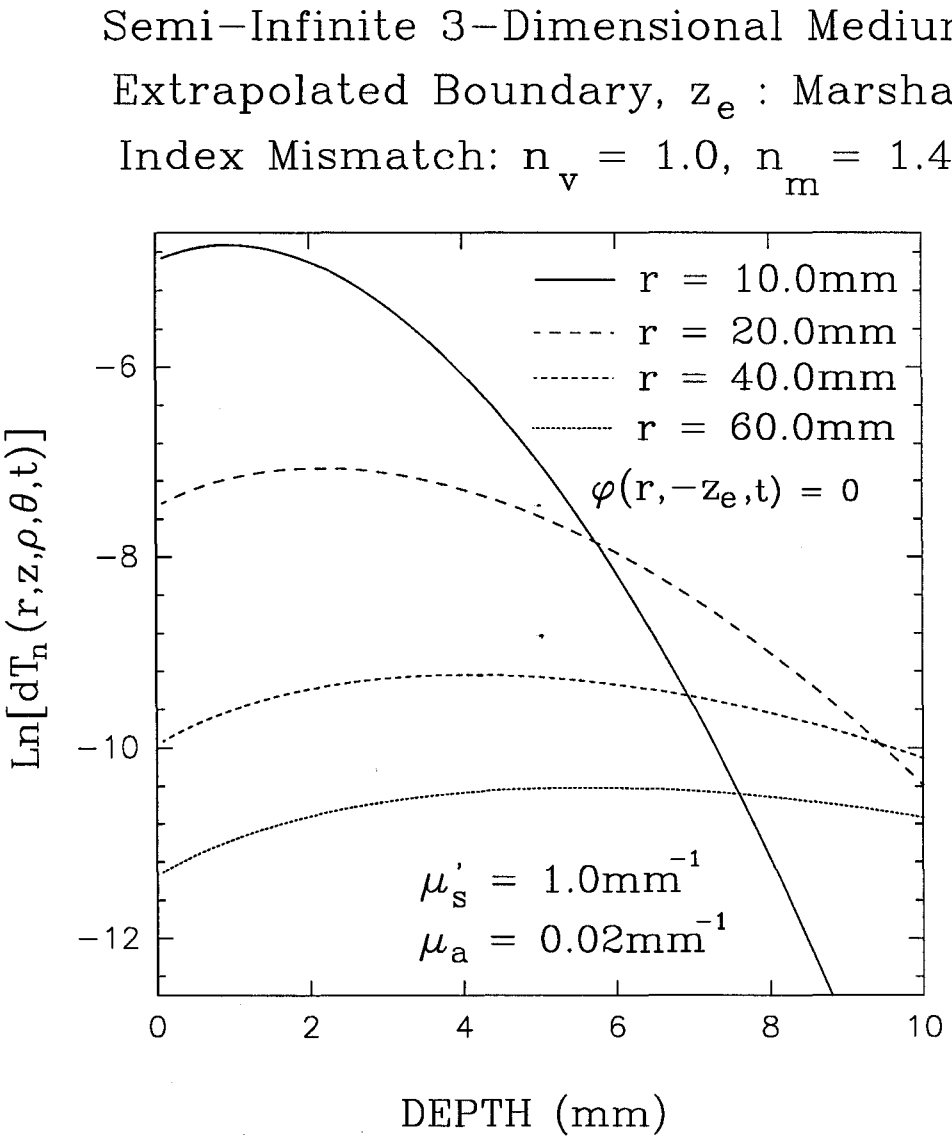

Figure 4.2.1.1

The residency time of a photon in an elemental volume dV in tissue before reemitting at the surface, normalized to the total time spent in the tissue, and given as a function of depth, for different values of the fiber separation. The curves have been calculated for early times using equation 3.50.

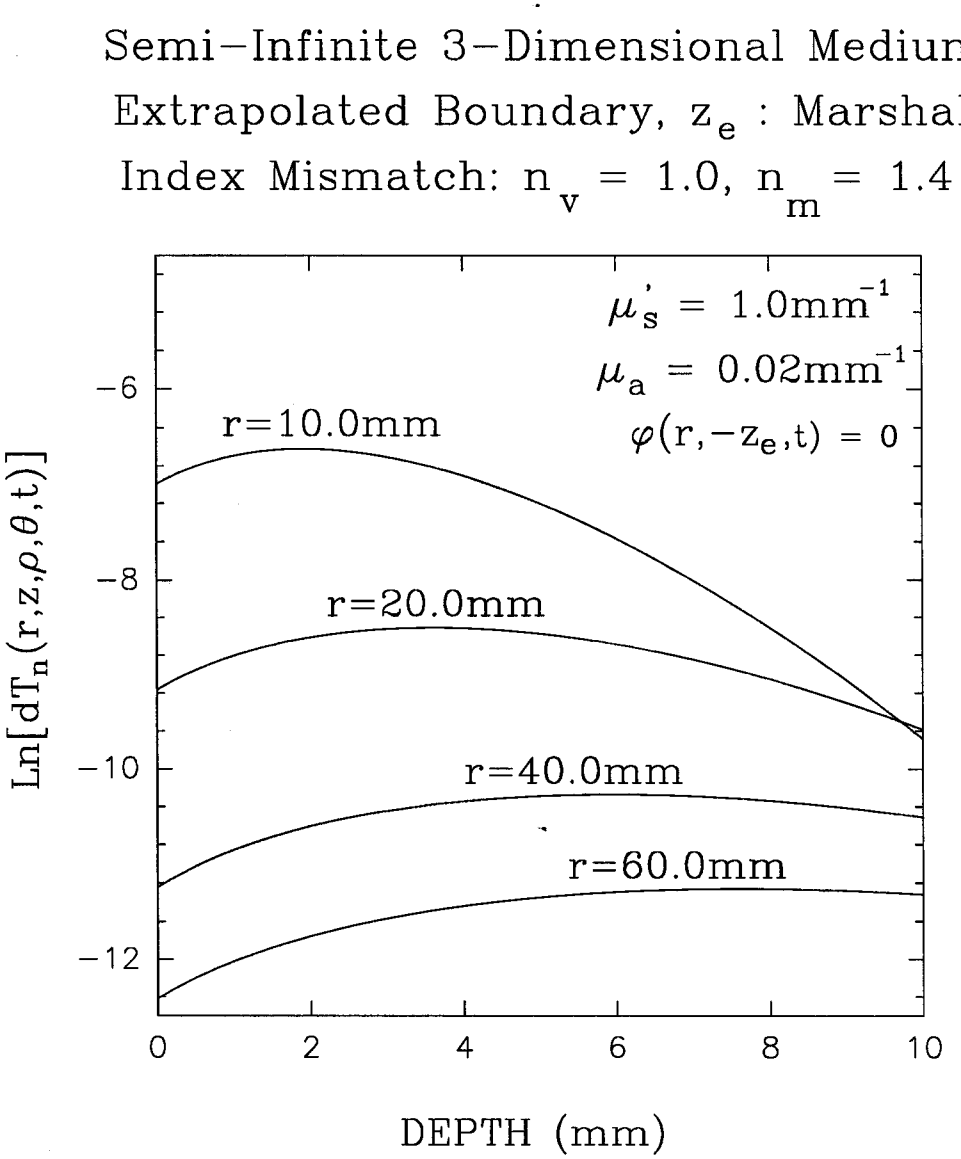

Figure 4.2.1.2

The residency time of a photon in an elemental volume dV in tissue before reemitting at the surface, normalized to the total time spent in the tissue, and given as a function of depth, for different values of the fiber separation. The curves have been calculated for late times using equation 3.50.

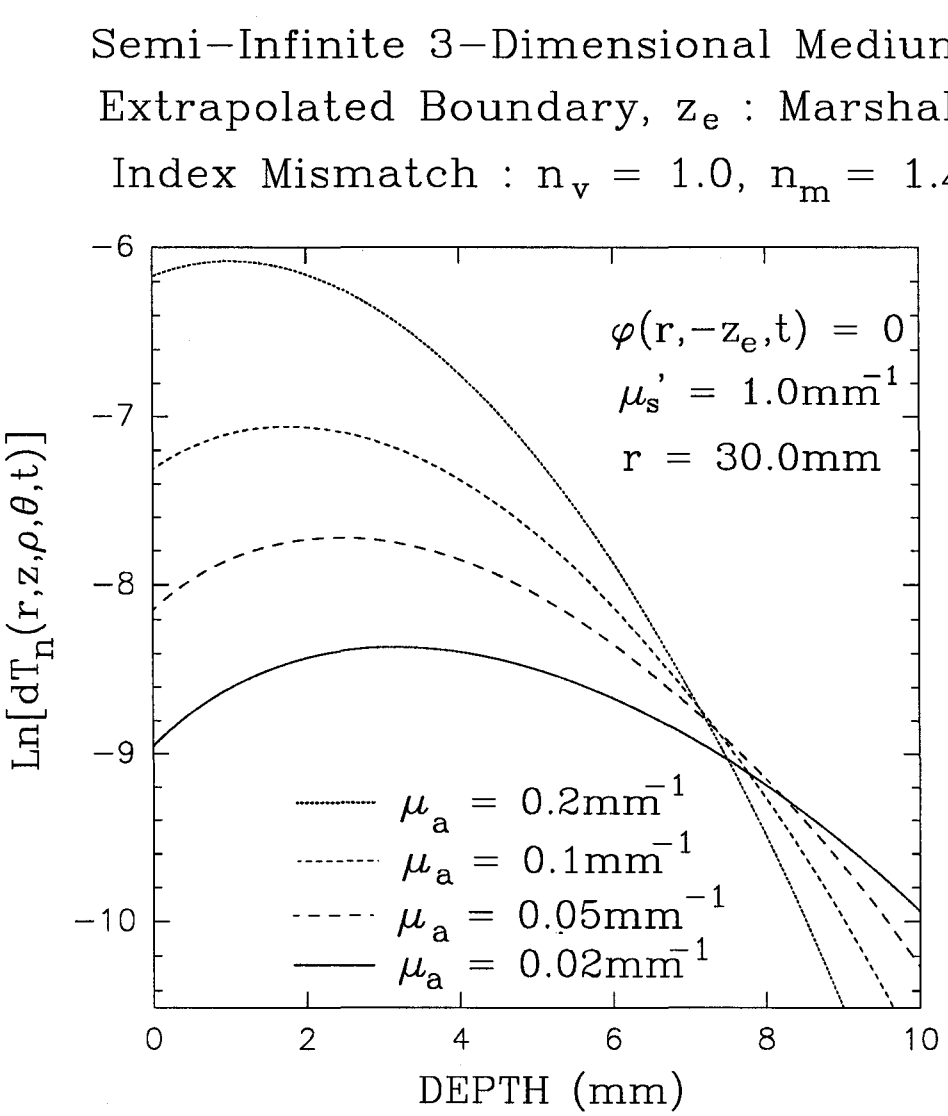

Figure 4.2.1.3

The time spent by a photon in an elemental volume dV in tissue before reemitting at the surface, normalized to the total time spent in the tissue, and given as a function of depth, for different values of the absorption coefficient. The curves have been calculated for early times using equation 3.50. The optical parameters are typical of soft tissue. The Marshak approximation was used to calculate z_e.

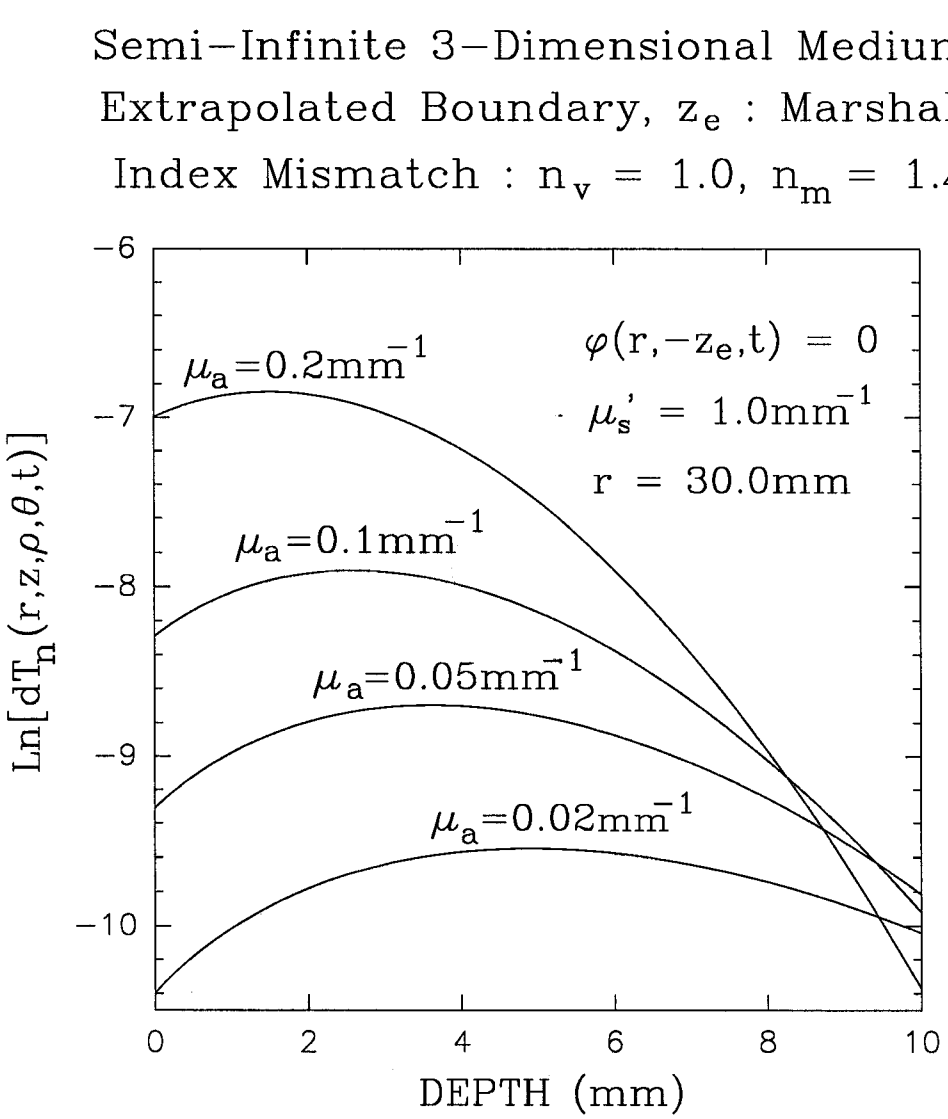

Figure 4.2.1.4

The time spent by a photon in an elemental volume dV in tissue before reemitting at the surface, normalized to the total time spent in the tissue, and given as a function of depth, for different values of the absorption coefficient. The curves have been calculated for late times using equation 3.50. The optical parameters are typical of soft tissue. The Marshak approximation was used to calculate z_e.

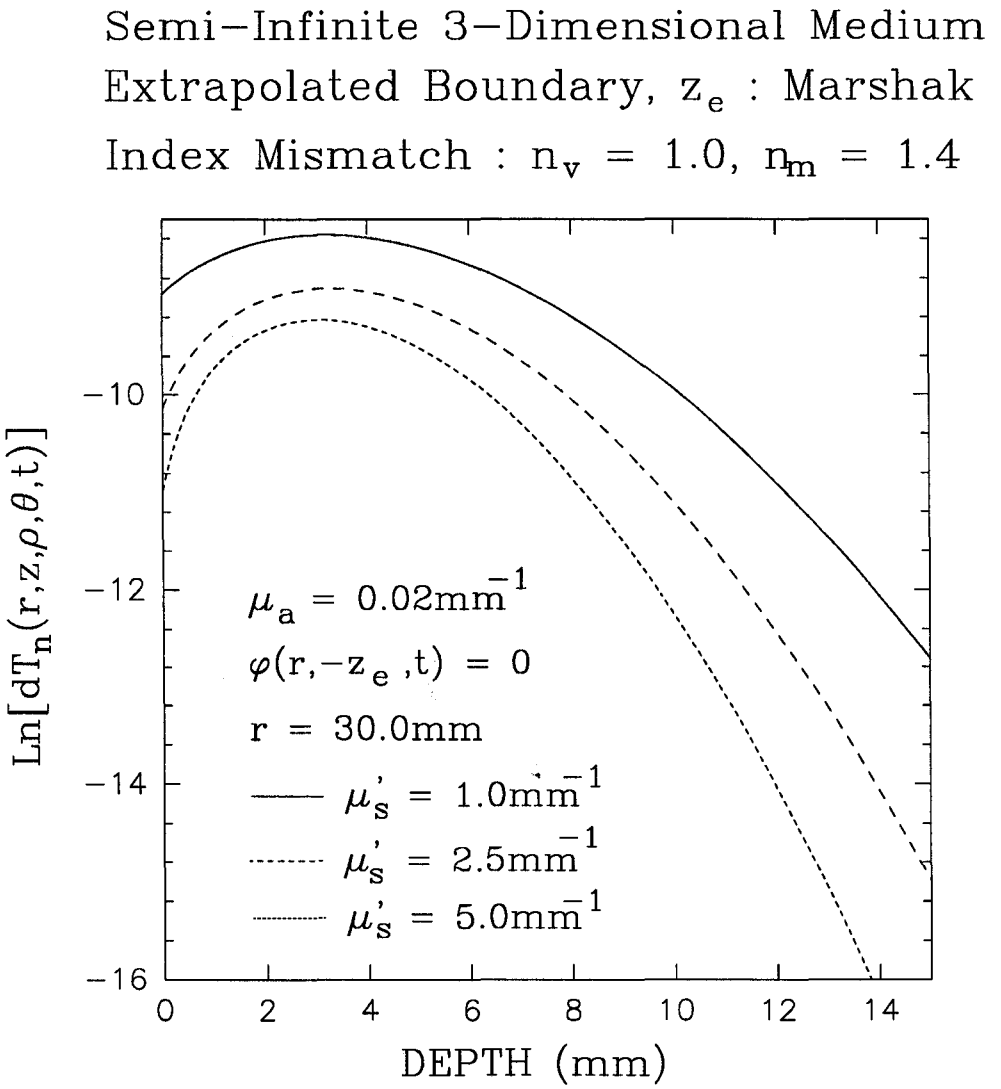

Figure 4.2.1.5

The time spent by a photon in an infinitesimal volume in tissue before reemitting at the surface, normalized to the total time spent in the tissue, and given as a function of depth, for different values of the transport scattering coefficient. The curves have been calculated for early times using equation 3.50.

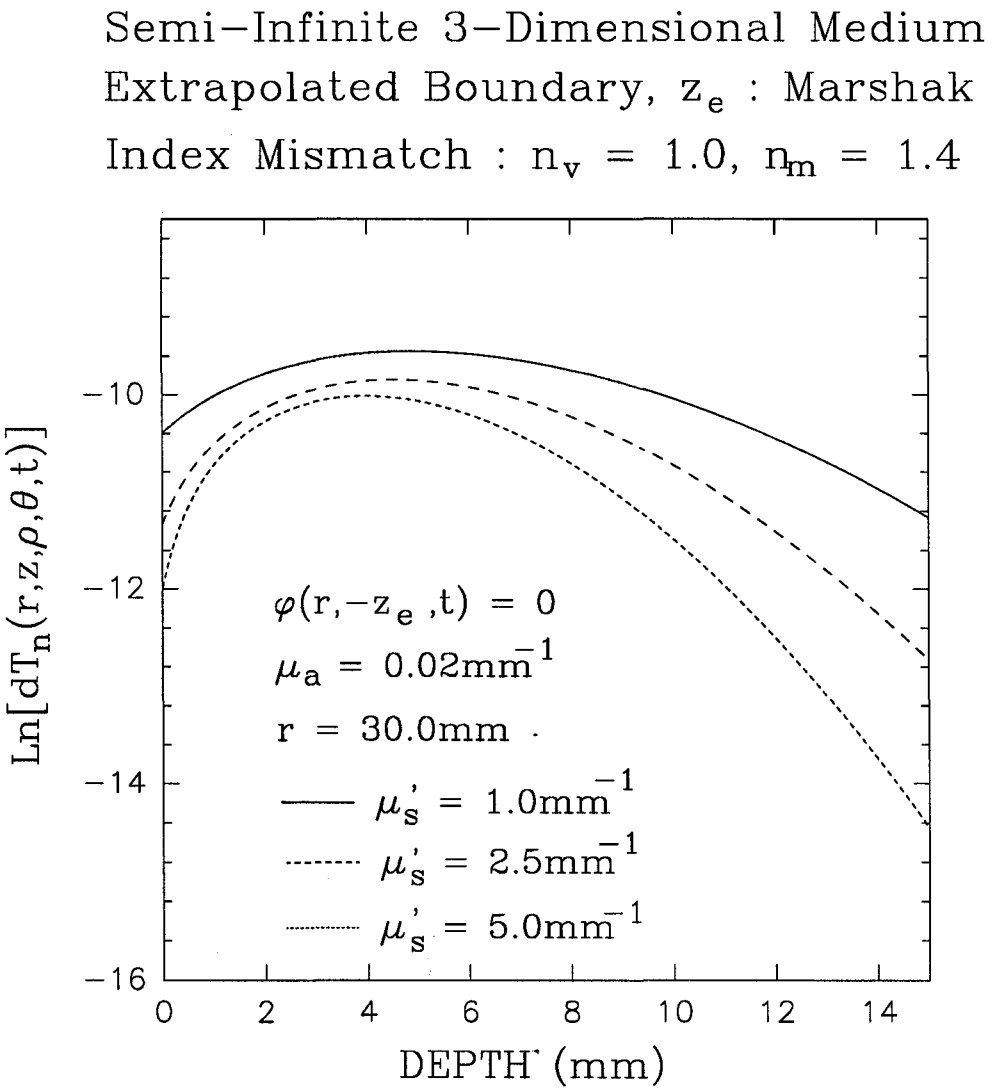

Figure 4.2.1.6

The time spent by a photon in an infinitesimal volume in tissue before reemitting at the surface, normalized to the total time spent in the tissue, and given as a function of depth, for different values of the transport scattering coefficient. The curves have been calculated for late times using equation 3.50.

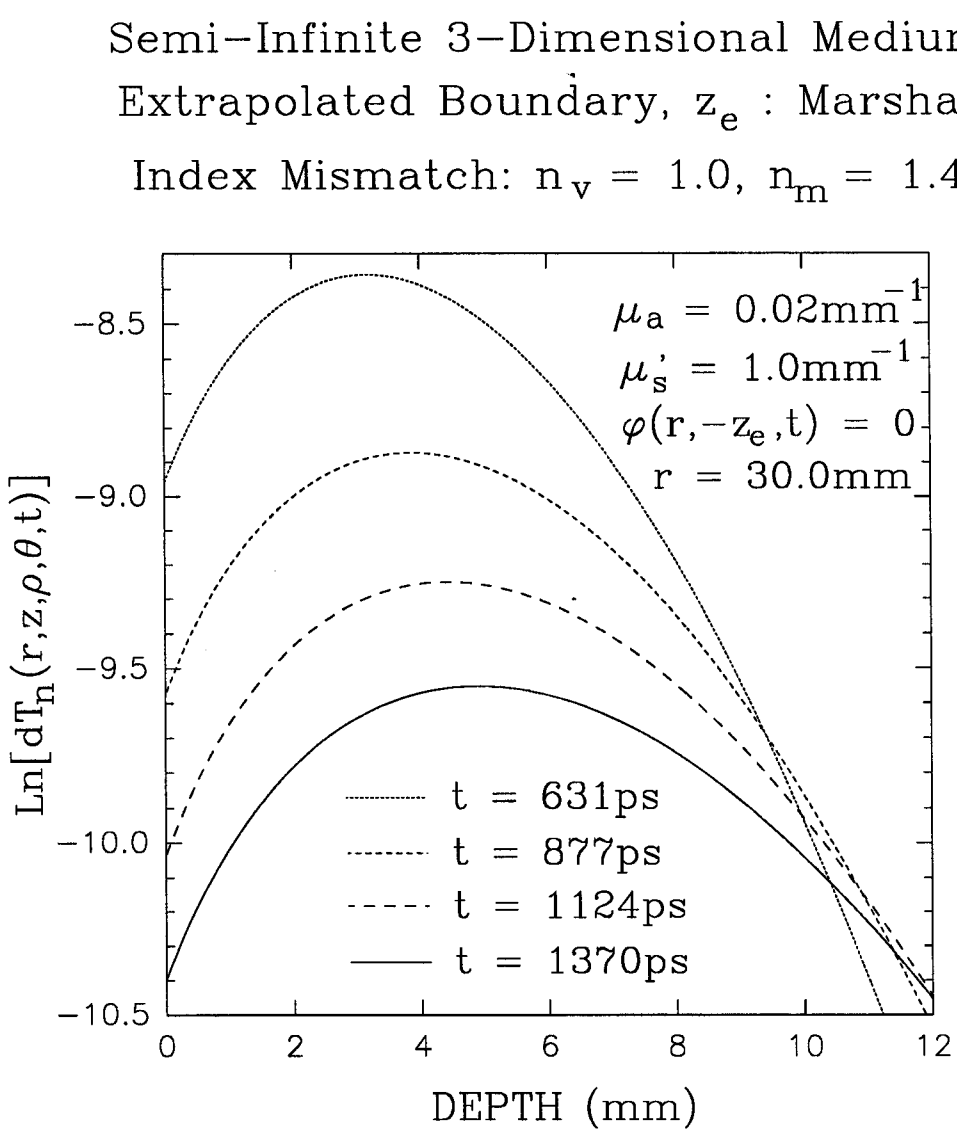

Figure 4.2.1.7

The residency time of a photon in an infinitesimal tissue volume dV before escaping through the surface, normalized to the total time spent in the tissue, and given as a function of depth, for different detection times. The curves have been calculated using equation 3.50.

photons on the distribution is shown in figure 4.2.1.7 and as expected, the depth distribution widens and flattens with delay in the detection time.

Figure 4.2.1.9 shows the distribution of the residency time as a function of both z and ρ for pulse irradiation in a semi-infinite medium and a zero boundary condition. The results have been obtained using equation 3.45. The orientation of the plane in which measurements were made is θ = 0 degree (i.e plane A in figure 4.2.1.8) with the source and detection fibers positioned at -10mm and +10mm respectively. Figure 4.2.1.10 shows the same distribution as in figure 4.2.1.9 but measurements in this case were made in a vertical plane midway between the source and detector and perpendicular to the plane containing the source and detection fibers (i.e plane B). In both cases the fiber separation is r = 20mm, μ_a = 0.02mm^{-1} and μ_s' = 1.0mm^{-1}. The most significant difference between the plots appears in their symmetry. It could be observed that the plot in figure 4.2.1.9 is symmetrical about a line midway between the two fibers, whereas the plot in figure 4.2.1.10 is symmetrical about the plane containing the source and detector. This result is not surprising, since in the first instance, for θ = 0 degree, the source and detection fibers are separated by a distance and are in the same plane, but in the second instance, θ = 90 degrees, the position of the source and detection fibers appears to be located at a single point (in this case at the origin) and hence the distribution should always be symmetrical about the plane containing that virtual single point. As it has usually been the case for

Planes in which Measurements were made.

Plane A: θ = 0 degree

Plane B: θ = 90 degrees

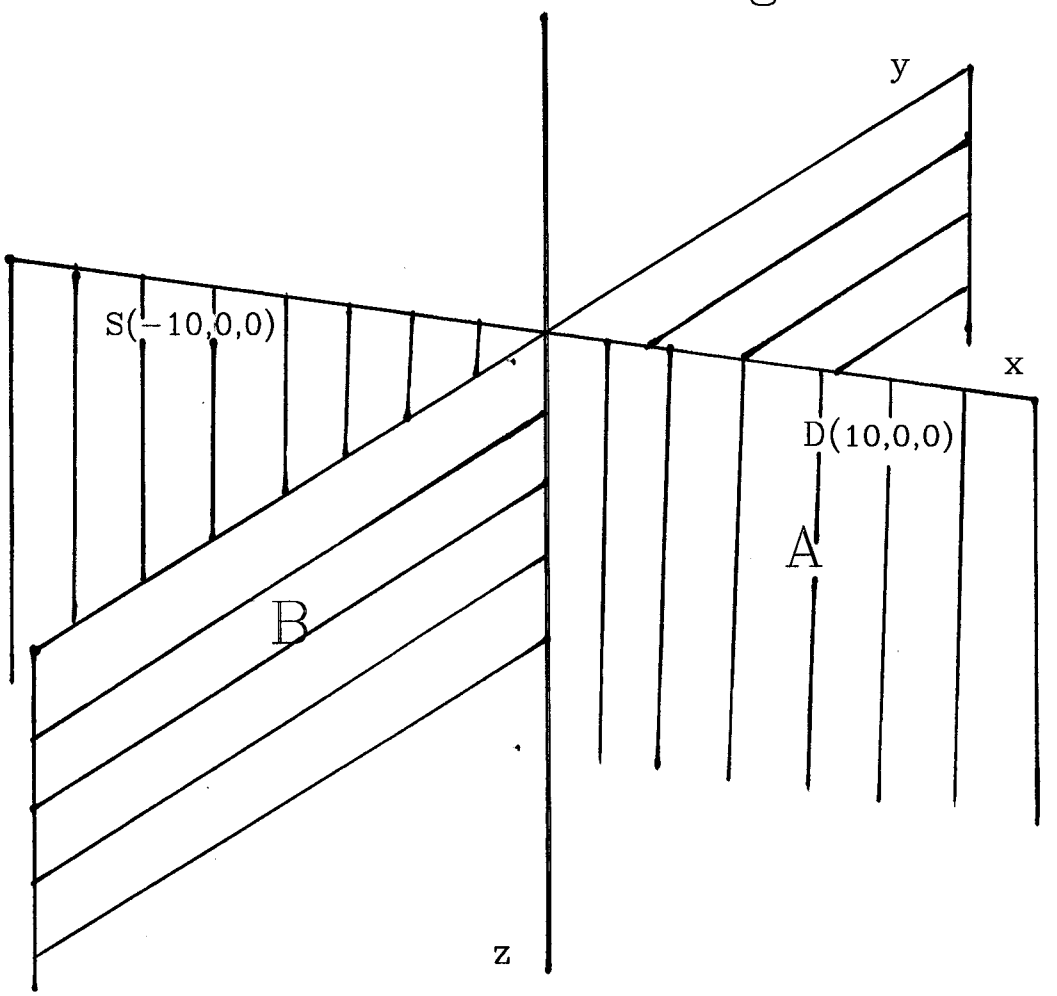

Figure 4.2.1.8

Diagrammatical presentation of the planes in which calculations were made to obtain figs 4.2.1.9, 4.2.1.10, 4.2.2.8 and 4.2.2.9. Plane A contains both the source and the detection fibers, positioned at −10mm and +10mm respectively. Plane B is midway between source and detector.

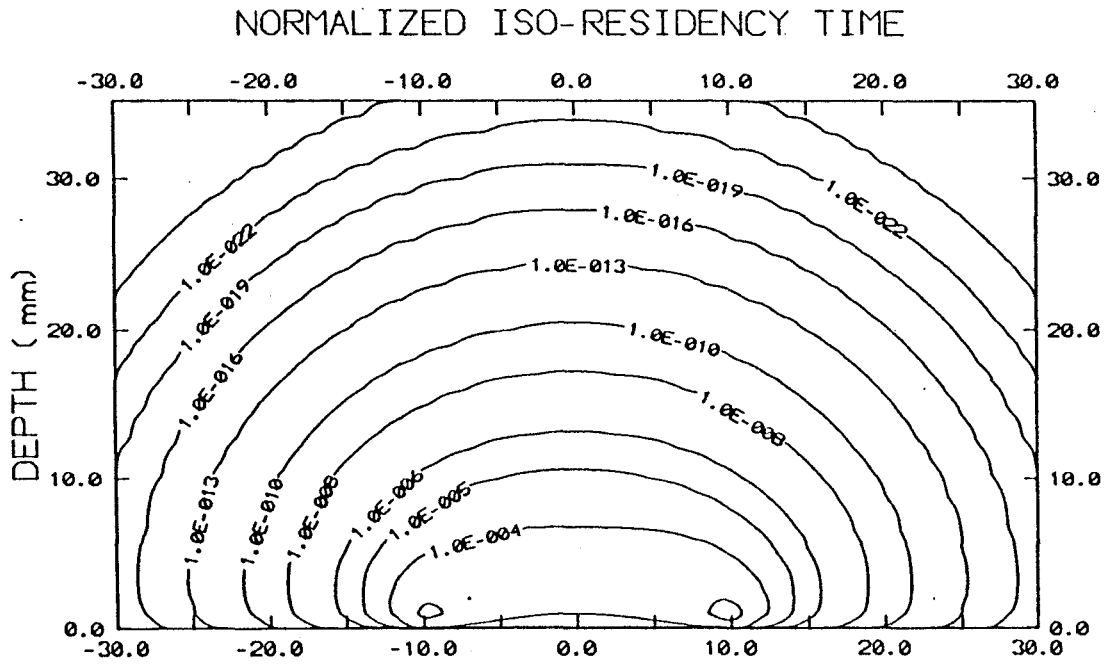

Figure 4.2.1.9

Iso-residency time distribution of photons incident on the surface of a semi-infinite homogeneous medium and detected at a radial distance of 20mm away. The lines have been calculated using equation 3.45, and the detection time is $t = t_{max}$. Calculations are made in the plane containing the source (positioned at −10mm) and the detector (positioned at +10mm).

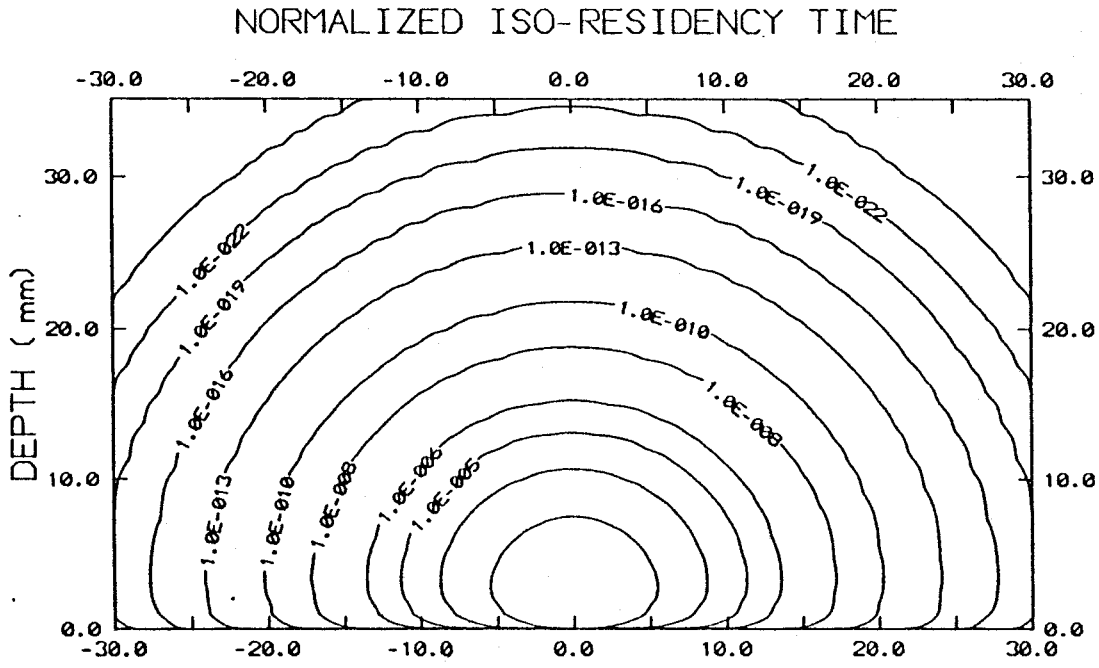

Figure 4.2.1.10

Examines the same iso-residency time distribution shown in figure 4.2.1.9. But in this case calculations are made in a plane perpendicular to and midway between the source and detection fibers.

almost all the results in the pulse state, the detection time used was the value for the 'early time'. It is worth mentioning here that at points very close to the surface of the tissue, there is some asymmetry about the two fibers.

Finally, figures 4.2.1.11 and 4.2.1.12 show the same depth distribution as in figure 4.2.1.9 but for a point source and a point detector in an infinite homogeneous medium. The main difference between the two plots is that figure 4.2.1.11 has been determined for a time of t = 700ps and figure 4.2.1.12 has been for a late time of t = 2000ps. Both plots have been calculated using equation 3.55. The absorption and the transport scattering coefficients used are $0.02mm^{-1}$ and $1.0mm^{-1}$ respectively which are typical of soft tissue, and the fiber separation is r = 20mm. Notice the symmetry in both cases.

4.2.2 STEADY STATE.

The solution of the steady state problem has been obtained from two different approaches. First by using the time integral of the time-resolved problem and secondly from the diffusion approximation to the steady state radiative transport equation. Almost all the results obtained in the steady state method have been calculated using equation 3.74.

Comparison shows that

$$c'\int_0^\infty L(r,z,\rho,\theta)dt = \phi(z,\rho)E(r,z,\rho,\theta) \qquad 4.3$$

at least to the fourth decimal place. A plot of this comparison is presented in

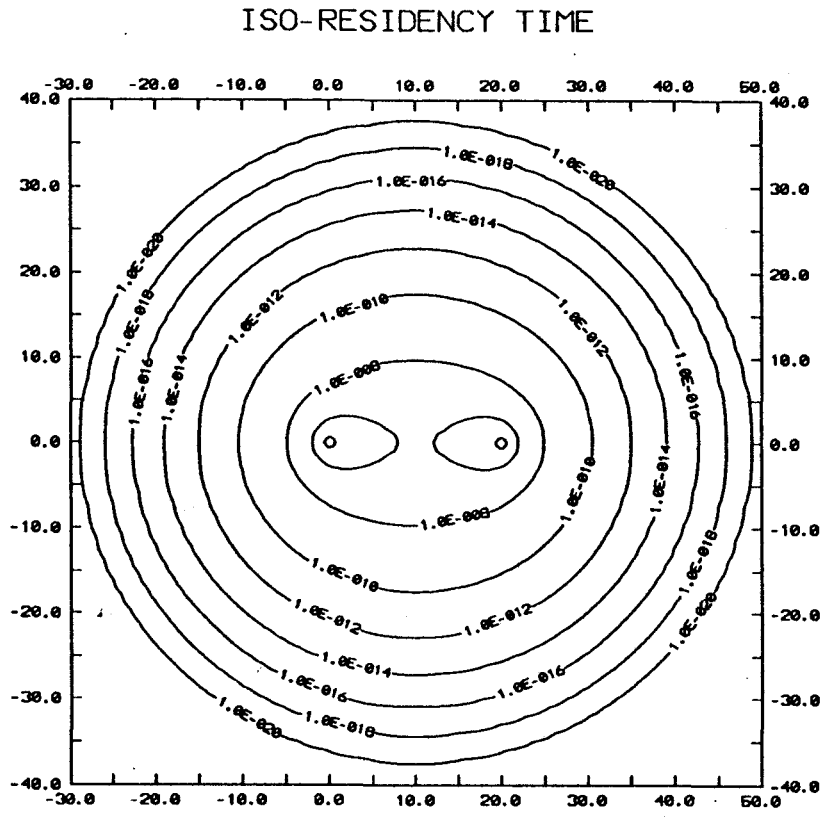

Figure 4.2.1.11

Iso-residency time of photons emitted from a point source (0,0) and observed in a point detector (20,0), in an infinite homogeneous medium, in the pulse state. The detection time of the detected photons is t = 700 ps and the lines have been obtained from equation 3.55.

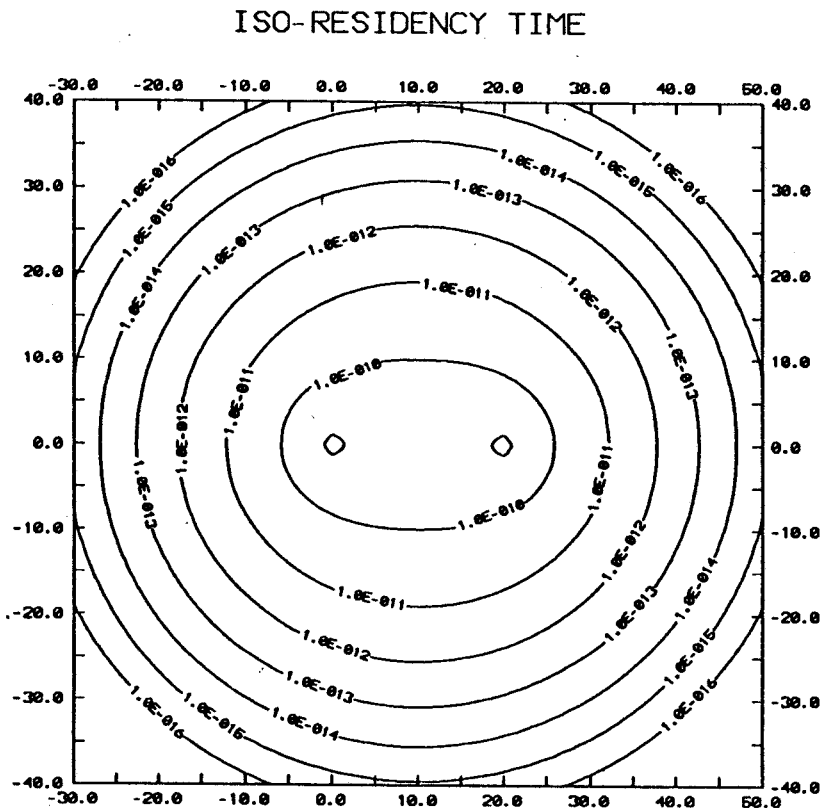

Figure 4.2.1.12

Iso-residency time distribution of photons emitted from a point source and observed in a point detector in an infinite homogeneous medium. This plot is similar to figure 4.2.1.11 but for a detection time of t = 2000 ps

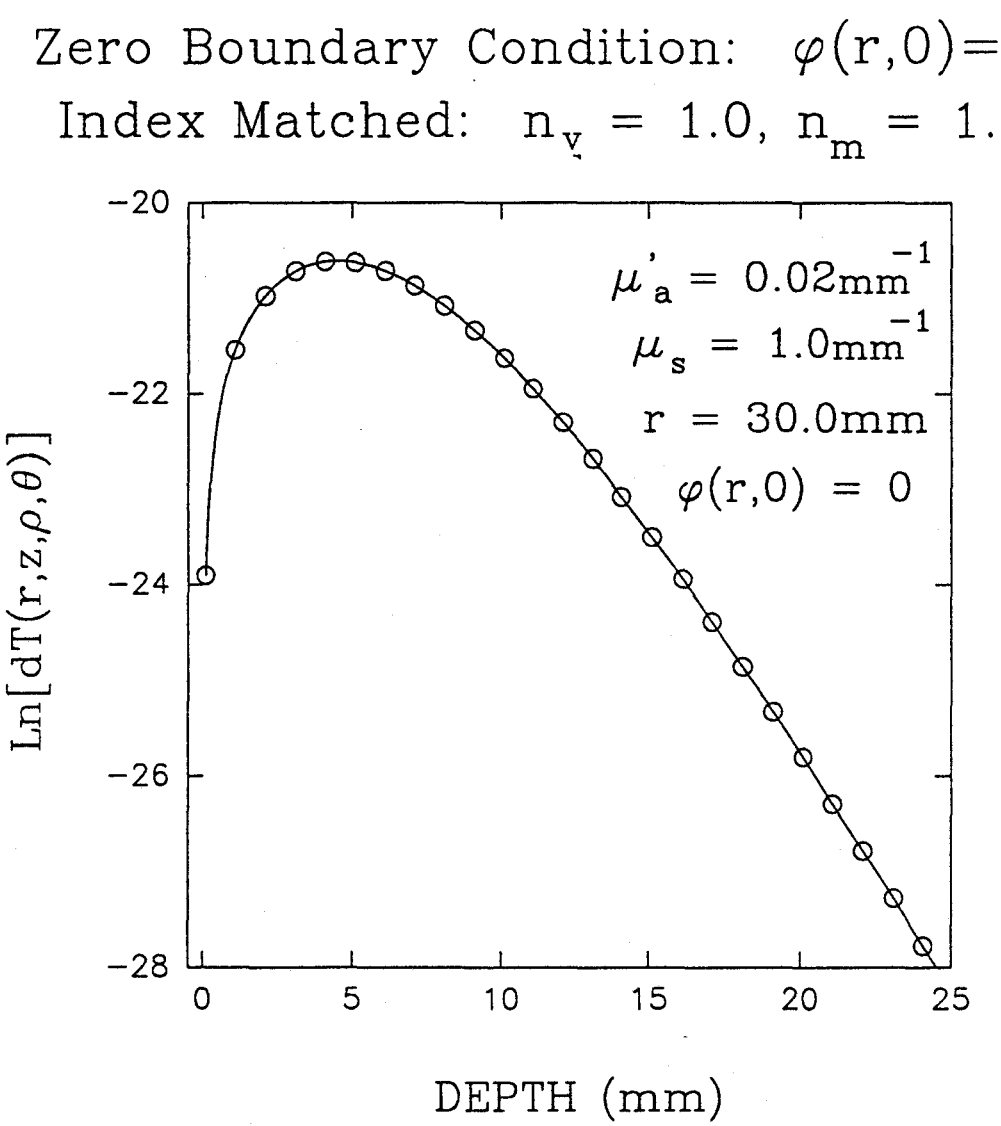

Figure 4.2.2.1

Comparison of the residency time of a photon in an elemental volume dV in tissue in the steady state obtained from the time integral of the time resolved problem (——) and from the steady state radiative transfer equation (symbols).

figure 4.2.2.1. The comparison of these two results is very important, as it serves as a test of the adequacy of the integration performed numerically using the computer. It also affirms that the residency time obtained in the steady state method from the time integral of the time-resolved problem is in fact equal to that obtained from the diffusion approximation to the steady state radiative transfer equation. A second test of the adequacy of the numerical integration has been to show that the volume integral of equation 3.45 and/or 3.59 is unity. The results obtained for both cases are reasonable, though the method used was crude. When the residency times in elemental tissue volumes were summed over both z and ρ from 0mm to 60mm at a grid size of 1.5mm and over θ from 0 to 360 degrees at a grid size of 1.0 degree, equation 3.45 gave a value of 0.99 for the pulse state relation (i.e a rough estimate of the volume integral of equation 3.44) and equation 3.59 gave a value of 0.98 for the steady state relation (i.e a rough estimate of the volume integral of equation 3.59). The reason for using such a crude method has been the difficulty encountered in performing an n-dimensional ($n \geq 3$) integration using the IMSL/LIB on the Microvax computer system, especially in this situation where the limits of integration of the innermost integral are not constants.

Figure 4.2.2.2 examines the comparison presented in figure 4.2.1.1 and 4.2.1.2 for a steady state technique. And as expected, as it was in the time-resolved method, the depth distribution of the residency time widens and flattens

Semi–Infinite 3–Dimensional medium
Extrapolated Boundary, z_e : Marshak
Index Mismatch: $n_v = 1.0$, $n_m = 1.4$

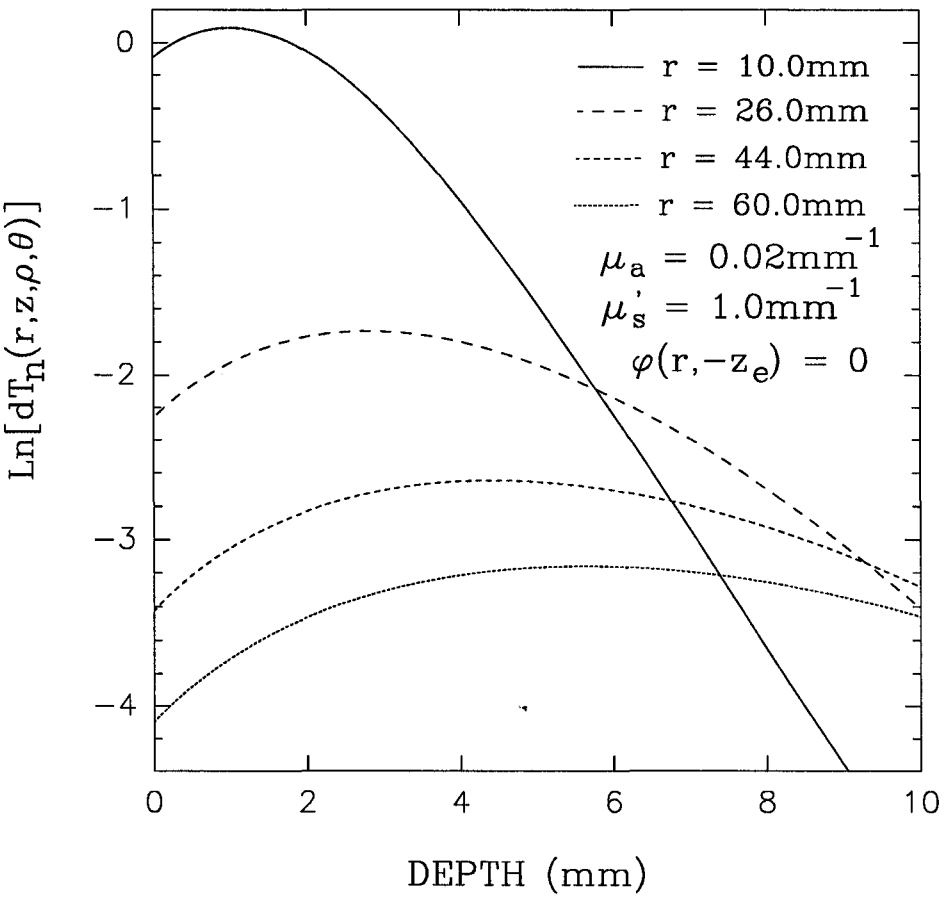

Figure 4.2.2.2

Examines the comparison presented in figures 4.2.1.1 and 4.2.1.2 for a steady state method. The curves have been calculated using equation 3.74. Note that the results are normalized to the total number of photons leaving the tissue per unit area. The optical parameters are typical of soft tissue.

with increase in the fiber separation. Figures 4.2.2.3 and 4.2.2.4 show the behaviour of the residency time depth profile for various values of the fundamental optical parameters. Comparison with the corresponding plots in the pulse state shows the same trend of variations. For example, the depth distribution tends to sharpen with increase in absorption.

In figure 4.2.2.5, the residency time as calculated from the diffusion model (equation 3.76) and the Random walk model (equation 3.77) for index matched and zero boundary condition is plotted versus depth for a semi-infinite homogeneous medium. The interesting thing to note here is that, both models predict the same residency-time depth profile, i.e, a build-up region near the surface and exponential fall far away from the surface of the medium in the 'diffusion region'.

Plots of the residency time in a vertical plane containing the source and detection fibers (i.e plane A in figure 4.2.1.8) which were positioned at -4.8mm and +4.8mm respectively, as a function of horizontal probe position at different probe depths in a homogeneous semi-infinite medium is shown in figure 4.2.2.6. The fundamental optical parameters are $\mu_s' = 1.0mm^{-1}$ and $\mu_a = 0.05mm^{-1}$. In figure 4.2.2.7, the residency time as calculated in a vertical plane perpendicular to the source and detection fibers (i.e plane B) is plotted versus a horizontal probe position at different depths. The fiber separation is r = 9.6mm and the optical parameters are the same as those used in figure 4.2.2.6.

Semi-Infinite 3-Dimensional Medium
Extrapolated Boundary, z_e: Marshak
Index Mismatch: $n_v = 1.0$, $n_m = 1.4$

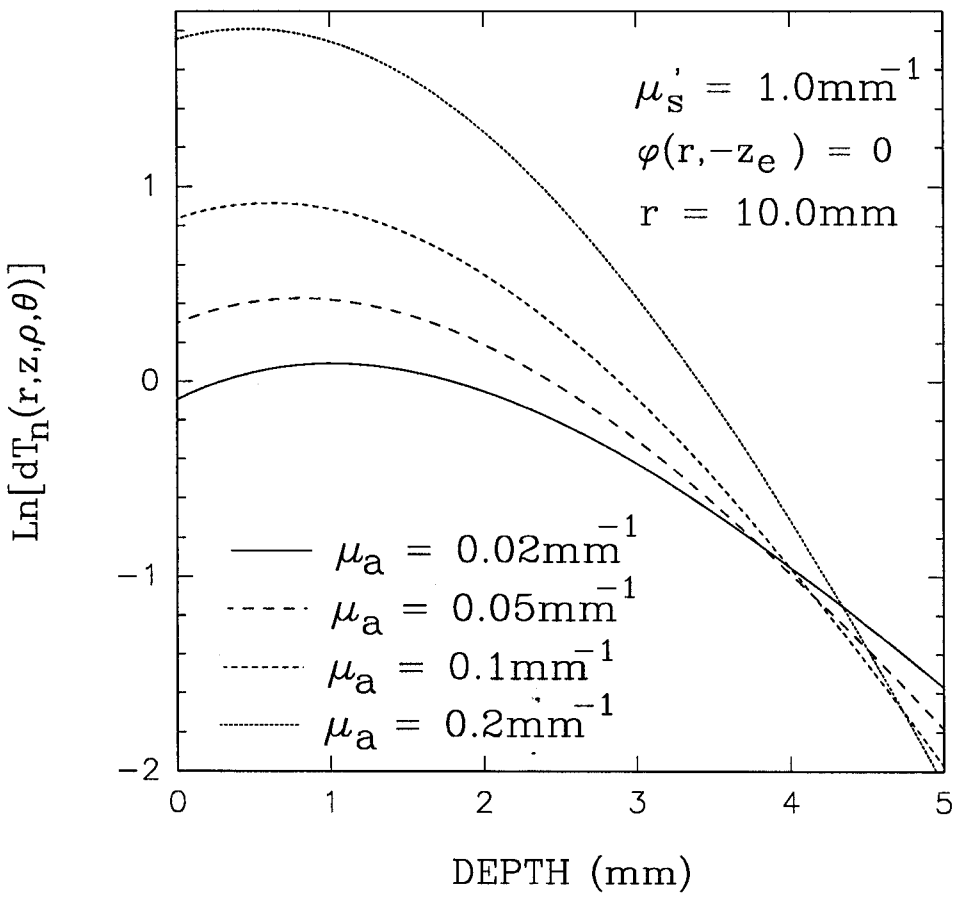

Figure 4.2.2.3

Examines the comparison presented in figures 4.2.1.3 and 4.2.1.4 for a steady state technique. The curves have been normalized to the number of photons leaving the tissue per unit area, and have been calculated using equation 3.74. The fiber separation is r = 10.0mm.

Semi–Infinite 3–Dimensional Medium
Extrapolated Boundary, z_e : Marshak
Index Mismatch: $n_v = 1.0$, $n_m = 1.4$

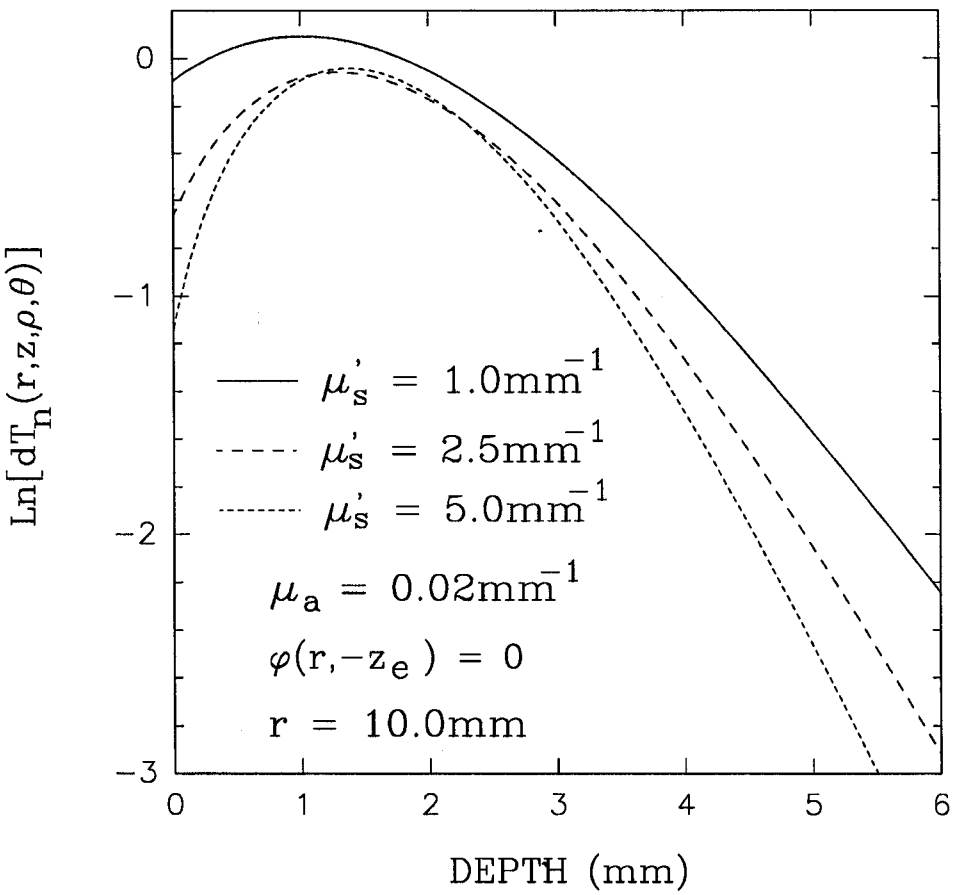

Figure 4.2.2.4

Examines the comparison presented in figures 4.2.1.5 and 4.2.1.6 for a steady state method. The curves have been normalized to the number of photons leaving the tissue per unit area and are calusing equation 3.74. The fiber separation is r = 10.0mm.

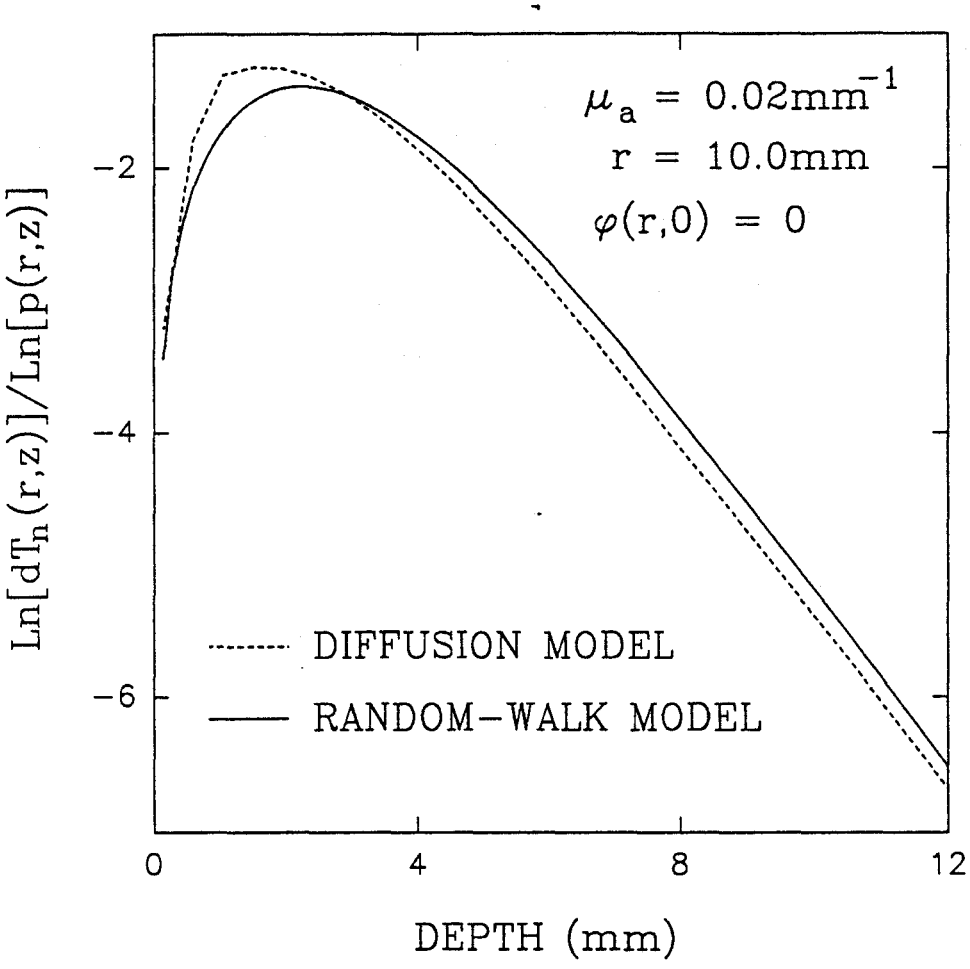

Figure 4.2.2.5

A comparison of the Residency time from both the Diffusion and the Random Walk models, given as a function of depth. The curve (·····) has been calculated using equation 3.76 and (——) from equation 3.77. The fiber separation is r = 10.0mm, and the fundamental optical parameters are typical of soft mammalian tissue.

Measurements from vertical plane containing the source and detection fibers (Plane A).

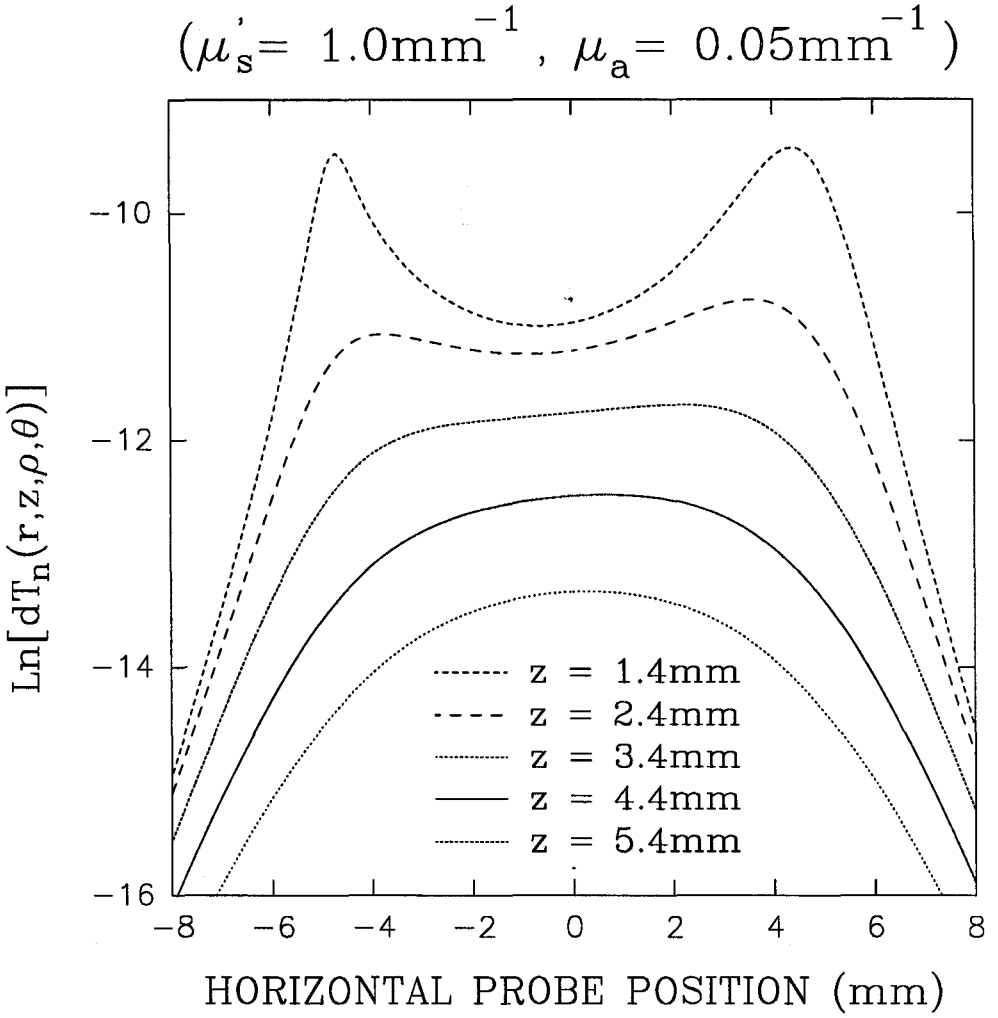

Figure 4.2.2.6

Plots of the residency time from a vertical plane containing the source and detection fibers, positioned at −4.8mm and +4.8mm respectively, as a function of horizontal probe position at different probe depths.

Measurements from vertical plane perpendicular to the source and detection fibers (plane B).

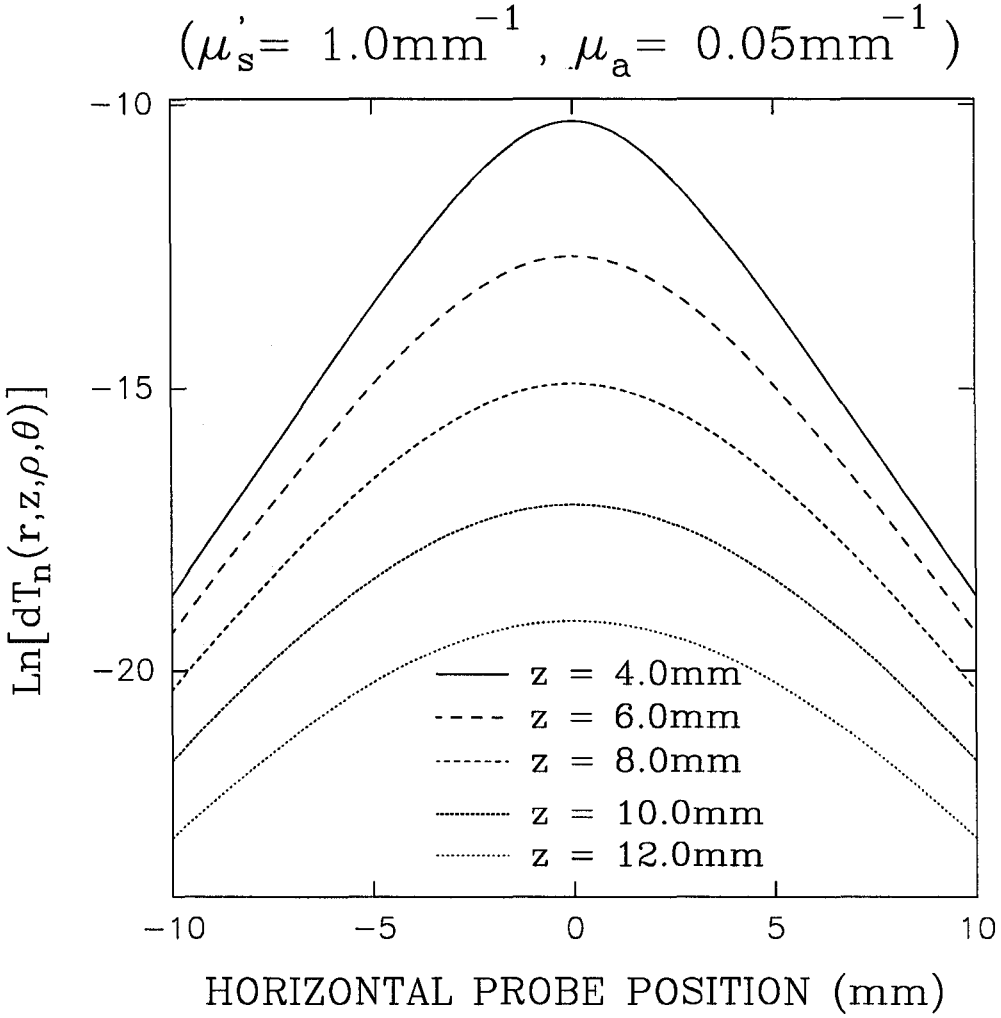

Figure 4.2.2.7

Plots of the residency time from a vertical plane perpendicular to the source and detection fibers, as a function of horizontal probe position at different probe depths. The fiber separation is r = 9.6mm.

Figures 4.2.2.8 and 4.2.2.9 examine the same comparison presented in figures 4.2.1.9 and 4.2.1.10 but for steady state measurements. The curves have been calculated using equation 3.76. In this case, the position of the extrapolated boundary has been calculated for an index matched boundary using the Milne approximation (equation 3.16). The optical parameters $\mu_a = 0.02mm^{-1}$, and $\mu_s' = 1.0mm^{-1}$ are typical of soft tissue and the fiber separation is r = 20mm. The source was positioned at -10mm and the detector at +10mm. Finally, figure 4.2.2.10 shows the spatial distribution of the residency time for a point source and a point detector in an infinite medium separated by a distance r = 20mm. The curves have been calculated using equation 3.63, and once again the optical parameters are typical of soft mammalian tissue.

4.3 DISCUSSION.

If a narrow impulse of collimated light enters a tissue, it expands into a distribution of diffuse light. The dynamics of the light distribution can be considered in terms of two phases.

phase i. The initial rapid increase in population. This phase occurs in the first few picoseconds depending on the optical properties of the tissue, and the dynamics of collected light are dominated by scattering, and

phase ii. The subsequent 'depopulation' of the photons. This phase occurs after the build-up of the photon population. The dynamics of collected light become dominated by absorption.

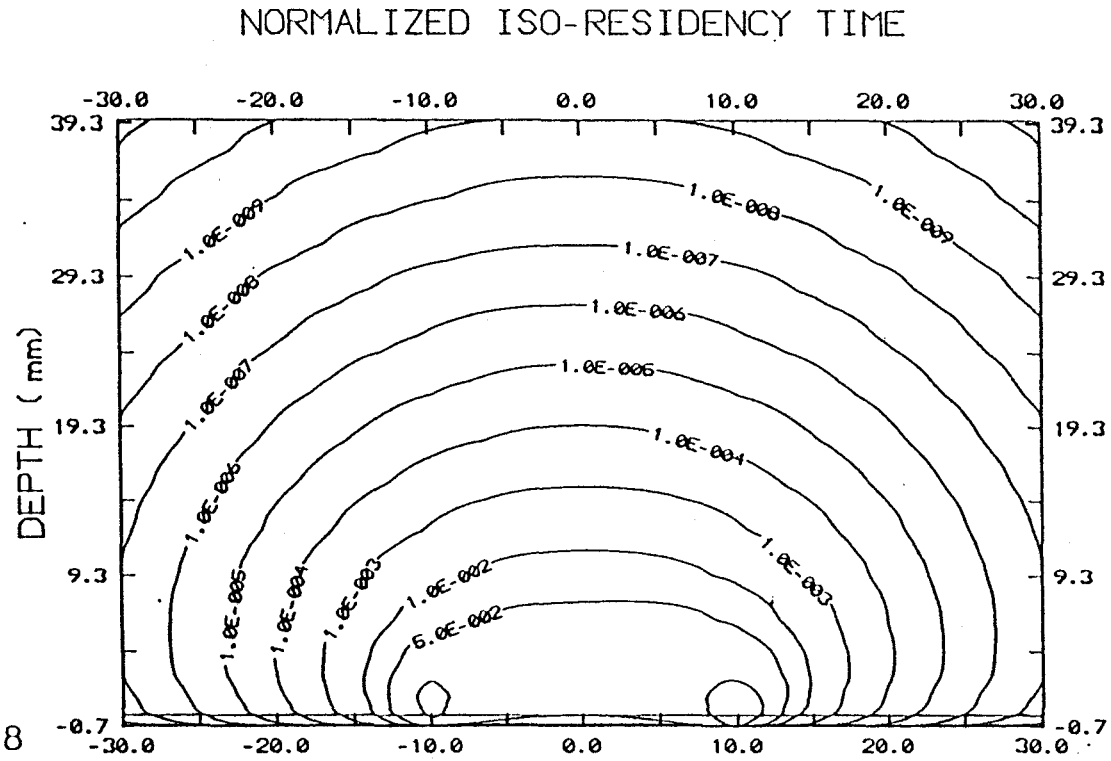

Figure 4.2.2.8

Examines the iso-residency time distribution for a semi-infinite homogeneous medium in the steady state. The photon fluence is set to zero at an extrapolated boundary calculated from equation 3.16 (Milne approximation). Calculations are made in the plane containing the source (positined at -10mm) and detector (positioned at +10mm).

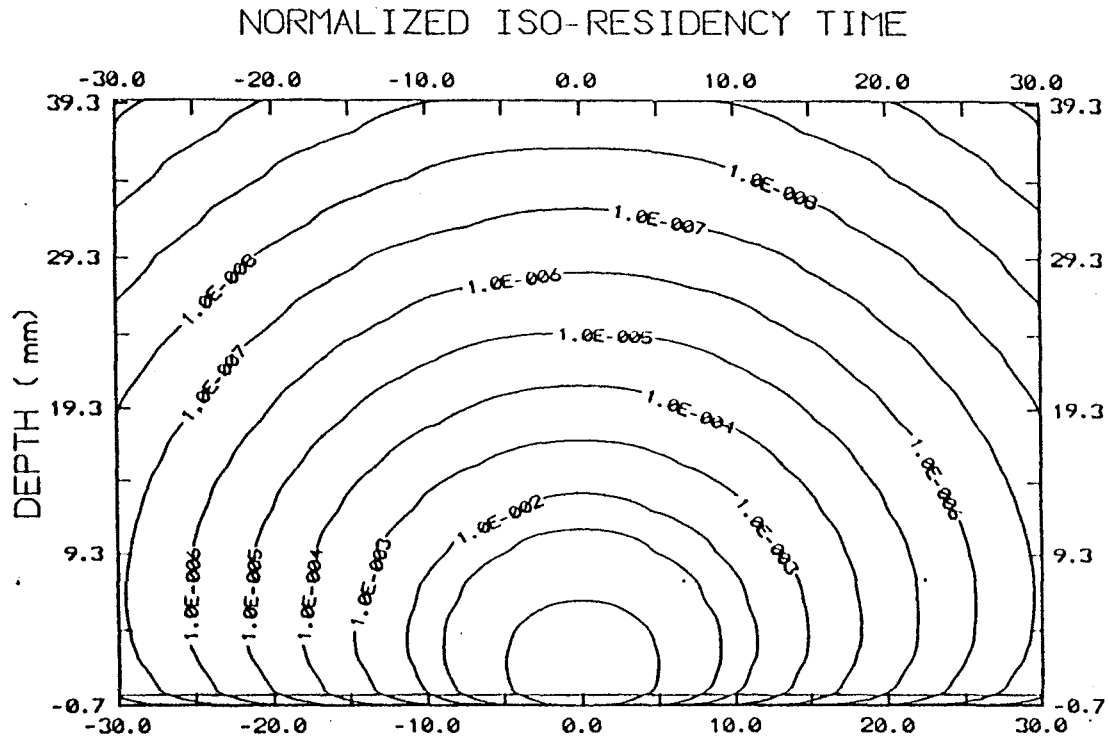

Figure 4.2.2.9

Examines the distribution in figure 4.2.2.8. But the plane in which calculations are made is perpendicular to and midway between the source and the detection fibers.

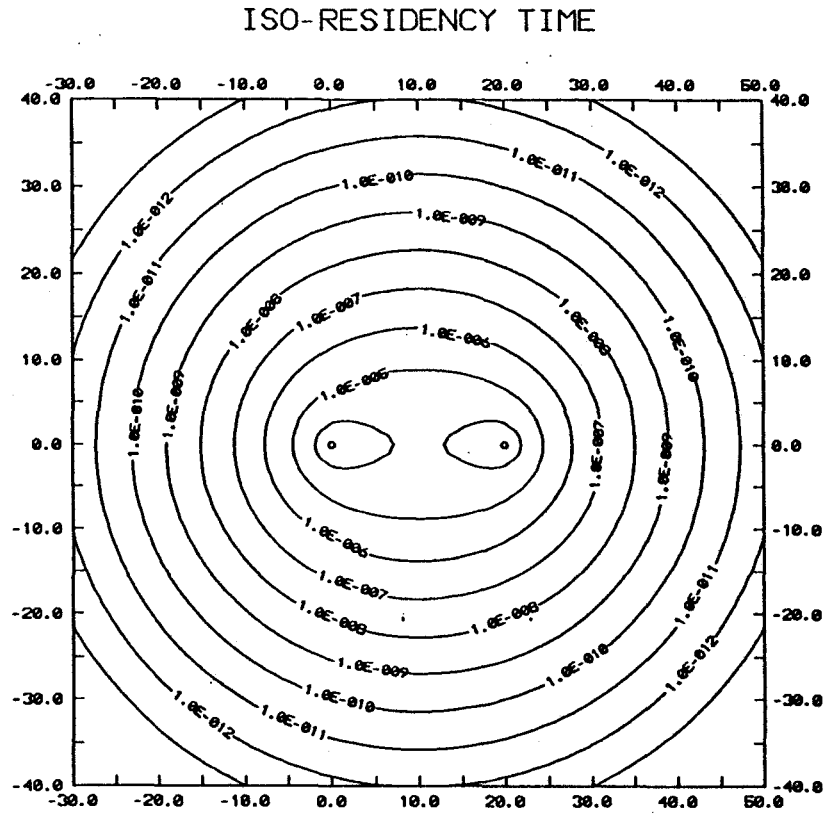

Figure 4.2.2.10

A plot of lines of the same residency time (iso-residency time) of photons emitted from a point source (0,0) and detected in a point detector at (20,0) in an infinite homogeneous medium, in the steady state. Points have been calculated using equation 3.63.

For a continuous beam of light incident on a tissue (i.e steady state), the spatial distribution of the reflectance becomes of prime importance. But a disadvantage of these steady state techniques is that they require absolute measurements at a number of different locations on the surface of the tissue, whereas the time-resolved methods appear to overcome this complication.

The optical properties of tissue greatly influence the volume interrogated by emergent photons. For example, increased transport scattering coefficient decreases the volume. Such a result is expected, because the mean-free-path between scattering sites ($\lambda = 1/\mu_s'$) is reduced with increase in μ_s'. Detected photons therefore have less chance of survival in the interior of the tissue and hence tend to remain close to the surface. Such photons will only carry information about the tissue optical properties from a smaller tissue volume. The fact that the residency time distribution tends to sharpen as the absorption coefficient increases is attributed to the fact that, long trajectories become less likely with large absorption probabilities. Another thing worth mentioning is the shift in the peak of the profiles. It could be observed that with increase in the absorption probabilities (or decrease in the transport scattering coefficient) the peak shifts towards the surface of the tissue.

It is of interest to note from the results that, for a given tissue with specified bulk optical properties, the volume involved in the measurement of its optical properties can be controlled by varying the fiber separation both in the steady

state and in the time-resolved techniques. Moreover, in the pulse state method, a further control of the volume is possible by varying the detection time. For instance, measurement at late times will involve the use of increasingly larger tissue volume. These observations are demonstrated in figures 4.2.1.1, 4.2.1.2, 4.2.1.7 and 4.2.2.2, where it can be observed that the distribution widens and flattens with increase in the fiber separation and/or the detection time of the emergent photons.

The adequacy of the model to predict parameters that control the volume of tissue interrogated during reflectance spectroscopy has been tested by comparing its results to results obtained from a 3-dimensional random walk model. The two models predict similar residency-time depth profile and also tend to agree well. They also predict the same changes in the distribution obtained by increasing the source-detector separation and μ_a (Weiss et al 1989). Weiss et al (1989) have demonstrated analytically that the mean penetration depth of a photon that emerges on the tissue surface at a distance r from the point of injection varies as $r^{1/2}$. This model numerically predicts the same variation with 6% uncertainty. Figure 4.2.2.11 shows the dependence of the mean penetration depth of a photon, $\langle dT(r,z) \rangle$, as a function of $r^{1/2}$ for relatively small values of r as calculated from this model. The data serve to confirm the theoretical prediction that $\langle dT(r,z) \rangle$ is proportional to $r^{1/2}$ even for quite small r values, as proposed by Weiss et al (1989).

The model can be refined in order to consider the effects of possible macroscopic spatial inhomogeneities in the optical parameters. Monte Carlo simulations may be well suited for this purpose. Further work could also be done using a Monte Carlo approach, at least for the steady state technique as a further test of the potential of this model to predict photon depth distribution in a turbid homogeneous tissue.

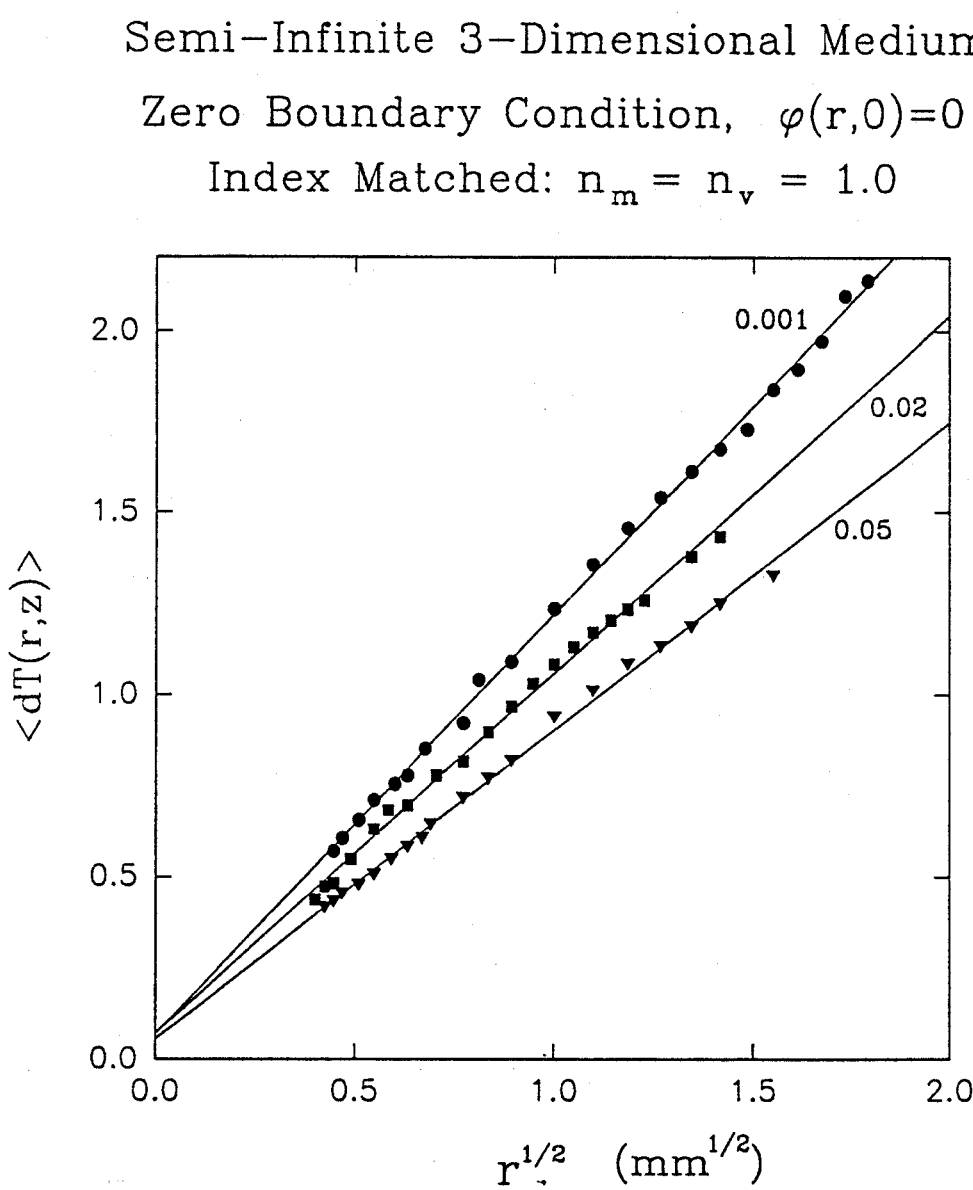

Figure 4.2.2.11

Average residency time of photons that emerge at a distance r from the point of entry, plotted as a function of $r^{1/2}$, for different values of the absorption coefficient. The points have been calculated using equation 3.76.

CHAPTER FIVE

CONCLUSION

The model described in this report holds promise of providing insight to the control of the volume interrogated by photons during both time-resolved and steady state reflectance spectroscopy. However, the problem of inhomogeneities in the optical properties need to be dealt with. Further work could also be done using a Monte Carlo approach, at least in the steady state technique as a further test of the adequacy of this model to predict diffusely re-emitted photon depth distributions in tissue. It has been demonstrated that time-resolved and steady state reflectance spectroscopy is a powerful technique in biological medical research, since it could non-invasively supply both diagnostic and therapeutic informations of tissues.

In this analysis it has been observed that the volume of tissue from which information about the interaction coefficients is contained can be controlled in a number of different ways. In the time-resolved measurements, the tissue volume can be increased by either increasing the source-detector separation or considering late-time photon reflectance measurements. Such measurements may be useful in determining the μ_a value in larger volumes, e.g brain, liver, kidney and tumours. Photons that reach the surface at larger times or fiber separations after

the excitation pulse have, in general, migrated farther from the immediate vicinity of the source and detector and hence 'carry' information about a larger volume of tissue. Early-time or smaller source-detector reflectance data will give information from a smaller tissue volume, and may be useful in measuring blood and clots within vessels, the superficial wall of the gastrointestinal and oesophageal tracts or the first mm of tissue at a catheter tip which receives strong therapeutic laser irradiation (Jacques 1989).

However, in the steady state, the only means of controlling the volume of tissue sampled by the re-emitted photons is to change the fiber separation. This observation has been predicted earlier by Weiss (1989) in his publication.

As discussed by Bonner et al (1987), knowledge of this volume is critical to understanding which parts of the microvasculature contribute to the flow signal and in absolute quantitation of the measurements used to quantify tissue metabolism or photochemistry.

Since both steady state technique and pulse irradiation were used in the analysis, it is worth mentioning here some of their advantages and disadvantages. One major disadvantage of time-resolved reflectance spectroscopy is in its economic constraints, for example, the requirement for picosecond laser and fast detector currently makes time-resolved techniques more expensive and hence less suited for routine clinical use. But this may change in the future as solid state and diode lasers become available in the appropriate wavelength

range (Patterson et al 1990).

A major advantage, however, of time-resolved scattering measurements is the ability to deduce the absorption and the transport scattering coefficients of tissue from measurements of the detected pulse shape at one location on the tissue surface. Such a strategy is relatively insensitive to some noise sources and tends itself to endoscopic applications where geometrical constraints make it difficult to measure the spatial dependence of the diffusely reflected light (Patterson et al 1990).

REFERENCES

Andersen, R. R., Hu, J. and Parrish, J. A., 1984, "Optical Radiation Transfer in Human Skin and Applications to in vivo Remittance Spectroscopy", In Bio-engineering and the Skin, (Edited by Marks, R. and Payne, P. A., 253-265. MTP Lancaster.

Bacci, M., Bandettini, L., Barel, A., Filipponi, F., Jori, G., Linari, R. and Romanndini, P., 1986, "In vivo Diffuse Reflectance Spectra of Mice Treated with Hematoporphyrin", In Photodynamic Therapy of Tumours and Other Diseases, (Edited by Jori, G. and Perria, C.), 409-412. Libreria Progetto Editore, Padova.

Bonner, R. F., Nossal, R., Havlin, S. and Weiss, G. H., 1987, "Model for Photon Migration in Turbid Biological Media", J. Opt. Soc. Am. A **4**, 423-432.

Bonner, R. and Nossal, R., 1981, "Model for Laser Doppler Measurements of Blood Flow in Tissue", Appl. Opt. **20**, 2097-2107.

Carter, L. L. and Cashwell, E. D., 1975, "Particle Transport Simulation with the Monte Carlo Method", Tech. Inform. Centre, Office of Public Affairs, U.S. Energy Res. Develop. Admin.

Chance, B., Nioka, S., Kent, J., McCully, K., Fountain, M. Greenfeld, R. and Holtom, G., 1988, "Time Resolved Spectroscopy of Haemoglobin and Myoglobin in Resting and Ischemic Muscle", Anal. Biochem., **174**, 698-707.

Chandrasekhar, S., 1943, "Stochastic Problems in Physics and Astronomy", Rev. Mod. Phy. **15**, 1-89.

Delpy, D. T., Cope, M., van der Zee, P., Arridge, S., Wray, S. and Wyatt, J., 1988, "Estimation of Optical Path length Through Tissue from Direct Time of Flight Measurement", Phys. Med. Biol., **33**, 1433-1442.

Doiron, D. R., Svaasand, L. O. and Profio, A. E., 1983, "Light Dosimetry in Tissue, Application to Photoradiation Therapy", In Porphyrin Photo sensitization, (Edited by Kessel, D. and Dougherty), Plenum, New York, 63-76.

Dougherty, T. J., Kaufman, J. E., Goldfarb, A., Weishaupt, K. R., Boyle, D. G. and Mittelman, A., 1978, "Photoradiation Therapy for the Treatment of Malignant Tumours", Cancer Res. **38**, 2628-2635.

Dougherty, T. J., Grindley, G. B., Fiel, R., Weishaupt, K. R. and Boyle, D. G., 1975, J. Natl Cancer Inst., **55**, 115-121

Duderstadt, J. J. and Hamilton, L. J., 1976, Nuclear Reactor Analysis, John Weily & Sons, New York.

Feather, J. W., Dawson, J. B., Barker, D. J. and Cotterill, J. A., 1981, "A Theoretical and Experimental Study of the Optical Properties of in vivo Skin", In Bioengineering and the Skin, (Edited by Marks, R. and Payne, P. A.), 275-281. MTP, Lancaster.

Flock, S. T., Patterson, M. S., Wilson, B. C. and Wyman, D. R., 1989, "Monte Carlo Modelling of Light Propagation in Highly Scattering Tissues-I: Model Predictions and Comparison with Diffusion Theory", IEEE Trans. Biomed. Eng., **36**, 1162-1168.

Flock, S. T., Wilson, B. C. and Patterson, M. S., 1989, "Monte Carlo Modelling of Light Propagation in Highly Scattering Tissues-II: Comparison with Measurements in Phantoms", IEEE Trans. Biomed. Eng., **36**, 1169-1173.

Flock, S. T., Wilson, B. C. and Patterson, M. S., 1988, "Hybrid Monte Carlo - Diffusion Theory Modelling of Light Distributions in Tissues", In Laser interaction with Tissue, (Edited by Berns, M. W.), Proc. SPIE, **908**, 20-28

Flock, S. T., Wilson, B. C. and Patterson, M. S., 1987, "Total Attenuation Coefficients and Scattering Phase Functions of Tissues and Phantom Materials at 633nm", Med. Phys., **14**, 835-841.

Furutsu, K., 1980, "Diffusion Equation Derived From Space-Time Transport Equation", J. Opt. Soc. Am., **70**, 360-365.

Gomer, C. J., Ed, 1987, "Photodynamic Therapy", Special Issue of Photochem. Photobiol., **46**, 561-952.

Groenhuis, R. A. J., Ferwerda, H. A. and Ten Bosch J. J., 1983, "Scattering and Absorption of Turbid Materials Determined from Refection Measurements.

1: Theory", Appl. Opt., **22**, 2456-2462.

Groenhuis, R. A. J., Ten Bosch, J. J. and Ferwerda, H. A., 1983, "Scattering and Absorption of Turbid Materials Determined From Reflectance Measurements. 2: Measuring Method And Calibration", Appl. Opt., **22**, 2463-2467.

Hoek, A. V., Vos, K. and Visser, A. J. W. G., 1987, "Ultrasensitive Time-Resolved Polarized Fluorescence Spectroscopy as a Tool in Biology and Medicine", IEEE J. Quan. Elec., **23**, 1812-1820.

Ishimaru, A., 1989, "Diffusion of Light in Turbid Material", Appl. Opt., **28**, 2210-2215.

Ishimaru, A., Kuga, Y. and Brucker, A. P., 1983, "Experiments on Picosecond Pulse Propagation in a Diffuse Medium", J. Opt. Soc. Am. A., **73**, 1812-1815

Ishimaru, A., 1978, "Diffusion of a Pulse in Densely Distributed Scatterers", J. Opt. Soc. Am., **68**, 1045-1049.

Ito, S. and Furutsu, K., 1980, "Theory of Light Pulse Propagation Through Thick Clouds", J. Opt. Soc. Am., **70**, 366-368.

Jacques, S. L., 1989, "Time Resolved Propagation of Ultrashort Laser Pulses within Turbid Tissues", Appl. Opt., **28**, 2223-2229.

Jacques, S. L., 1989, "Time-Resolved Reflectance Spectroscopy in Turbid Tissues", IEEE Trans. Biomed. Eng., **36**, 1155-1160.

Jacques, S. L. and Prahl, S. A., 1987, "Modelling Optical and Thermal Distributions in Tissue During Laser Irradiation", Laser Surg. Med., **6**, 494-503.

Jerlov, N. G., 1976, "Marine Optics", Elsevier, Amsterdam.

Johnson, C. C., 1970, "Optical Diffusion in Blood", IEEE Trans. Biomed. Eng. BME-**17**, 129-133.

Kessel, D., 1984, "Yearly Review: Hematoporphyrin and HPD: Photophysics, Photochemistry and Phototherapy", Photochemistry and Photobiology, **39** (6), 851-859.

Kuga, Y., Ishimaru, A. and Bruckner, A.P., 1983, "Experiments on Picosecond Pulse Propagation in a Diffuse Medium", J. Opt. Soc. Am. A. **73**, 1812-1815.

Lee, L. C. and Jokipii, J. R., 1975, "Strong Scintillation in Astrophysics, II: A Theory of Temporal Broadening of Pulses", Astrophys. J. **201**, 532-543.

Madsen, S. J., 1988, "A Remote Electro-Optical Technique for Monitoring Singlet Oxygen Generation during Photodynamic Therapy", Project Report, McMaster University, Hamilton, Canada.

Marchesini, R., Bertoni, A., Andreola, S. Melloni, E. and Sichirollo, A. E., 1989, "Extinction and Absorption Coefficients and Scattering Phase Functions of Human Tissues in vitro", Appl. Opt. **28**, 2318-2324.

Marijinissen, J. P. A., Star, W. M. and van Gemert, J. C., 1987, "Light Dosimetry: Status and Prospects", J. Photochem. Photobiol. **1**, 149-167.

Marijinissen, J. P. A. and Star, W. M., 1984, "Phantom Measurements for Light Dosimetry Using Isotropic and Small Aperture Detectors", In Porphyrin Localization and Treatment of Tumours, 133-148, (Edited by Doiron, D. R. and Gomer, C. J.), New York: Alan R. Liss.

Moulton, J. D., 1990, "Diffusion Modelling of Picosecond Laser Pulse Propagation in Turbid Media", M. Eng. Thesis, McMaster University, Hamilton, Canada.

Nishioka, N. S., Teng, P., Deutsch, T. F. and Anderson, R. R., 1987, "Mechanism of Laser-Induced Fragmentation of Urinary and Biliary Calculi", Laser Life Sci. **1**, 231-245

Parsa, P., Jacques, S. L. and Nishioka, N. S., 1989, "Optical Properties of Rat Liver Between 350 and 2200nm", Appl. Opt., **28**, 2325.

Patterson, M. S., Moulton, J. D., Wilson, B. C. and Chance, B., 1990, Applications of Time-Resolved Light Scattering Measurements to Photodynamic Therapy Dosimetry", SPIE Progress in Biomedical Optics, **1230**, 62-74.

Patterson, M. S., Schwartz, E. and Wilson, B. C., 1989, "Quantitative Reflectance Spectrophotometry for the Noninvasive Measurement of Photosensitizer Concentration in Tissue During Photodynamic Therapy", SPIE Proceedings, **1065**, 115-122.

Patterson, M. S., Chance, B. and Wilson, B. C., 1989, "Time Resolved Reflectance and Transmittance for the Non-Invasive Measurement of Tissue Optical Properties", Appl. Opt. **28**, 2331-2336.

Patterson, M. S., Wilson, B. C., Feather, J. W., Burns, D. M. and Pushka, W., 1987, "The Measurement of Dihematoporphyrin Ether Concentration in Tissue by Reflectance Spectrophotometry", Photochem. Photobiol. **46**, 337-343.

Peters, V. G., Wyman, D. R., Patterson, M. S. and Frank, G. L., "Optical Properties of Normal and Diseased Human Breast Tissue in the Visible and near Infra-red", Phys. Med. Biol., (in press).

Prince, M. R., Anderson, R. R., Deutsch, T. F. and LaMuragiia, G. M., 1987, "Pulsed Laser Ablation of Calcified Plaque", Proc. Soc. Photo-Opt. Itrum. Eng., 906-956.

Profio, A. E., 1989, "Light Transport in Tissue", Appl. Opt. **28**, 2216-2222.

Puliafito, C. A. and Steinert, R. F., 1983, "Laser Surgery of the Lens: Experimental Studies", Ophthalmology, **90**, 1007-1012.

Reynolds, C., Johnson, C. and Ishmaru, A., 1976, "Diffuse Reflectance from a Finite Blood Medium: Applications to the Modelling of Fiber Optics Catheters", Appl. Opt. **15**, 2059-2067.

Rybicki, G. B., 1971, "The Searchlight Problem with Isotropic Scattering", J. Quant. Spectrosc. Radiat. Transfer, **11**, 827-849.

Shishov, V. I., 1974, "Effect of Refraction on Scintillation Characteristics and Average Pulse Shape of Pulsars", Sov. Astron. **17**, 598-602.

Simmons, E. L., 1975, "Diffuse Reflectance Spectroscopy: A Comparison of the Theories", Appl. Opt. **14**, 1380-1385.

Stern, M. D., 1985, "Laser Doppler Velocimetry in Blood and Multiply Scattering Fluids:, Appl. Opt. **24**, 1968-1986.

Tahmoush, A. J., Bowen, P. D., Bonner, R. F., Mancini, T. J. and Engel, W. K., 1983, "Laser Doppler Blood Flow Studies During Open-Muscle Biopsy in Patients with Neuromuscular Diseases", Neurology, **33**, 547-551.

Weinman, J. A. and Shipley, S. T., 1972, "Effect of Multiple Scattering of Laser Pulses Transmitted Through Clouds", J. Geophys. Res., **77**, 7123-7128.

Weiss, G. H. and Nossal, R., 1989, "Statistics of Penetration Depth of Photons Re-emitted from Irradiated Tissue", J. Mod. Opt., **36**, 349-359.

Welch, A. J., Toon, G. and van Gement, M. J. C., 1987,"Practical Models for Light Distribution in Laser-Irradiated Tissue", Lasers Surg. Med. **6**, 488-493.

Wilson, B. C., 1990, "The Nature of the Light Field in Biological Media", (In press).

Wilson, B. C., 1990, "Modelling and Measurements of Light Propagation in Tissue for Diagnostic and Therapeutic Application", Laser Systems for Photobiology, 1-15.

Wilson, B. C., Park, Y., Hefetz, Y. Patterson, M. S., Madsen, S. and Jacques S., 1989, "Thermal and Optical Interactions with Biological and Related Composite Materials", SPIE Proceeding, **1064**, 97-105.

Wilson,B. C., Patterson, M. S., Flock, S. T. and Moulton, 1988, "The Optical Absorption and Scattering Properties of Tissue in the Visible and near Infrared Wavelength range", In Light in Biology and Medicine, **1**, 45-52 (Edited by Douglas, R. H., Moan, J. and Dall'Acqua, F.), New York: Plenum.

Wilson, B. C., Patterson, M. S. and Flock S. T., 1987, "Indirect versus Direct Techniques for the Optical Properties of tissues", Photochem & Photobio., **46**,601-608.

Wilson, B. C. and Patterson, M. S., 1986, "The Physics of Photodynamic Therapy", Phy. Med. Biol., **31**, 327-360.

Wilson, B. C., Jeeves, W. P. and Lowe, D. M., 1985, "In vivo and Post Mortem Measurements of the Attenuation Spectra of Light in Mammalian Tissue", Photochem. Photobiol. **42**, 153-162.

Wilson, B. C., Jeeves, P., Lowe, D. M. and Adam, G., 1884, "Light Propagation in Animal Tissues in the Wavelength Range 375-825 nanometres", Porphyrin Localization and Treatment of Tumours, 115-132.

Wilson, B. C. and Adam, G., 1983, "A Monte Carlo Model for the Absorption and Flux Distributions of Light in Tissue", Med. Phys., **10**, 824-830.